BARE SOIL EROSION DEPENDENCE ON SOIL AND RAINFALL PROPERTIES

A Dissertation

Presented to

the Faculty of the Department of Civil and Environmental Engineering

University of Houston

In Partial Fulfillment

of the Requirements for the Degree

Doctor of Philosophy

in Environmental Engineering

by

Hu Liu

August, 1999

ACKNOWLEDGMENT

I would like to express my appreciation to the many people who have helped me complete this research and made my doctoral program an enriching experience. The following have been particularly important to me in this process:

Dr. Theodore G. Cleveland, for his constant encouragement, skillful instruction and thoughtful suggestions to improve the clarity of the manuscript.

Dr. K. H. Wang, for his essential guidance of the hydraulic methods used in this research.

Dr. W. Dupre, Dr. C. Vipu and Dr. J. Hunsucker, for their scientific instructions and professional help.

My wife, Qin Yin, for her always 100% backing up my studies and research.

My parents, for their love and support. Without them, this dissertation would not have been possible.

BARE SOIL EROSION DEPENDENCE ON SOIL AND RAINFALL PROPERTIES

An Abstract

of a

Dissertation

Presented to

the Faculty of the Department of Civil and Environmental Engineering

University of Houston

In Partial Fulfillment

of the Requirements for the Degree

Doctor of Philosophy

in Environmental Engineering

by

Hu Liu

August, 1999

ABSTRACT

As of October 1, 1992, industrial discharge on project sites larger than 5 acres are required by the 1987 Water Quality Act to apply for storm water permits. The new standard will reduce the 5 acres to 1 acre in the near future. A Storm Water Pollution Prevention Plan (SW3P) is required for the application of the storm water discharge permit. The basis of organizing and designing the SW3P for a construction project is the knowledge of the amount of soil that could be eroded by rain storms during the construction period.

Two hundred and thirty seven rainfall-induced soil erosion experiments were conducted to assist in predicting soil loss and subsequent increase in total suspended solids leaving a highway construction site during a rainfall event. Soil shear strength, compressive strength, rainfall intensity, soil bed slope and water erosion power were treated as variables during the experiments. A rainfall simulator and an inclined, 4.8 m-long and 1.2 m-wide water flume were used for the research**.** Rainfall duration is fixed to 30 minutes to compare with other researcher' work. Soil loss was approximated by estimating the volume change before and after each run.

The results of this study confirmed that higher rainfall intensity produced more erosion. The soil with higher shear strength resisted soil erosion better than the soils with lower shear strength at high rainfall intensities. Soil loss was nearly independent of shear strength at low rainfall intensity. Lower soil loss is expected for cohesive soil if the

compressive strength is high. In the situation of low slope steepness and short slope length, soil loss is independent to the slope steepness. A water erosion power concept was developed but is not good enough to predict the amount of soil erosion solely, in part because it neglects soil properties.

Multiple regression analysis was conducted because none of the variables studied could individually predict the amount of soil erosion. Two empirical equations, in which one is an additive model, the other is a product model, were developed for soil erosion prediction induced by single rainfall event. Multiple regression suggested that both models can predict soil erosion better than single parameters. The product model was selected because it is similar to earlier models, and at zero rainfall it predicts zero erosion whereas the additive model violates this intuitive limit. The validity of the empirically derived model is reduced by errors introduced by using a low sampling density for estimating soil loss for most runs. Nonetheless, the general relationships shown in the model are felt to be valid.

The Universal Soil Loss Equation (USLE), the Revised Universal Soil Loss Equation (RUSLE) and modified Universal Soil Loss Equation (MUSLE) are not precise enough for estimation of seasonal or single rainfall-induced soil erosion events yet these tools are in use for these types of estimates. They are poor tools for estimating soil loss over short construction periods (less than 1 year). Based on the comparison conducted in this research, the distribution of soil erosion predicted by RUSLE and MUSLE at the bare soil condition are much more scattered than the developed product model. Most of the

estimations are over-estimations. Therefore, the USLE, RUSLE and MUSLE are not a good tool to predict soil erosion amount in the current research conditions.

Volume measurements can accurately estimate soil loss only when taken in a high-density sampling grid (approximately 350 measurements/m^2). Under such conditions, volume-based measurements can be as accurate as the mass-based measurement widely used by other researchers. The volume method has extreme value in the highway construction sites and field conditions. The approach developed in this research, and similar future approaches could be applied in the field without difficulties associated with collecting and weighing solids. The advantage of this approach is that the use of directly measurable properties of the soils reduces the need to rely upon non-measurable properties such as erosion control factors, cover and management factors, and support practice factors in predicting soil erosion.

TABLE OF CONTENTS

LIST OF ABBREVIATIONS

ASAE	American Society of Agricultural Engineers
ASCE	American Society of Civil Engineers
BMP	Best Management Practice
CREAMS	Chemicals Runoff and Erosion from Agricultural Management Systems
DOT	Department of Transportation
EPA	Environmental Protection Agency
FIFRA	Federal Insecticide, Fungicide, and Rodenticide Act
MaxD	Maximum Deviation
MinD	Minimum Deviation
MUSLE	Modified Universal Soil Loss Equation
NAHB	National Association of Home Builders
NPDES	National Pollutant Discharge Elimination System
NRCS	Natural Resources Conservation Service
NURP	Nationwide Urban Runoff Program
PAH	Polycyclic Aromatic Hydrocarbon
RMS	Root Mean Square Deviation
RUSLE	Revised Universal Soil Loss Equation
SW3P	Storm Water Pollution Prevention Plan
TSC	Temporary Sediment Control
TSS	Total Suspended Solids
TXDOT	Texas Department of Transportation

ULI	Urban Land Institute
USDA	United States Department of Agriculture
USEPA	United States Environmental Protection Agency
USGS	United States Geological Survey
USLE	Universal Soil Loss Equation
WEPP	Water Erosion Prediction Project
WEQ	Wind Erosion Equation

LIST OF TABLES
(with captions)

LIST OF FIGURES
(with captions)

CHAPTER 1

INTRODUCTION

Storm water runoff draining from large surface areas, such as agricultural and urban land, has been found to be a major cause of adverse water quality, including non-attainment of designated uses. Storm water discharges can carry a number of pollutants that can occur from land development, illicit discharges, construction site runoff, and improper disposal of materials (EPA, 1998).

1.1 SUSPENDED SOLIDS TRANSPORT POLLUTANTS

Storm water runoff is rainwater or snowmelt that runs off the land and into streams, rivers, and lakes. The suspended solid particles in storm water runoff come from soil eroded by rainfall and surface flow. Storm water runoff from lands modified by human activities can harm surface water resources, and, in turn, violate water quality standards, in two ways: (1) by changing natural hydrologic patterns and (2) by elevating pollutant concentrations and loading.

Suspended solids serve as a transport mechanism for pollutants that can pose a threat to the health of people and the natural environment. The Nationwide Urban Runoff Program (NURP) suggested that the total suspended solids (TSS) is an indicator of other pollutants including heavy metals, oxygen demanding pollutants, and nutrients commonly found in storm water discharges (EPA, 1983). High lead and cadmium

concentrations have been associated with fine grained soils of 20 to 50 microns, and polycyclic aromatic hydrocarbons (PAHs) are adsorbed by soil particles in the 6 to 60 micron range (Xanthopoulous and Augustin, 1992). Bomboi and Hernandez (1991) discovered a strong correlation between traffic density and high levels of PAHs and n-alkanes in the particles carried in storm water runoff from a highway. Most of the pollutants were associated with particle sizes in the range of 6-60 microns.

More than half of the particles found in typical storm water samples fall in the size range of 6 to 60 microns. A sedimentation study of Barker Reservoir (Winslow Associates et al., 1985) in Houston reported over 60% of the particles in sediment were smaller than 60 microns in size. In another study using 89 storm water samples from the Dallas-Fort Worth Metroplex that were collected prior to entering the receiving streams, the researcher discovered that over 85% of the particles were smaller than 30 microns (Pechacek, 1993). These two studies, in different geological provinces of Texas, indicate that the potential for pollutant transport by storm water sediments is significant.

Thus, the storm water runoff may contain or mobilize high levels of contaminants, such as sediment, suspended solids, nutrients, heavy metals, pathogens, toxins, oxygen-demanding substances, and floatables. Such contaminants are carried to nearby streams, rivers, lakes, and estuaries. Individually and combined, these pollutants can reduce water quality and threaten one or more designated beneficial uses (EPA, 1998).

1.2 STORM WATER RUNOFF FROM HIGHWAY CONSTRUCTION SITES POLLUTES WATERS

Driver and Mustard (1984) studied the monitoring data compiled during the mid-1980s, covering 717 storm events at 99 sites in 22 metropolitan areas throughout the United States. The study revealed that 38 states reported urban runoff as a major cause of designated beneficial use impairment, and 21 states reported storm water runoff from construction sites as a major cause of beneficial use impairment.

Storm water discharges generated during construction activities can cause an array of water quality impacts. Specifically, the biological, chemical, and physical integrity of the waters may become severely compromised. Water quality impairment results, in part, because a number of pollutants are preferentially absorbed onto mineral or organic particles found in fine sediment. The interconnected process of erosion (detachment of the soil particles), sediment transport, and delivery is the primary pathway for introducing key pollutants, such as nutrients (particularly phosphorus), metals, and organic compounds into aquatic systems (Novotny and Chesters, 1989).

In a study of TSS load as a function of land use in Virginia (Vice et al, 1969), highway construction areas varying from less than 1% to more than 10% of the basin contributed 85% of the sediment load. The sediment yield of the highway construction area was 10 times that of cultivated land, 200 times that for grassland and 2000 times that of forestland. These results suggested that highway construction activities could

significantly increase the soil erosion potential and the total suspended solids load to the natural receiving water bodies during rainstorms.

Concrete and asphalt products, herbicides, insecticides, oils, gasoline, degreasers, and paints are commonly used in the construction and maintenance of roads and highways. These materials and chemicals are easily spilled onto the soil in the construction sites. Road construction and maintenance generate pollution when these pollutants are carried off the construction site with soil particles during rainstorms and carried by runoff to streams, rivers, and lakes. The prevention of storm water pollution is focused at all levels of legislation and administration to protect not only the aquatic lives, but also the health of human beings.

1.3 LEGAL REQUIREMENTS

As of December 1990, industrial storm water dischargers and municipalities of 100,000 or more are required by the Environmental Protection Agency (EPA) to apply for the National Pollutant Discharge Elimination System (NPDES) permit. As of October 1, 1992, industrial dischargers and contractors working on project sites larger than 5 acres are required by the 1987 Water Quality Act to apply for storm water permits. In the near future, the 5-acre standard will be changed to 1 acre. The general permit is applicable only to facilities in states that do not have delegated federal facility authority for the NPDES. The general permit requires dischargers: (1) to prepare storm water pollution prevention plans (SW3P) that identify potential sources of pollution which might affect

the quality of storm water discharges from the facility, and (2) to describe and implement best management practices (BMPs) to reduce the pollutants in the discharges.

Construction companies have to prepare the SW3P to apply for the storm water discharge permit from EPA. SW3P, which includes site description, erosion and sediment control, storm water management, maintenance plans, inspections, and non-storm water discharges, is crucial in the permit application package. Without the plan, a permit will not be granted from EPA. Construction companies have to incur expenditures of capital for preparing a SW3P before they receive the discharge permit from EPA, and for the assessment, installation, and maintenance of sediment control devices over the construction period.

A number of provisions to reduce environmental impacts of road construction should be specified in an erosion and sediment control plan. Those operations are listed as follows:

1) Minimum expose of working surfaces.
2) Optimal placement of rock filter dams, silt fences, and sediment traps to prevent sediment from reaching drainage systems.
3) Wash mud from vehicles when leaving a construction site.
4) Provide a coarse rock surface on temporary exit/entry roads to construction sites to prevent the transfer of soil off site where it will be washed into nearby drainage channels.

5) Restrict herbicide and pesticide use in highway rights-of-way to applicators certified under the Federal Insecticide, Fungicide, and Rodenticide Act (FIFRA) to ensure safe and effective application.
6) Limit the use of chemicals such as soil stabilizers, dust palliatives, sterilants, and growth inhibitors to avoid excess application and consequent intrusion of such chemicals into surface runoff.

To prepare a SW3P, construction companies must first investigate the amount of soil that could be eroded and transported out of its original site during a rainfall event. Second, they must optimally locate the prevention devices and operations. Therefore, soil erosion estimates are crucial in predicting the effect of storm water runoff, and in installing and executing pollution prevention plan effectively and economically.

1.4 OBJECTIVES OF THE RESEARCH

This research has four objectives.

1) Develop an empirical equation describing soil erosion as a function of measurable properties of rainfall, soil, and overland flow to help highway construction engineers to estimate the soil erosion on the rainfall event basis. The equation will be an extension of the RUSLE-type erosion models.
2) Explore a concept of erosion power that combines the raindrop impact power and surface flow entrainment power to further describe soil erosion.

3) Compare the prediction results of the empirical equation to those from the Revised Universal Soil Loss Equation (RUSLE) and Modified Universal Soil Loss Equation (MUSLE), which are using for soil erosion estimation at construction sites.
4) Test the applicability of the developed model with censored data.

The empirical equation developed in this study is based on laboratory measured rainfall intensity, soil shear strength, compressive strength, soil moisture content, slope steepness, rainfall intensity, overland flow velocity, and depth. It can be used as an alternative to the RUSLE and MUSLE to predict soil loss and subsequent increase in total suspended solids of storm water leaving a highway construction site during a rainfall event. The parameters related to soil erosion in the empirical model can be obtained from simple field measurements. The empirical equation is a part of an erosion model that allows a highway engineer to quickly and precisely estimates the amount of soil erosion during a rainfall event. Therefore, the effectiveness of temporary sediment controls (TSCs) applied under a Storm Water Pollution Prevention Plan required before and during construction can be evaluated. The usefulness of the model is compared to results calculated by RUSLE and MUSLE.

CHAPTER 2

BACKGROUND AND LITERATURE REVIEW

Although soil erosion from highway construction sites is getting more and more attention from environmental engineers, the study of soil erosion began in the early 1900s, with contributions from agricultural engineers. Federal- and state-supported natural-runoff and erosion-plot research began in the 1930s. A. W. Zingg and other researchers started compilation and analysis of that information in the 1940s. The USLE, which is an empirically based erosion prediction tool, was developed in 1950s and 1960s.

The research of mathematical theory for soil erosion mechanics began in the late 1960s. The theory was tested and refined, using new equipment, including field rainfall simulators. This new theory led to the tools used in the Chemicals Runoff and Erosion from Agricultural Management Systems (CREAMS) model, which served as the prototype for the Water Erosion Prediction Project (WEPP) erosion prediction technology.

2.1 SOIL EROSION PROCESSES

2.1.1 Introduction

Soil erosion may be defined as the detachment and removal of soil material from the soil surface of the ground, either by water or by wind, (Finkel, 1986). In this dissertation the

only mechanism studied is water erosion. Several distinctive processes are involved in erosion of surface materials by water. They are raindrop splash, unconcentrated wash (includes sheet flow erosion), concentrated wash (rill, gully, stream bank, and channel erosion), and a mixed process in which entrainment is by raindrop splash and transport is by wash. The occurrence and significance of each of these processes are governed by variety of climatic, topographic, hydrologic, and vegetative conditions, and also by the entrainment resistance of surface materials (Bryan, 1974). Gully, stream bank, and channel erosion are not considered in this research.

2.1.2 Characteristics of Rainfall

The characteristics of natural rainfall are important because rainfall is the driving force for flow that causes soil erosion. The sizes of natural raindrops range from near zero to about 7 mm in diameter, with a median drop diameter between 1 and 3 mm, and a tendency for the median to increase with rainfall intensity. Table 2-1, from Finkel (1986), is a list of values of rainfall intensity and the corresponding mean drop diameter.

The fall velocities (terminal velocities) of raindrops vary from near zero to more than 9 m/s, and tend to increase with the increase of raindrop diameter. For example, the terminal velocity of a 2 mm diameter raindrop is about 6.49 m/s. Table 2-2, from Finkel (1986) is a list of drop diameters and corresponding terminal velocities.

Table 2-1. Relation of drop size to precipitation intensity (after Finkel 1986)

Rainfall Intensity (mm/h)	Mean Diameter (mm)	Mass (g)
2.5	1.47	1.66
12.7	2.12	4.99
25.4	2.50	8.18
50.8	2.92	13.04
76.2	3.22	17.48
101.6	3.47	21.88
127	3.62	24.84
154.2	3.80	28.73
177.8	3.92	31.54
203.2	4.07	35.30
228.5	4.15	37.42
254	4.25	40.19

Table 2-2. Terminal velocity of falling drops (after Finkel 1986).

Drop Diameter (mm)	Minimum fall height (m)	Terminal velocity (m/s)
1	2.2	4.03
2	5.0	6.49
3	7.2	8.06
4	7.8	8.83
5	7.6	9.09
6	7.2	9.18

2.1.3 Raindrop Splash

Raindrop splash erosion is caused by the kinetic energy of the raindrop released at the instant of impact, causing detachment of soil particles. Generally, on hitting the soil surface, raindrop breaks up into a ring of droplets. These droplets and the soil particles detached by the kinetic energy of the falling drop rebound into air in a crown-shaped structure, and re-deposit to the surface when the droplets fall. The muddy secondary droplets may reach as high as 70 centimeters, and, as far as 2 meters horizontally (Finkel,

1986). Figure 2-1 is a photograph of raindrop impact. The crown-shaped droplets of raindrop and the attached soil are rebounding from the soil surface radially from the point of impact.

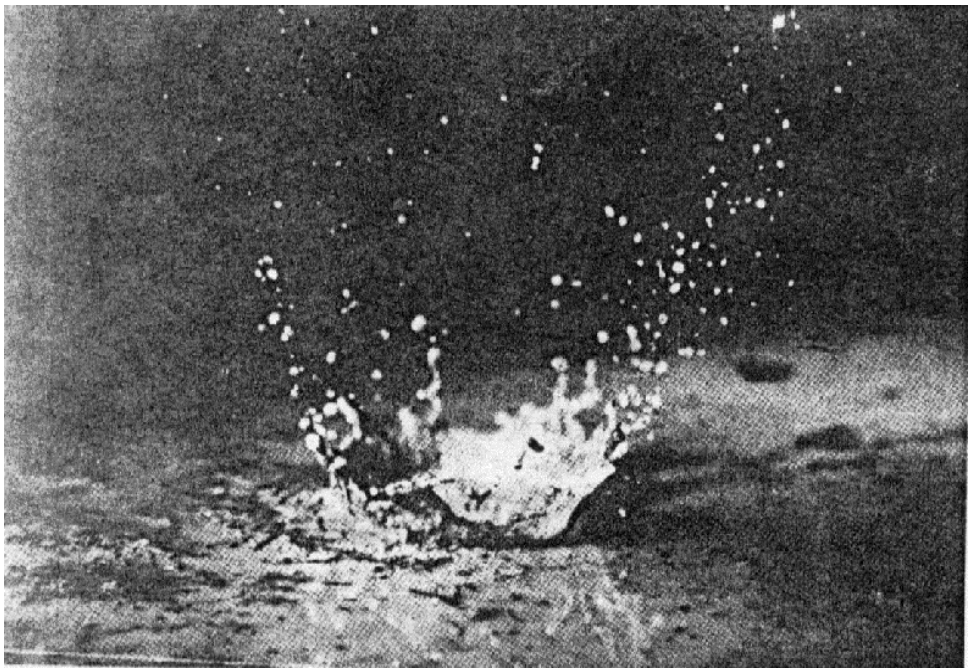

Figure 2-1. Raindrop splash at the instant of impact (after Finkel 1986).

Al-Durrah and Bradford (1982b) studied the mechanism of raindrop splash on soil surfaces using single drop experiments. They observed that the impulsive loading caused by the impacting drop occurs too fast for drainage; thus there is no change in total soil volume or bulk density. The soil surface is deformed under the impulsive load application of the drop; however, the vertical strain under the impact area is compensated by a bulge around the perimeter of the depression. The vertical force of the drop is transformed to lateral shear caused by radial flow of the impacting drop. They found that splash shape is influenced by surface shear strength and splash angle was highly

correlated with soil shear strength. The relationship between splash angle and shear strength is given by

$$\theta_s = 40.5 \cdot \tau^{-0.425}, \qquad \text{Eq. [2-1]}$$

where

θ_s = the splash angle (degree),
τ = the shear strength (kPa).

They also showed that this relationship is independent of soil type. Low soil strength resulted in a larger cavity and surrounding bulge, a greater detachment of soil particles, and a greater splash angle with the horizon. Figure 2-2 is the sketch of the drop splash from Al-Durrah and Bradford (1982b), that shows the transformation of compression of drop to shear stress and the detachment of soil particles.

The kinetic energy of a raindrop is a function of two fundamental characteristics of the raindrop: the size (or mass) and the impact velocity (terminal velocity). The soil detaching power of falling drops is far greater than that of a flowing stream over a given area of land surface (Finkel, 1986).

On level ground the soil particles splash uniformly in all directions and, assuming a uniform distribution of raindrops, the net transport is zero. However, on a slope, the flying droplet strikes the ground surface at a greater distance on the downhill side than on the uphill side. This way, soil particles are moved down the slope in progressive steps in the absence of surface water. Figure 2-3 is the sketch from Finkel (1986) showing the down slope soil transport by the raindrop impact.

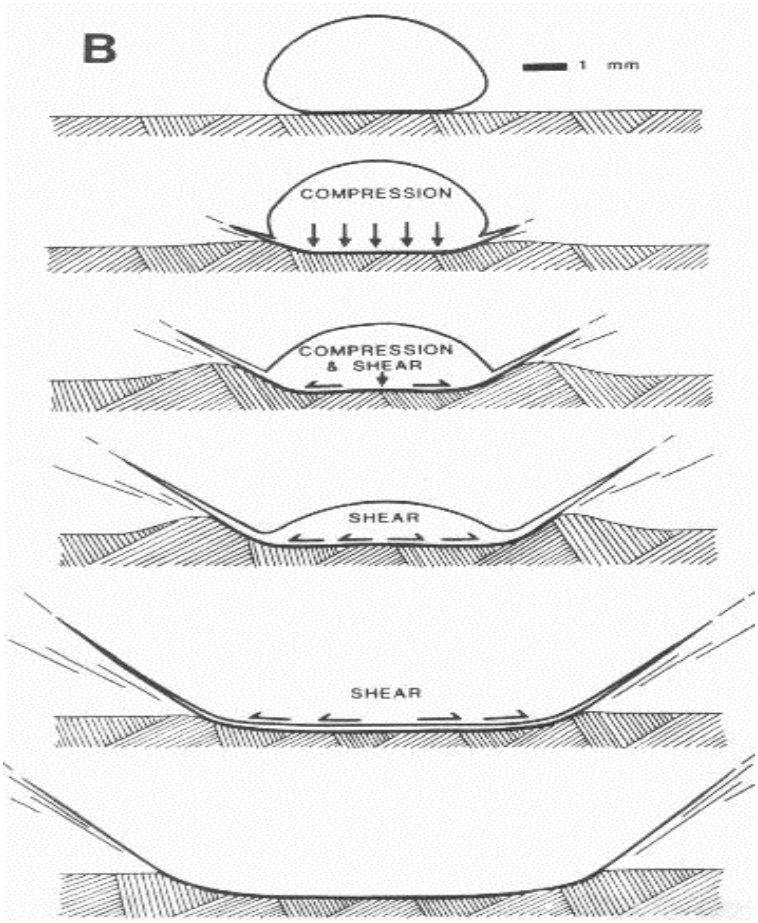

Figure 2-2. Compression transferring to shear stress during drop splash (after Al-Durrah and Bradford 1982b).

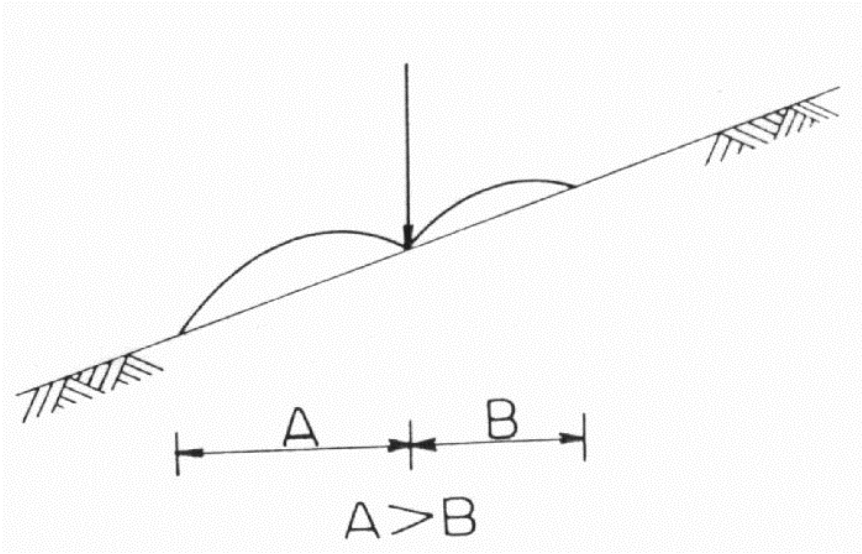

Figure 2-3. Down slope soil transport by raindrop impact (after Finkel 1986).

According to Tan (1989b), raindrop impact is the dominant detachment agent of soil erosion in the interrill area, because the soil surface may not be totally covered by water, and surface water is not deep enough to cushion the soil from impact by raindrops. The detached soil particles are usually dispersed into or onto surface water and are kept in suspension by turbulent flow that transports these particles down the slope or to rills.

Young and Wiersma (1973) experimentally studied the role of rainfall impact on soil detachment and transport. They showed that reducing raindrop impact energy by 89% (with same rainfall intensity) resulted in a 90% reduction in soil erosion. Singer and Blackard (1982) suggested that raindrops contributed significantly to the soil loss up to 35 to 40% soil slope steepness, and cannot contribute more when the slope steepness is higher than 40%, because there is less direct raindrop impact on the soil surface at high slope angles. However, the natural angle of repose of most natural loosely consolidated materials is less than 40%.

Singer and Walker (1983) compared the effects of rainfall, overland flow, and rainfall plus overland flow. They found that raindrop impacts increase both the erosive power of runoff and the volume of water discharged from the bed because of the development of a surface seal. Soil surface seals and crusts resulting from aggregate breakdown reduce the soil infiltration rate and may induce erosion by increasing runoff (Le Bissonnais, et al. 1995). They also found that rain-flow transportation was an effective erosive agent. A partitioning of soil loss indicated that raindrop splash made only a minor contribution to the soil transport.

Kung (1984) showed that the terminal velocity and the curvature of the lower half of the drop are important physical characteristics of a raindrop. It is the raindrop size spectrum instead of rainfall intensity that will determine the total amount of soil splash. Turner et al. (1985) reported that, for land surfaces having slopes steeper than 3%, overland flow resulting from intense rainfall can become a dominant process in removing and transporting soil particles. For slopes that are less than 3%, removal and transport of soil particles are more likely to be caused by raindrop splash.

Tan (1989a, b) suggested that eroding pressure, (p_e), which is caused by water drop impact on soil surface, showed a functional trend in relation with erosion. The eroding pressure could be treated as a suitable parameter when raindrops' impact is involved in the erosion process. The eroding pressure was defined as:

$$p_e = \frac{4}{3}\rho w^2 \frac{1}{\beta}\exp(-\frac{1}{\beta}), \qquad \text{Eq. [2-2]}$$

$$\beta = \frac{3}{8}(\frac{d}{D})^2, \qquad \text{Eq. [2-3]}$$

where

p_e = eroding pressure (Pa),
w = terminal velocity of rain drop in air (m/s),
ρ = density of water (g/cm^3),
d = depth of surface water (mm),
D = diameter of raindrop (mm).

By assuming that raindrop impact is the only erosive agent, overland flow simply transports the sediment eroded under the action of raindrops. Sander et al. (1996)

suggested an unsteady soil erosion model to explain the soil erosion behavior. The model consisted of 20 partial differential equations. The analytical solution could reproduce the rapid initial increase to a peak in the total sediment concentration, which occurs about 3-5 minutes after the commencement of rainfall, as well as the subsequent declining exponential tail towards steady-state conditions. It is also able to show that the fraction of shielding of the original soil bed resulting from depositing sediment reaches its equilibrium value on about the same time-scale as the total peak suspended sediment concentration.

2.1.4 Interrill Erosion

If the infiltration rate is less than the rainfall intensity, overland flow occurs. Interrill flow could just transport the soil particles detached by raindrops to rills or downstream. However, when shear stress of interrill flow exceeds a critical shear stress value for the particular soil condition, the flow begins to detach soil particles and transport them. Nearing (1991) discussed a probabilistic model for the detachment of cohesive soil particles by shallow turbulent flows. Generally soil shear strength is about 1000 times higher than that of flow. The detachment of cohesive soil particles occurs only when a turbulent "burst" occurs and the flow shear stress exceeds the local tensile strength on the soil surface. The flow shear strength need to detach non-cohesive soil particles is much smaller than that of cohesive soil particles.

Soil erosion models typically represent interrill erosion empirically as a power function, e.g. Meyer (1981), Meyer and Harmon (1989), and Line and Meyer (1988). That is,

$$E = aI^b, \qquad \text{Eq. [2-4]}$$

where

E = the interrill erosion rate for a given rainfall duration (ton/ha-h),
a, b = constants related to soil properties,
I = the rainfall intensity during the rainfall duration (mm/min).

Reported b values range from 1.3 to 2.2. For soil with low-clay content (less than about 20%), b value is typically reported near 2.0.

Nearing et al. (1989) developed a process-based soil erosion model-Water Erosion Prediction Project (WEPP) for the United States Department of Agriculture (USDA). In WEPP, the interrill erosion is conceptualized as a process of sediment delivery to concentrated flow channels, or rills. The interrill sediment is then either carried off the hill slope by the flow in the rill or deposited in the rill. Sediment delivery from the interrill areas is

$$D_i = K_i I^2, \qquad \text{Eq. [2-5]}$$

where

D_i = interrill erosion rate (kg/m^2-s),
K_i = interrill soil erodibility (kg-s/m^4),
I = rainfall intensity (m/s).

Interrill soil erodibility (K_i) is dependent on time, experimental methodology, form, and assumptions of equations used to describe interrill erosion and soil conditions. Rainfall

intensity, slope steepness, and antecedent water content each affect interrill sediment delivery and can contribute to detachment and/or transport-limiting conditions (Truman and Bradford, 1993).

Generally raindrop and overland flow combine to remove soil from the original cohesive soil. Once eroded soil enters overland flow, either as aggregates or primary particles, a significant proportion of it returns to the soil bed, forming a cohesionless deposited layer which could be removed again by the same erosion processes. By delineating between the processes of entrainment, which acts upon the original cohesive soil, and reentrainment, which acts upon the deposited layer, a physical description of the erosion of cohesive soils had been provided by Hairsine and Rose (1992a) and Rose et al. (1983a, b). The model was based on two distinct equilibrium situations. The first case occurs when the deposited layer does not completely shield the original soil surface, and sediment concentration is affected by the cohesive strength of the soil, the so called entrainment-limiting case. For this case, the dynamic equilibrium could be described as

$$q\frac{dc_i}{dx} + c_i\frac{dq}{dx} = r_e, \qquad \text{Eq. [2-6]}$$

where

q = the water flux per unit width,
c_i = the sediment concentration of class i (kg/m^3),
x = distance down slope (m),
r_e = the entrainment process rate.

The second case happens when the deposited layer completely shields the original soil. It appears to correspond with what has been previously called a "transport-limited" situation. The transport limit has been derived as, (Rose et al. 1983a)

$$\frac{d(qc)}{dx} = \sum_{i=1}^{I} r_{gi} = \frac{F\rho[\frac{\sigma}{\sigma-\rho}]S(2-\frac{1}{m})}{\sum_{i=1}^{I}\frac{\upsilon_i}{I}} \bullet K^{1/m} Q^{2-1/m} x^{1-1/m}, \qquad \text{Eq. [2-7]}$$

where

r_{gi} = gravity processes,
F = a effective fraction of (Ω-Ω_0),
Ω = stream power,
Ω_0 = the threshold stream power,
ρ = the water density (g/cm^3),
σ = sediment density (g/cm^3),
S = slope,
m = an integer or a non-integer,
υ_i = the settling velocity representative of class I,
I = total number of classes,
K = calculated from Manning's or Chezy's equations.

2.1.5 Rill Erosion

Rills are small, shallow, ephemeral, concentrated flow paths. Merritt (1984) observed and identified four stages during the development of a rill by taking videos and stereo-photographs during the experiments. 1) Sheetflow stage: a relatively even, laminar sheetflow flows over the smooth surface. Sediment concentration and particle velocities rise rapidly as erosion starts to take place, and erosion is localized and involves only individual grain movements. 2) Flowline stage: flow concentrates into minute channels at random points. Depth, Reynolds number and sediment concentration increase while

velocity decreases because of increased roughness. Small, straight ripples start to appear. 3) Micro-rills stage: most of the water is flowing in well-defined, very small channels. The ripples grow in size. A ripple could become larger and more unstable than the rest, then, it creates localized turbulence and scouring occurs downstream, a small headcut forms and the headcut retreats rapidly upstream. 4) Micro-rills with headcuts stage: a zone of deposition downstream of the headcut occurs as the headcut retreats upslope. The channel becomes wider and deeper carrying all of the runoff, and if left to grow by more headcuts, it becomes a small rill. During all these four stages, Froude Numbers were all over 1, indicating a supercritical flow situation at all times. In all experiments, soil bed slope was 5 degree.

Fullerton and Fullerton (1973) observed that, when all the other factors are held constant and only slope is varied, the rill development is unaffected by slope angle. McCool et al. (1987) also suggested that little or no rill erosion occurs on the low slopes, and interrill erosion is not greatly affected by slope. Slattery and Bryan (1992) observed that prior smoothing of the soil surface by entrainment and redistribution of sediment by overland flow facilitated supercritical flow. The development of supercritical flow and waves, which mold and incise the soil bed was the critical condition for knickpoint initiation. Rills always developed through the formation of a knickpoint and were usually found on soils of high detachability. Figure 2-4 is a picture of rills formed on the soil surface, observe that the rill depth is quite shallow.

Proffitt and Rose (1991) conducted experiments to study the relative importance of rainfall detachment and runoff entrainment. They applied rainfall only, overland flow only, and a combination of rainfall and overland flow to the soils and found that compared with experiments with overland flow alone, rainfall prevented rill formation at 1% slope and delayed rill development at 3 and 5% slopes.

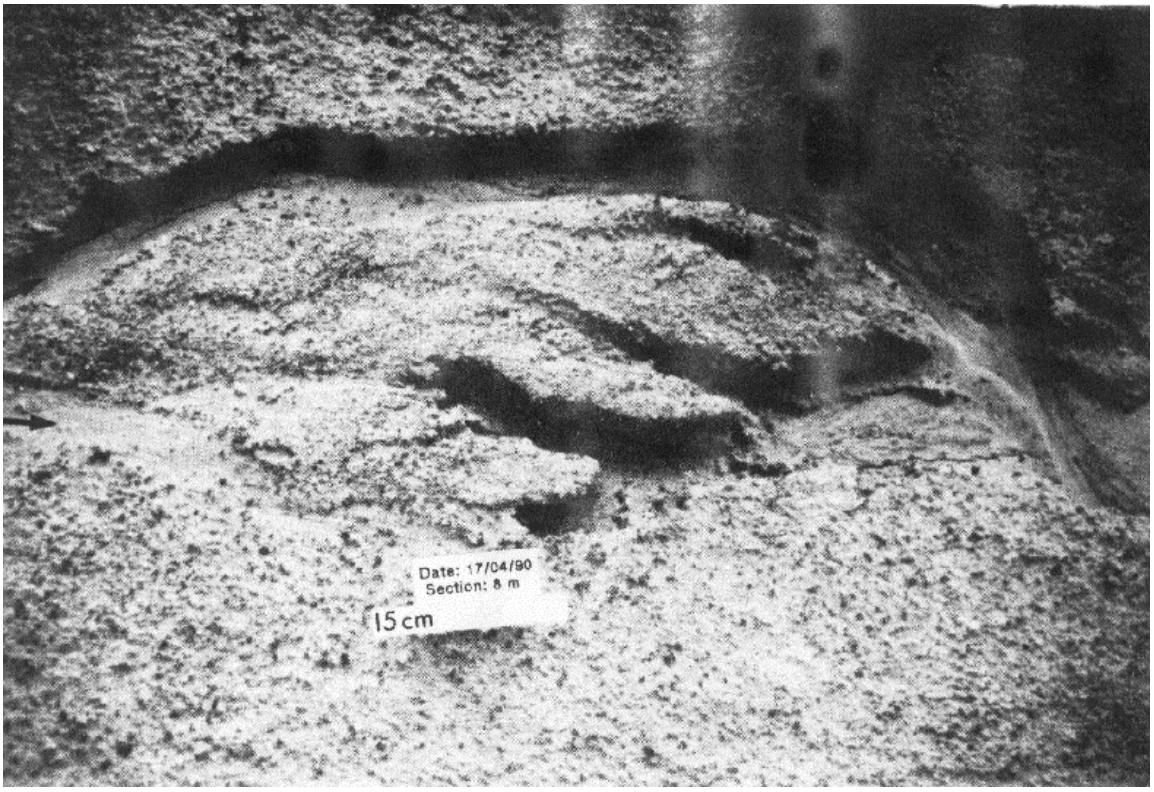

Figure 2-4. Rills formed on the soil surface (after Slattery and Bryan 1992).

Water in rill flows is deeper than in the interrill area and the effect of raindrop impact may not reach the rill bed. However, the considerable disturbance induced by raindrops makes rill flow more turbulent than overland flow in the interrill area. Generally, researchers thought that the flow begins to detach soil particles only when shear stress of

rill flow exceeds the critical shear stress for a particular soil. The turbulent flow causes rapid fluctuation of pressure and bed shear stress. As a result, rill flow not only is more effective in widening and deepening the rill, but also more effective in transporting loose fragments and particles of soil than interrill flow.

Rill erosion is geomorphically significant because runoff reaches its maximum detachment and transportation power when channeled into rills (Rauws and Govers, 1988). Because of roughness in the land surface the rills will eventually flow together and concentrate into fewer, deeper channels. These eventually form gullies, if the slope is long enough.

Researchers have presented a number of equations and models to estimate the soil erosion contributed by rills. Line and Meyer (1988) suggested the following equation,

$$ER = b(Q - Q_c), \qquad \text{Eq. [2-8]}$$

where

ER = the rill erosion rate in unit of g/min-m,
b = the slope of the regression line (regression parameter),
Q = the midpoint runoff rate (kg/min),
Q_c = the critical runoff rate (kg/min) or conceptually, the rate of runoff at which rill erosion begins.

Using the same principles from Hairsine and Rose (1992a), Hairsine and Rose (1992b) introduced a model to estimate water erosion by rill flow. They assumed that there is a dynamic equilibrium in the deposited layer at the base of the rill. The equation is

$$G\frac{dc_i}{dx} + c_i\frac{Q}{N} = [(1-H)W_b + W_s][\frac{F(\Omega - \Omega_0)}{IJ}] + q_{syi}, \qquad \text{Eq. [2-9]}$$

where

G = the volumetric flow rate per rill,
Q = the runoff rate per unit land area,
N = the number of rills,
W_b = the base width of the rill,
W_s = the unshielded sidewall length,
F = the fraction of the excess stream power (Ω-Ω_0) used in entraining or reentraining sediment,
J = the specific energy of entrainment (J/kg),
q_{syi} = the lateral sediment flux to any rill in mass rate per unit rill length and

$$H = \frac{cgD\dfrac{\sigma-\rho}{\sigma}\displaystyle\sum_{i=1}^{I}\frac{\upsilon_i}{I}}{F(\Omega-\Omega_0)} f \frac{W_b+W_s}{W_b} \qquad \text{Eq. [2-10]}$$

where

c = total sediment concentration,
g = gravitational constant,
D = the flow depth,
f = a nondimensional factor related to rill shape.

According to this model, sediment concentration at the transport limit was sensitive to rill shape, whereas the shape of the rill cross section was shown not to greatly affect the sediment concentration at the entrainment limit (Hairsine and Rose 1992b).

The USDA WEPP model suggested an equation for the rill erosion rate. Based upon Nearing et al. (1989), Nearing et al. (1990) and Zhang et al. (1996), the equation for net soil detachment is

$$D_r = K_r(\tau-\tau_c)(1-\frac{G}{T_c}), \qquad \text{Eq. [2-11]}$$

where

D_r = the rill erosion rate(kg m^{-2} s^{-1}),
K_r = rill erodibility (s/m),
τ = shear stress in the rill (Pa),
τ_c = the critical hydraulic shear stress of the soil (Pa),
G = sediment load (kg m^{-1} s^{-1}),
T_c = the transport capacity of the flow in the rill(kg m^{-1} s^{-1}).

In this equation, K_r and τ_c are soil dependent and τ and T_c are flow dependent. However, the greatest limitation to this equation is that it was based on detachment by flow only. Other individual processes such as rill sidewall sloughing and headcutting are not considered.

Based on the models in this review, these researchers focused on sediment erosion and transportation estimation for open channel flow, such as streams and rivers, to rills. This focus is because researchers assumed that relationships derived for sheet flow or larger channel flow are applicable to actively eroding rills. Nearing et al. (1997) challenged this assumption and pointed out that based on their research, flow velocity of rills did not vary with slope. Reynolds number was not a consistent predictor of hydraulic friction. Stream power was found to be a consistent and more appropriate predictor for unit sediment load for their experiments. However, stream power is a concept used in larger channel flows, therefore, further research is still necessary for choosing proper sediment erosion and transportation models for rill erosion.

2.2 RAINFALL SIMULATION

2.2.1 Introduction

Rainfall simulation is an experimental method used to determine the relative erodibilities of different soil materials and other hydrological model parameters. Rainfall simulators are research tools designed to apply water in a form similar to natural rainstorms.

The major advantages of using simulated rainfall to study soil erosion, as Meyer (1988) described, are:

1) More rapid results. The time required to get conclusive result is much shorter.
2) More efficient. Test plot maintenance prior to application of artificial storms is much easier.
3) More controllable. The necessary conditions, for example, rainfall intensity, duration, topography and surface treatments, can be well regulated.
4) More adaptable. In addition to greater control for field studies, simulated rainfall is readily adaptable to highly controlled laboratory research. Erosion studies that would be impossible to properly control in the field, e.g., temperature, humidity and wind, can often be conducted in the laboratory using the rainfall simulator.

Meyer (1988) also pointed out that the ideal rainfall simulator should be inexpensive to build, easy to operate, simple to move, and could be used whenever and wherever needed. The most important is that the rainfall can also be adequately generated.

2.2.2 Types of Rainfall Simulators.

During the last 60 years, researchers have used a broad range of techniques and equipment to simulate rainfall. According to the drop-forming method, which is the most important part in designing a rainfall simulator, there are 3 major categories of rainfall simulators -- hanging yarns, tubing tips and nozzles (Mutchler and Hermsmeier, 1965).

2.2.2.1 Hanging yarns

Parsons (1943) mentioned a rainfall simulator that was called dripolator or stalatometer. It was made by using hanging-yarn drop former. A piece of muslin cloth is laid loosely on a chicken wire screen to form a depression at each screen opening. A piece of yarn is attached to the cloth at each depression. The water sprayed to the cloth is collected at the depressions and travels down the hanging yarns to form drops. The screen should have a regular spacing to give a uniform distribution of intensity over the test area. Average intensity was controlled either by the nozzle flow or by the water head of the supply tank. Drop size is dependent on yarn size and is limited to drops with diameters larger than about 4 mm. However, to prevent the drops from repeatedly falling in the same spot, either the applicator unit or test plot was moved.

2.2.2.2 Tubing tips

Tubing tip is a precise method of forming raindrops. Ekern and Muckenhirn (1947) used a simulator made of 22-gage hypodermic needles set in an aluminum container on a 25.4 mm grid. Drop sizes were changed from 2.8 to 5.8 mm by enclosing the needles in various sizes of glass tubes. Velocities of drops approached terminal velocities by virtue of a 10.67 m fall. Also, the air currents deflected the falling drops to produce an essentially random impact pattern at the plot surface.

Mutchler and Moldenhauer (1963) introduced a rainfall simulator whose drop former was made by telescoping pieces of tubes. As a small tube at the top controls the flow, the largest tube produces the drops at the lower end of each drop former. The drop formers were set in a rotating water tank so that a uniform intensity distribution was achieved.

Gabriels and Boodt (1975) built their rainfall simulator by suspending a circular iron water tank from a frame assembly 2.75 m above the soil surface. Copper capillary tubes inserted through the bottom of the tank allow for the raindrops to pass through. Changing the tip-diameter of the capillary tubes can vary drop sizes. Intensity can be controlled by changing the number of dripping capillaries per unit area and their sizes, as well as by adjusting the hydrostatic head above the drop formers. The water tank is chosen to turn at one revolution per minute to attain the desired drop distribution.

Onstad et al. (1981) built a trailer mounted rainfall simulator. The simulator has four identical modules, and each module covers an area of 0.61 m by 0.91 m. The drop formers are stainless steel capillary tubes with inside diameter of 0.69 mm. Water is applied through these drop-forming tubes, and air is forced to flow around the tubes. Increasing air pressure increases the air velocity passing, which resulting in smaller drops. The drop size distribution is narrower than the natural rainfall with the same intensity. The simulator can generate rainfall intensity range from zero to 200 mm/h. The height of drop formers from soil surface is 2 m.

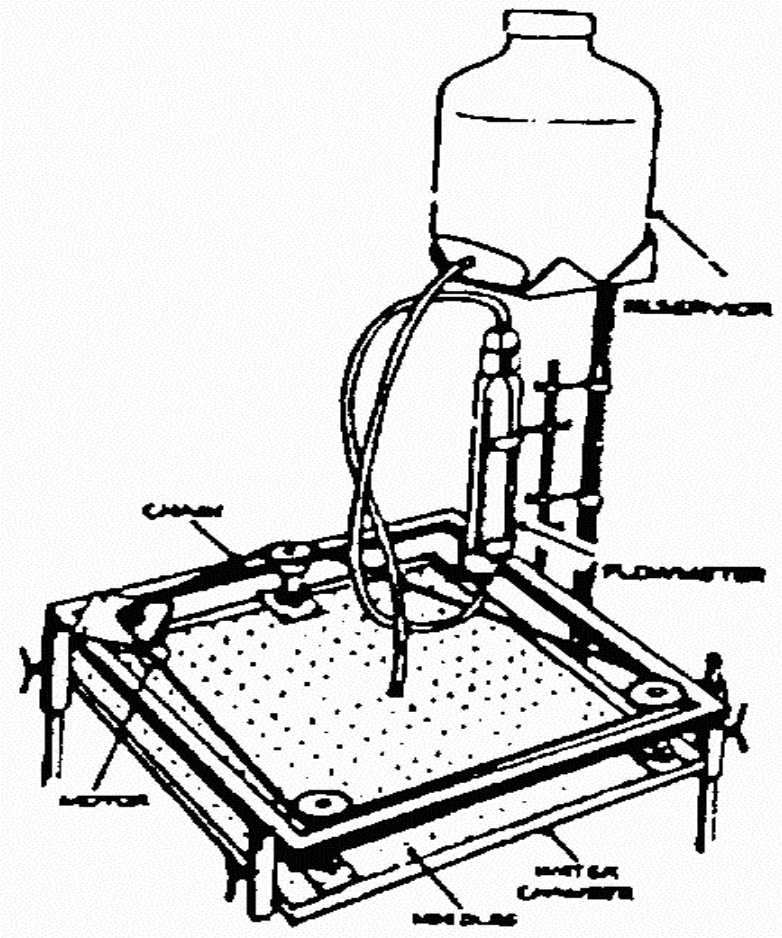

Figure 2-5. A tubing tip typed rainfall simulator (after Meyer, 1988).

2.2.2.3 Nozzles

A nozzle is the only method practically available to produce a distribution of drop sizes and it is the most common type of simulator in use. It forms drops with an initial velocity dependent on pressure that can accelerate raindrops to terminal velocity.

Meyer and McCune (1958) introduced a rainfall simulator that became the "USDA rainulator". The rainfall simulator is made of aluminum to minimize the weight and prevent corrosion by weathering. It is simple to separate, assemble, operate, and transport because the individual pieces can be disassembled into long, narrow, and easily loaded shapes. The rainfall simulator was successfully used to analyze soil erodibility (both qualitatively and quantitatively). The rainulator uses the Spraying System Company 80100 Veejets. The nozzles are installed at a height of 2.44 m above the soil plot surface spraying water drops vertically downward. The pressure applied to nozzles are 41.4 kPa (6 psi), so that the impact velocities of raindrops are very close to the terminal velocity of most natural rain drops. Nozzles are moved back and forth across slope and each unit can cover an effective soil surface of 24.3 m^2. Units could be combined together. In this research, 12 units had been combined to form the rainfall simulator assembly. Two rainfall intensities, 63.5 and 127 mm/hour, could be achieved by the rainulator.

Swanson (1965) developed a rotating-boom rainfall simulator. It is comparatively cheap and easy to operate, separate, assemble, and transport. The spraying nozzles are the same

as that of Meyer-McCune rainulator. The rainfall intensity applied by this simulator was 127 mm/hour. However, the intensity is not very uniform all over the plots. Therefore, it can not be combined into larger groups as can the Meyer-McCune rainulator. Figure 2-6 shows this type of rotating boom simulator.

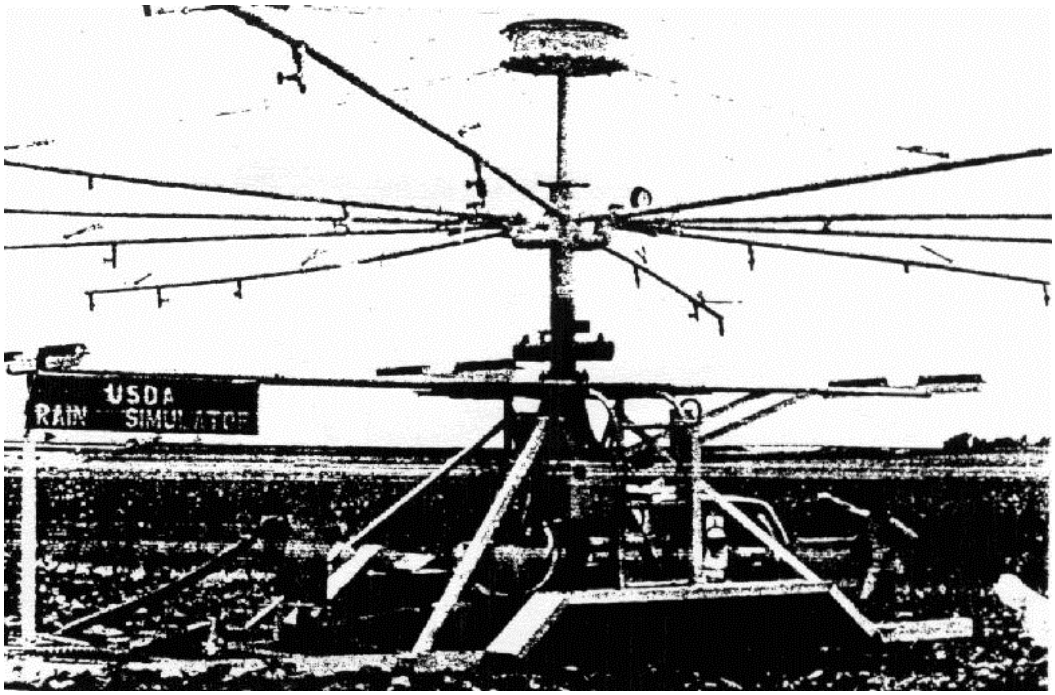

Figure 2-6. A rotating-boom rainfall simulator (after Meyer, 1988).

Neibling et al. (1981) introduced a programmable rainfall simulator that can vary rainfall intensities both in time and space. Nozzles are the same as those of the rainulator, but cycle times of a nozzle have been reduced from about 20 to 0.5 s for a rainfall intensity of 64 mm/h. Nozzles were oscillated continuously during the operation. The kinetic energy of the raindrops is approximately 75% that of natural rainfall and drop size distribution is slightly smaller than that of natural rainfall. Comparing with the rainulator, repeatable intensities are easier to obtain in programmable simulator. The ease of assembly, short

cycle times for minimal effects from intermittent rainfall bursts, and programmable intensities gives the programmable simulator definite advantages. Figure 2-7 is a picture of this type of programmable rainfall simulator.

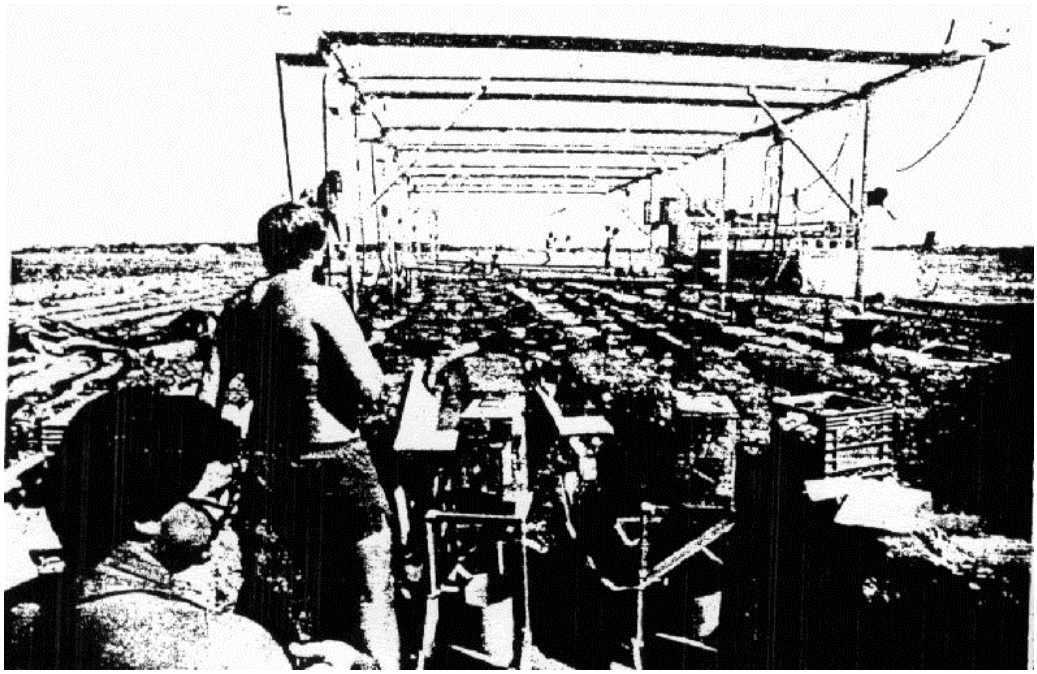

Figure 2-7. A programmable rainfall simulator (after Meyer, 1988).

Miller (1987) introduced a portable, variable-intensity, low-cost, and nozzle-typed rainfall simulator. This simulator could be used both in small pan runoff-erosion studies and field studies. Electrically operated solenoid valves control intensity. The opening and closing of the solenoid valves, controlled by a rotating cam or microcomputer, varies the intensity of rainfall from approximately 1.44 to 86.4 mm/h, at 29 kPa water pressure. Kinetic energy of the rainfall is within the range for natural rainfall. The problem of varying intensity was addressed by oscillating the nozzles, diverting part of the spray from the plot, or injecting air into the water stream.

2.2.3 Limitations of Rainfall Simulators

There are two major limitations for hanging yarn and tubing tip type rainfall simulators. First of all, these two types of rainfall simulators cannot simulate the terminal velocities of natural raindrops close enough because of the height limitation of the simulator. For example, to attain at least 95% of the terminal velocity, the height from simulator to soil surface should be set at 5.0 m for a 2 mm diameter drop, and about 7.8 m for a 4 mm diameter drop. Secondly, only one or a very limited range of drop sizes could be formed in one configuration of these categories of rainfall simulators. Therefore, as suggested by Meyer (1988), these types of rainfall simulators are used mostly for fundamental studies when a carefully controlled drop size is important or for the detailed studies of particular rainfall characteristics.

Several problems have been addressed when using nozzles to simulate rainfall. First of all, numerous nozzles give a drop-size distribution similar to rain, but the median drop size is too small. In natural rainfall, median drop size increases with increasing rainfall intensity. In a network of nozzles, an increase in working pressure increases the average intensity but decreases the drop sizes (Hall, 1970). Secondly, nozzle type rainfall simulators have energy characteristics similar to natural rainfall, but apply water at a very high rate. To achieve low rainfall intensities, nozzles should be moved back and forth, turned around a center horizontally or switched off-and-on periodically. Therefore, low intensities are made up of high-intensity periods and zero-intensity periods, which would allow infiltration capacity to partly recover. Because nozzles are more likely to duplicate

the drop distribution of rainfall, they are best suited for large plot erosion studies (Mutchler and Hermsmeier, 1965).

Meyer (1988) suggested that the goal of rainfall simulator research is to collect accurate and useful data, not optimize a simulator. Generally, one square meter and smaller plots may be sufficient for studying raindrop impact (interrill) erosion. The rainfall simulators used for such kind of rainfall simulation should be capable of achieving fairly uniform, continuous rainfall intensity application over the study area. The simulators should also be capable of applying almost vertical impacts for most raindrops, and applying repeatable simulated rainstorms.

2.3 SOIL EROSION PREDICTION METHODS.

Soil erosion has been studied for more than 60 years. Many empirical and theoretical formulas have been developed to predict or estimate soil erosion. Although many researchers have pointed out the limitations they inherited, USLE and its modifications are still the most important soil erosion prediction tools ever been developed for soil erosion prediction.

2.3.1 Soil Erosion Prediction Methods prior to USLE

Zingg (1940) first began to use empirical equations to estimate soil erosion by water. He recommended an equation as

$$A = CS^{1.4} L^{0.6}, \qquad \text{Eq. [2-12]}$$

where

A = average soil loss per unit area from a land slope of unit width (lb/ft^2),
C = a constant of variation,
S = degree of land slope (%),
L = horizontal length of land slope (ft).

By 1956, more than 7500 plot-years and 500 watershed-years of erosion research data were compiled from 21 states. Starting in 1957, Smith and Wischmeier published a series of empirical equations about soil erosion based on these data, ultimately publishing the Universal Soil Loss Equation.

Smith and Wischmeier (1957) indicated that the principal factors in addition to rainfall that could also affect the soil erosion are the slope, length of slope, cover or cropping system, soil and the management. An empirical equation for estimating field soil loss is as follows (which was the best approach then available)

$$A = C \cdot S \cdot L \cdot K \cdot P \cdot M, \qquad \text{Eq. [2-13]}$$

where

A = average annual field soil loss (ton/acre),
C = average annual plot soil loss (ton/acre) for a selected rotation with farming up and down slope,
S and L = relative factors for percent (S) and length (L) of slope adjusted to give unity loss on a three per cent slope 90 ft long,
K = soil factor whose values must be relative to a unity value for the soil of the plots from which C values are secured,
P = factor for conservation practices in relation to a unity value for up-and-down-hill farming,
M = management factor.

Wischmeier and Smith (1958) combined raindrop diameter and velocity data to determine the kinetic energy of rainfall. They suggested

$$E = 916 + 331 \log_{10} I, \qquad \text{Eq. [2-14]}$$

where

E = kinetic energy (ft-ton/acre-in),
I = rainfall intensity (in/h).

Multiplication of E by total amount of rainfall (inches) gives total kinetic energy. Also, they found that, EI_{30}, the product of kinetic energy (E) and the maximum 30 minute intensity (I_{30}), was the best single rainfall parameter for prediction of soil loss.

Wischmeier et al. (1958) proposed another equation for estimating soil loss,

$$Y_c = b_0 + b_1 X_e + b_2 X_i + b_3 X_p + b_4 X_c, \qquad \text{Eq. [2-15]}$$

where

Y_c = computed soil loss (ton/acre),
X_e = energy of the rain (ft-ton/acre),
X_i = X_e times maximum 30-min. intensity (in/h), actually equals to EI_{30},
X_p = antecedent precipitation index,
X_c = accumulated rainfall energy since last tillage of the soil.
b_0, b_1, b_2, b_3, and b_4 = regression coefficients.

Although they mentioned that this equation was more accurate than the equations they proposed before, this equation disappeared in the later papers.

2.3.2 Universal Soil Loss Equation (USLE)

The most widely used method of predicting soil erosion is the Universal Soil Loss Equation (USLE). In 1965, Agriculture Handbook 282 was published, which served as the main reference manual for USLE until it was revised in 1978 as Agriculture Handbook 537 (Wischmeier and Smith, 1978). The USLE was derived from statistical analysis of 10,000 plot-years of natural runoff plots data and the equivalent of 1000 to 2000 plot-years of rainfall simulators' data. The authors emphasized that the USLE is an erosion model designed to predict the longtime average soil losses from sheet and rill erosion, and from specific field areas in specified cropping and management systems. Many variables and interactions influence sheet and rill erosion. The USLE groups these variables under six major erosion factors, the product of which, for a particular set of conditions, represents the average annual soil loss (Wischmeier, 1976). The USLE (Wischmeier and Smith, 1978) is expressed as

$$A = R \cdot K \cdot L \cdot S \cdot C \cdot P, \qquad \text{Eq. [2-16]}$$

where

A = the estimated soil loss (ton/acre-year),
R = the rainfall and runoff factor (hundreds of ft-ton-in/acre-year),
K = the soil erodibility factor (ton-acre-h/hundreds of acre-ft-ton-in),
L = the slope length factor,
S = the slope steepness factor,
C = the cover and management factor,
P = the supporting practice factor.

The rainfall and runoff factor, R. The local value of rainfall erosion index generally equals R for the soil loss equation and may be obtained directly from the Isoerodent Map

from Wischmeier and Smith (1978). The rainfall erosion index for a particular locality is the average annual total of the storm EI_{30} values in that locality, which is

$$R = EI_{30} = (9.16 + 3.31 \lg I) I_{30}, \qquad \text{Eq. [2-17]}$$

where

I = rainfall intensity (in/h),
I_{30} = maximum 30-min intensity (in/h).

Rain showers of less than 1/2 inch and separated from other rain periods by more than 6 hours were omitted from the erosion index computations. A limit of 3 in/h is imposed on I because the median raindrop size does not continue to increase when intensities exceed 3 in/h.

The soil erodibility factor, K. K is a quantitative value determined experimentally. Experiments should be carried under the "standard condition", which is a 22.13 m (72.6 ft) long unit plot with a uniform length-wise slope of 9%. The plot should be in continuous fallow, tilled up and down the slope, free of vegetation for more than 2 years. Soil loss data from plots that meet all the specified conditions except the 9% slope should be adjusted to this standard by S. Actually, measuring K value is very tedious and costly, so that a nomograph method has been developed. To use the nomograph method to find K value of a certain soil, soil textural data such as, particle size distribution, organic matter concentration, soil structure, and permeability, are required. K value could be found after those data had been plotted to the nomograph shown in Figure 2-8. However, Wischmeier (1977) pointed out that soil erodibility is the inherent susceptibility of a particular soil to erosion and therefore is site-specific.

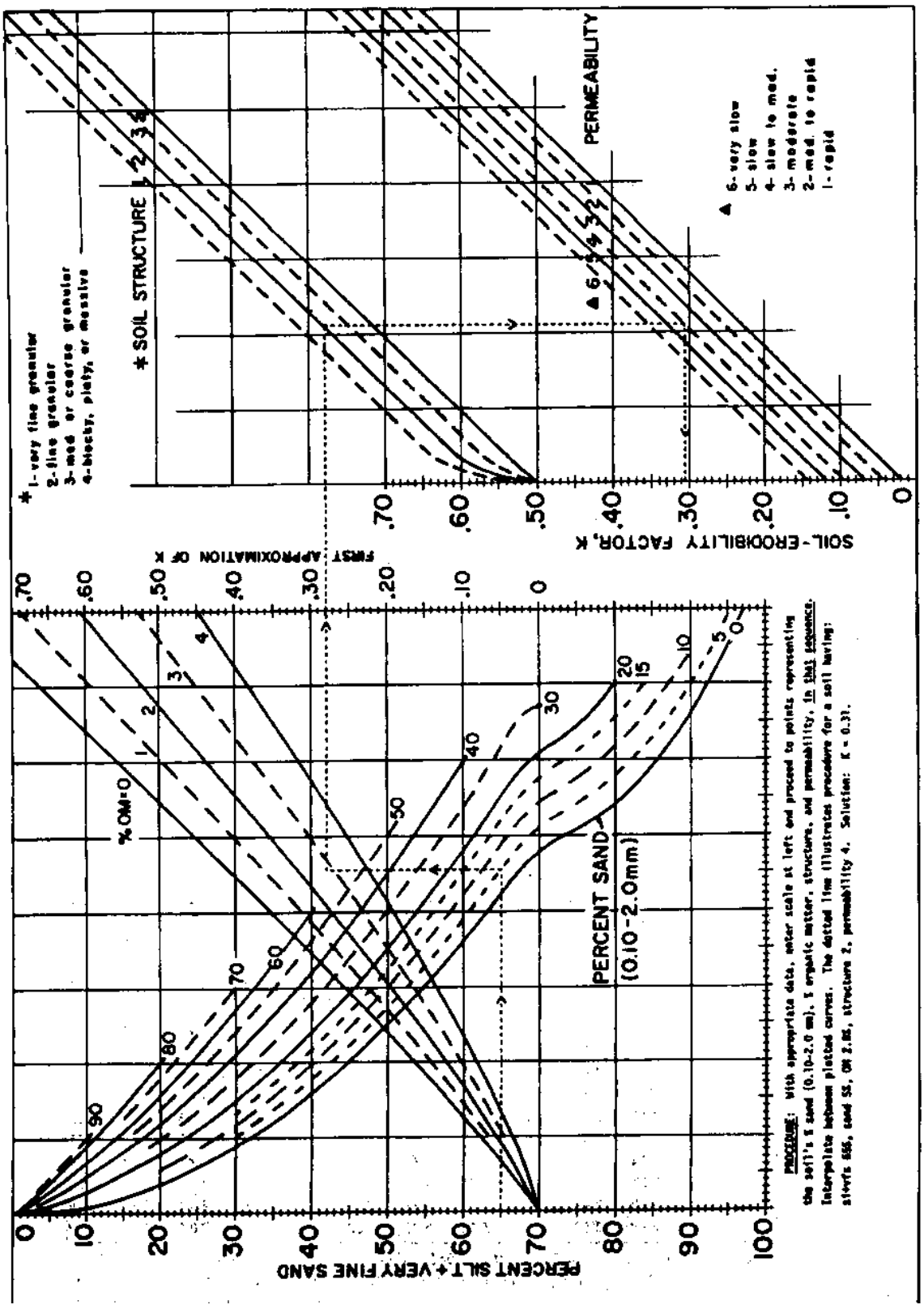

Figure 2-8. The soil-erodibility nomograph of Wischmeier and Smith (1978).

The topographic factor, L and S. LS is the expected ratio of soil loss per unit area from a field slope to that from a 72.6 ft length of uniform 9% slope under otherwise identical conditions. The numerical values could be obtained directly from the slope effect chart or data table from Wischmeier and Smith (1978). The calculation equation of LS is

$$L = (\lambda / 72.6)^m, \qquad \text{Eq. [2-18]}$$

where

λ = slope length (ft),
m = 0.5 if slope is >5%, 0.4 on slopes of 3.5-4.5%, 0.3 on slopes of 1-3% and 0.2 on uniform slope <1%.

Then $S = 65.41\sin^2\theta + 4.56\sin\theta + 0.065$, Eq. [2-19]

where

θ = angle of slope.

Cover and management factor, C. C is the ratio of soil loss from land cropped under specified conditions to the corresponding loss from clean-tilled, continuous fallow. For construction areas, the site preparations that remove all vegetation and also the root zone of the soil not only leave the surface completely without protection but also remove the residual effects of prior vegetation. Therefore, this condition is comparable to the previously defined continuous fallow condition, i.e., C equals to 1.0.

Support practice factor, P. P is the ratio of soil loss with a specific support practice to the corresponding loss with up-and-down-slope culture. For construction sites, P equals to 1.0.

2.3.3 Limitations of USLE

Generally, the USLE applies only to sheet, rill, and inter-rill erosion; i.e., it cannot be used to predict gully or stream bed erosion. It applies only to large areas of loose, bare soil, exposed for 2 or more years. Also, the USLE uses a yearly rainfall erosion index and yearly distribution curves based on long-term averages. The USLE is designed to predict long term average annual soil loss, and would produce misleading soil loss values if it is applied to a seasonal or single storm situation (Wischmeier 1976).

Loch (1984) suggested that the nomograph method for estimating K factor is only valid for certain ranges of soil properties. It cannot be used with confidence for soils which have higher clay contents and more active clay minerals than the soils for which nomographs are available.

McCool et al. (1989) indicated that the USLE limits the shortest slope length to which the USLE can be applied. When the USLE is used for slope lengths shorter than 4 m, a value of 4 m is recommended for slope length. Therefore, the USLE is therefore not appropriate for short slopes. Weggel and Rustom (1992) stated that the USLE overestimates soil losses when applied to areas other than large areas of loose farm soil. It gives soil loss rates that are too large when applied to construction sites, highway embankments and small drainage basins. It is not applicable to steep slopes, small areas, and plots that with mixed soil types.

Singer and Blackard (1982) pointed out that the equation of slope steepness factor, i.e., Eq. [2-19] is not validated for slopes higher than 18%. Wischmeier and Smith (1978) indicated that the best estimate range for S and L factors of USLE is 3-18% in slope steepness and 30-300 ft in slope length. Mutchler and Murphree (1985) indicated that the USLE greatly over-predicted soil loss on the flatter slopes.

Researchers also tried to find other correlations between the characteristics of rainfall, runoff, soil, and soil erosion. Haji, et al. (1988) pointed out that, the universal soil loss equation involved so many variables that it was virtually impossible to adopt for estimating the magnitude of erosion. In spite of enormous efforts, no simple criteria could be adopted which can give a real insight into the process of erosion and which can be adopted for solving practical problems.

Kamalu (1992) reported that the runoff erosion rate becomes dominant on longer land (>2 m) or steeper slopes(9% or above), and becomes the least erosive form on gentle slopes. The interactive combination of rainfall and runoff was dominant over other erosive forms on intermediate slopes (5-7%). He concluded that the runoff is the most important contributor to road shoulder erosion. Huang and Bradford (1993) suggested that the effects of slope steepness on sediment loss rate depended on runoff intensity and vice versa after conducting an empirical analysis of slope and runoff factors for soil erosion. Therefore, it is really impossible to derive universal type, slope independent, and runoff adjustable factors to predict soil erosion. Le Bissonnais, et al. (1992) reported that drying of soil reduces runoff and sediment concentration. The reduction was most

effective with dry soils high in organic carbon content and with the dried then rewetted soils high in clay content. Thus, at least under controlled conditions, initial moisture greatly influences detachment and transport of soil particles and therefore interrill erosion.

2.3.4 Modifications of the USLE

The USLE provided the first tool for systematic soil erosion prediction and became widely used and discussed. Many modifications were suggested by subsequent research. The most important among all these modifications are the Modified Universal Soil Loss Equation (MUSLE) and the Revised Universal Soil Loss Equation (RUSLE).

Williams (1975) suggested the MUSLE for predicting sediment yield for individual storms. Compared with the USLE, MUSLE replaced the rainfall energy factor of the USLE with a runoff factor. The reason for this modification was because runoff factor proved superior to rainfall for predicting sediment concentrations, and runoff is more highly correlated to sediment loss than is rainfall (Williams, 1975). The equation of MUSLE is

$$S = 95(Q \cdot q_p)^{0.56} \cdot K \cdot LS \cdot C \cdot P\,, \qquad \text{Eq. [2-20]}$$

where

S = sediment yield in tons,
Q = volume of runoff in acre-feet,
q_p = peak flow rate in ft^3/sec,
All the other parameters are same as that of USLE.

The MUSLE contains a built-in delivery ratio. It uses volume of runoff and peak flow rate and should better account for watershed conditions, such as antecedent soil moisture, because runoff tends to integrate all of the factors. A data-based comparison of the USLE and MUSLE was conducted by Cooley and Williams (1985). The results indicated that the USLE predictions would be higher than the MUSLE predictions when equal values of K, LS, P, and C are used.

Farmer and Fletcher (1977) modified the USLE and suggested to use their equation in the erosion control practice in highway construction activities. The equation is

$$A = R \cdot K \cdot LS \cdot VM \,, \qquad \text{Eq. [2-21]}$$

where

A, R, K, LS are the same as that of USLE,
VM = erosion control factor.

The only difference between USLE and the modified USLE is that the C and P factors of USLE, which related specifically to agricultural lands were replaced by an erosion control factor, VM. The VM factor is applied as a single unit and accounts for the effects of all erosion control measures that may be applied on any given site. Since this method had been adapted by the Texas Department of Transportation, VM factor had been calculated based on various erosion control practices. The values of the VM factor for Texas can be found in the following table from Vose and Smith (1993).

Table 2-3. Erosion Control Factors (VM) for various practices (after Vose and Smith 1993)

Vegetative Management Practice	VM Value
Bare Soil - freshly disked to 6-8 inches	1.00
Bare Soil - after rain	0.89
Compacted Fill	1.24-1.71
Undisturbed soil - except for scraped	0.66-1.30
Soil Retention Blankets	0.015
Mulching (depends on application rate)	0.01-0.05
Hydromulch	0.05-0.10
Asphalt emulsion (depends on application rate)	0.01-0.57
Sediment Control Fence	0.25
Hay Bale	0.33
Triangular Sediment Dike	0.25
Inlet Protection	0.25-0.33
Sediment Trap - Stone Outlet	0.15 - 0.30
Sediment Basin	0.10
Sandbag Berm	0.30
Rock Filter Dam	0.30

Mutchler and Murphree Jr. (1985) reported their USLE modification in metric units and for soil slope steepness less than 3% as

$$A = RR_cKK_cLSC_1C_2C_3C_4C_5P, \qquad \text{Eq. [2-22]}$$

where

A = the estimated soil loss, in ton/ha.,
R = the rainfall erosion index, the average annual accumulation of specified storm EI,
R_c = the correction factor to reduce the USLE erosion prediction on low slopes,
K = a constant used with variable soil erodibility included in the average annual and cropstage C factor,
K_c = used to represent variable soil erodibility when the C subfactors are used,
L = the slope length factor, the same as L in the USLE except in metric system,
S = slope steepness factor, the same as S in the USLE,
C_1 = the land use residual,
C_2 = the incorporated residue,
C_3 = the tillage intensity and recency,
C_4 = the macro-roughness,
C_5 = the cover-canopy effects,
P = the erosion control practices.

McCool et al. (1987) recommended two equations to be used in the USLE for more reasonably soil loss estimation on slope steepness less than 9% and equal to or greater than 9%. The equations are:

slope steepness < 9%, $S = 10.8 \sin\theta + 0.03$, Eq. [2-23]

slope steepness ≥ 9%, $S = 16.8 \sin\theta - 0.50$, Eq. [2-24]

where

S = USLE slope steepness factor,
θ = angle of slope having a steepness of s expressed in percent.

McCool et al. (1987) also recommended a slope factor equation for short slopes (length ≤ 4 m) where all of the erosion is caused by raindrop impact and runoff freely discharges from the end of the slope, is

$$S = 3.0(\sin\theta)^{0.8} + 0.56 .$$ Eq. [2-25]

2.3.5 Revised Universal Soil Loss Equation (RUSLE)

In 1987, ARS, SCS, and several cooperators began a project to revise the USLE and its documentation. Renard et al. (1991) and Renard et al. (1994) introduced the Revised universal soil loss equation, the RUSLE. The RUSLE uses the same fundamental structure of USLE to link those thousands of plot-years of data under both natural and simulated rainfalls that derived the USLE, and the factors of RUSLE have been broken down further to allow better definition and more accuracy of prediction. The equation is as

$$A = R \cdot K \cdot LS \cdot C \cdot P ,$$ Eq. [2-26]

where

A = the estimated soil loss (ton/acre-year),
R = the rainfall and runoff factor (hundreds of ft-tonf-in/acre-yr),
K = the soil erodibility factor (ton-acre-h/hundreds of acre-ft-tonf-in),
L = the slope length factor,
S = the slope steepness factor,
C = the cover and management factor,
P = the supporting practice factor.

Table 2-4 from Renard et al. (1994) summarized the difference between the USLE and RUSLE. Briefly, RUSLE made additions and revisions that include:

1) Computerization of calculation algorithms.
2) New R values for western US.
3) Revisions and additions of R values for eastern US.
4) Seasonally variable K factors.
5) A subfactor approach for C factor calculation.
6) LS algorithms for varying shape.
7) New P values for different conditions, for example, rangelands, stripcrop rotations, contour factor values and subsurface drainage.

Both the USLE and RUSLE models are fundamentally statistical in nature. They are essentially statistical descriptions of several thousand plot-years of natural rainfall/runoff data collected on uniform slopes managed under common agricultural practices. Renard et al. (1997) described the RUSLE method in detail. Numerous new research results of soil erosion, detailed calculation procedure and computer program menu are included.

Table 2-4. Differences between the USLE and RUSLE (after Renard et al. 1994).

Factor	USLE	RUSLE
R	Based on long-term average rainfall conditions for specific geographic areas in the US.	Generally the same as USLE in the Eastern US Values for Western States (Montana to New Mexico and west) are based on data from more weather stations and thus are more precise for any given location. RUSLE computes a correction to R to reflect the effect of raindrop impact for flat slopes striking water ponded on the surface.
K	Based on soil texture, organic-matter content, permeability, and other factors inherent to soil type.	Same as USLE but adjusted to account for seasonal changes such as freezing and thawing, soil moisture, and soil consolidation.
LS	Based on length and steepness of slope, regardless of land use.	Refines USLE by assigning new equations based on the ratio of rill to interrill erosion, and accommodates complex slopes.
C	Based on cropping sequence, surface residue, surface roughness, and canopy cover, which are weighted by the percentage of erosive rainfall during the six crop stages. Lumps these factors into a table of soil loss ratios, by crop and tillage scheme.	Uses these subfactors: prior land use, canopy cover, surface cover, surface roughness, and soil moisture. Refines USLE by dividing each year in the rotation into 15-day intervals, calculating the soil loss ratio for each period. Recalculates a new soil loss ratio every time a tillage operation changes one of the subfactors. RUSLE provides improved estimates of soil loss changes as they occur throughout the year, especially relating to surface and near-surface residue and the effects of climate on residue decomposition.
P	Based on installation of practices that slow runoff and thus reduce soil movement. P factor values change according to slope ranges with some distinction for various ridge heights.	P factor values are based on hydrologic soil groups, slope, row grade, ridge height, and the 10-year single storm erosion index value. RUSLE computes the effect of stripcropping based on the transport capacity of flow in dense strips relative to the amount of sediment reaching the strip. The P factor for conservation planning considers the amount and location of deposition.

USDA-NRCS (1996) announced that the Natural Resources Conservation Service (NRCS) utilizes factors from equations of the USLE, the RUSLE, and the wind erosion equation (WEQ) to predict soil erosion due to water and wind. The EPA (1998) proposed to use the RUSLE and its factors as evaluation tools to approve discharge waivers, which could be obtained by construction site owners. Under different circumstances, three

kinds of discharge waiver could be granted. The first waiver would be based on "low predicted rainfall potential". The permitting authority would determine which times of year, if any, the waiver opportunity would be available for construction sites based on the table of R values published in the Renard et al. (1997). The second waiver would be based on "low predicted soil loss". The permittee would apply the RUSLE to determine whether or not this waiver would be available. The third waiver would be based on a consideration of ambient water quality. Therefore, the RUSLE is a de-facto official tool to estimate the soil erosion.

In terms of construction activities, no significant improvement was achieved in the RUSLE because it is still a tool designed for agricultural usage. Some limitations discussed in Section 2.3.3 still apply to the RUSLE. No improvement has been achieved in the RUSLE about the prediction of soil erosion occurring in seasonal and single rainstorm events, which is the most typical situation for many construction activities. There are improvements of calculation methods of the K factor. However, the calculation is still largely based on soil texture, organic matter content and permeability, which could be changed dramatically by construction activities. The RUSLE is still using the same method as the USLE for the erosion estimation on very low slope, therefore, the RUSLE will over-predict soil loss on the flat slopes.

2.3.6 Water Erosion Prediction Project (WEPP)

Nearing et al. (1990) claimed that the trend in erosion prediction technology in the USA, Australia, and Europe is toward the development of process-based simulation models. The emphasis in erosion research on strictly empirically based models, such as the USLE is declining. The WEPP consists of process-based soil erosion models. Also according to Nearing et al. (1990), the WEPP is now producing a new generation of soil-erosion prediction technology based on fundamentals of hydrologic and erosion science. The WEPP is being developed by the USDA aimed at replacing the USLE. It is going to be delivered in three versions: profile, watershed, and grid, with the profile version being the direct replacement of the USLE. However, no official WEPP model, documentation or computer program had been delivered yet.

Nearing et al. (1989) present the erosion model used in the WEPP technology. The steady state sediment continuity equation is shown as

$$\frac{dG}{dx} = D_r + D_i, \qquad \text{Eq. [2-26]}$$

where

x = distance downslope (m),
G = sediment load (kg/s-m),
D_i = interrill erosion rate (kg/s-m^2), which could be calculated from Eq. [2-5],
D_r = rill erosion rate (kg/s-m^2).

If sediment load, G, is smaller than sediment transport capacity, T_c, rill erosion rate could be calculated from Eq. [2-11], otherwise, rill erosion rate should be computed as:

$$D_r = (\frac{V_f}{q})(T_c - G)\,, \qquad \text{Eq. [2-27]}$$

where

V_f = effective fall velocity for the sediment (m/s),
q = flow discharge per unit width (m^2/s),
T_c = sediment transport capacity in the rill (kg/s-m).

The sediment transport capacity in the rill is calculated as

$$T_c = k_t \tau_f^{3/2}\,, \qquad \text{Eq. [2-28]}$$

where

k_t = a transport coefficient,
τ_f = hydraulic shear acting on the soil.

Three hydrologic variables required to drive the erosion model in the hydrology component of the WEPP are peak runoff rate, effective runoff duration and effective rainfall intensity. The calculation method is

$$t_r = V_t / P_r\,, \qquad \text{Eq. [2-28]}$$

where

t_r = effective runoff duration (s),
V_t = total runoff volume for the rainfall event (m^3),
P_r = peak runoff rate (m/s).

$$I_e = [(\int I^2 dt) / t_e]^{0.5}\,, \qquad \text{Eq. [2-29]}$$

where

I_e = effective rainfall intensity (mm/s),
I = rainfall intensity (mm/s),
t = time (s),
t_e = total time during which the rainfall rate exceeds infiltration rate (s).

The erosion computations are made by solving non-dimensional equations and then redimensionalizing the final solution. Several normalization parameters, such as rill and interrill detachment parameter, deposition parameter, and normalized erosion equations are also introduced in Nearing et al. (1989). Also, the WEPP can calculate soil loss for cases involving downslope variability such as surface roughness, cover, and canopy differences, soil type, and surface runoff rates. The WEPP does this by dividing the hillslope into homogeneous strips and treating each strip as an independent hillslope with added inflow of water and sediment equal to that coming from the upslope strip.

Zhang et al. (1996) evaluated the WEPP runoff and soil loss predictions using natural runoff plot data. They found that by using the WEPP, average runoff and soil loss rates for different cropping and management systems were adequately predicted. The accuracy and reliability of the predictions were shown best on average annual basis, less on annual basis, and worst for individual events. Because of high variations of soil loss rates, the WEPP did not predict event soil loss as well as it predicted event runoff. The WEPP model is considered a useful tool for predicting runoff and soil loss rates under cropped conditions, and it is more reliable in predicting longer term averages. However, the model tended to overpredict soil loss for the years with lower soil loss rates, and underpredict soil loss for the years with higher soil loss rates.

2.4 SOIL EROSION PREDICTION USED IN HIGHWAY CONSTRUCTION ACTIVITIES

Currently, the USLE and its modifications are the most widely used methods in soil loss estimation from the construction sites during rainfall events. Wischmeier and Smith (1978) announced that USLE could also be used as erosion prediction tool at construction activities, however, serious problems exist.

First of all, the USLE was designed to predict long term average annual soil loss from agricultural lands. The short time period during which the soil is exposed by construction activities makes it likely that the bare soil will experience lower net rainfall. Therefore, misleading soil erosion values might result if the USLE is applied on such kind of seasonal or single storm events.

Secondly, the USLE was developed for agricultural activities, where the setting normally involves relatively long, regular, gentle slopes, large, homogeneous area, and where changes during the season are relatively predictable. From its form, it is necessary to evaluate separately the soil loss for areas having different conditions. Also the number of calculations required for a construction site can be very large, because small areas, different types of soils, and conditions can change not only from pre-construction to post-construction phases, but almost daily.

Thirdly, USLE greatly overpredicts soil loss on the flatter slopes (slope less than 3%). In many highway construction sites, slopes are less than 3%. ULI et al. (1978) discussed the

applicability of USLE in construction sites and suggested that USLE is not reliable and too conservative for estimating general erosion behavior on construction sites, and it may lead to over-design.

Mining engineers have also intensively studied erosion, focusing on the erosion behavior of mining waste piles. The particle sizes in the waste piles are generally much bigger than that of soils because there are a lot of gravel and larger rocks in the waste piles. The slope angle of the sides of piles is higher than that of agricultural land; for example, the side angle of the coal mine waste pile could range from 14% to 33%.

Vipulanandan et al. (1982) conducted erosion research on coal mining waste piles under natural rainfall conditions. They found that a large amount of erosion took place during the first few hundred millimeters of rainfall and the rate of erosion decreased with cumulative rainfall. No apparent correlation was found between the amount of erosion and the slope angle. Erosion quantities predicted by USLE differ substantially from the measured quantities. The reason was that the USLE was developed for the application on agricultural lands. Because erosion is a consequence of the complex interaction of many factors, it is very difficult to generalize this phenomenon in a quantitative manner by means of a theoretical approach. An empirical model was developed as

$$\frac{100 \cdot Q}{\alpha \cdot \log(E/A)} = n \cdot Q + 4845 \cdot \alpha^{-1.83} + 365 \cdot \exp(-Q/132), \qquad \text{Eq. [2-30]}$$

where

Q = the cumulative rainfall (mm),
α = slope (%),
E = total erosion (g),

A = slope area (m^2),
n = slope of an empirical line (degree), which could be found by applying the regression method.

The model agreed fairly well with field results and took into account the time-dependent nature of the erosion process.

Montoya and Brown (1984) investigated the erodibility of strip-mine spoils. The spoil inclinations used were 2, 9, and 18%. The K factor was determined experimentally and also calculated by using the properties of spoils. The research indicated that K values estimated from the physical properties of mine spoil were larger than those experimentally determined. The adjusted K values for mine spoils could be used in the USLE to calculate the spoil erosion. The erodibility factor of mine spoil (K_m) could be calculated as

$$K_m = 0.339 K_w^{0.48}, \qquad \text{Eq. [2-31]}$$

where K_w is the erodibility factor estimated from the physical properties of the spoil using the equation from Wishmeier and Smith (1978).

Schroeder (1987) conducted an erosion research on reshaped spoil areas of surface mines, and found that spoil loss increased linearly with increasing slope gradient at both crusted and freshly respread spoil pile surfaces. In this research, the slope gradients ranged from 0.1 to 11.1% and slope length was 4.9 m. Also, the research found that the USLE underestimated the slope gradient effect on spoil loss for slopes < 9% and overestimated at slopes > 9%.

CHAPTER 3

EXPERIMENTAL METHODS AND MATERIALS

One part of this dissertation is to develop an empirical equation based on measurable soil and rainfall properties. The approach involves data acquisition, such as experimental measurement of rainfall properties, soil properties and soil erosion volumes, evaluation of the significance of different variables, and empirical equation development.

3.1 SELECTION OF SOILS

Both artificial soils and real soils have been used in prior soil erosion research. Those soils include pure sand, clays, and agricultural soils from most of the states in the US. To develop a plausible empirical soil erosion equation, we selected three artificial soils and three real soils. Table 3-1 shows the textural analysis results and the classification of these soils based on the USDA standard.

Table 3-1. Soil Texture Analysis and Classification (USDA Standard)

Soil	Gravel >2 mm	Sand 2 mm<s<50 um	Silt 50 um<s<2 um	Clay <2 um	USDA Classification
Soil 1	0.0%	100.0%	0.0%	0.0%	Sand
Soil 2	0.0%	19.9%	13.4%	66.7%	Clay
Soil 3	0.0%	82.3%	3.0%	14.7%	Sandy loam
Soil 4	7.4%	19.1%	40.6%	32.9%	Clay loam with gravel
Soil 5	1.2%	57.6%	23.4%	17.8%	Sandy loam
Soil 6	17.6%	48.2%	22.2%	12.0%	Gravelly sandy loam

Washed sand, clay, and a sand-clay mixture were used as artificial soils. Soil 1 is commercial 20-40 sieve (0.85-0.425 mm) washed, quartz sand. The reason for choosing

sand is because it is a non-cohesive soil, and should be easily eroded. It represents one end of a soil textural spectrum.

Soil 2 is pure bentonite, used for making drilling mud. It is a very fine powder (when dried) and can swell to 400% to its original volume when saturated with water. This soil is used to represent very fine textured clay soil. Soil 3 is a mixture of sand and bentonite clay, with 30% volume of bentonite clay and 70% volume of pure sand. It represents on possible mixture of these two ideal soils. Three artificial soils were selected to study the impact of different soil properties because washed sand was considered a non-cohesive soil and bentonite was considered a cohesive soil.

Real soils are also used in this research. Three different kinds of soils from three different locations were collected. Soil 4 is a clay loam with gravel collected from a highway construction site at NASA Road 1 in Houston, Texas. In the soil series, it is a Midland-Urban Land Complex based on Wheeler (1976). Soil 5 is a sandy loam from the National Geotechnical Test Site at the University of Houston at Houston, Texas. It is a Urban-Land in the soil series. Soil 6 is a gravelly sandy loam from highway construction site at the intersection of Highway 59 South and Beltway 8, Houston, Texas. In the soil series, it is a Lake Charles clay. This soil represented about 7.7% of the soils in Harris County, Texas. The real soils were selected from three geographically separate locations as representative of local conditions.

3.2 SOIL TEXTURAL ANALYSIS

Soil texture analysis can help us understand the texture properties of the soil. To compare the research result to other research, we need to analyze and classify the soils. The result of this research is compared with the results from agricultural engineers, and they use the USDA Soil Classification System to classify soils. Therefore, the sieve analysis and hydrometer analysis was chosen as the soil textural analysis methods in this research. The USDA Soil Classification System divide soils into different categories solely based on the soils' particle sizes and use the pure sand, silt and clay as three end elements. By plotting the weight percentages of sand, silt and clay from soil textural analysis data, the name of the soil could be determined from the area where the soil textural point is located in Figure 3-1. For comparison, the USGS soil texture analysis standard and classification are also shown in Table 3-2 and Figure 3-2.

Table 3-2. Soil Texture Analysis and Classification (USGS Standard)

Soil	Gravel >2 mm	Sand 2 mm<s<62.5 um	Silt 62.5 um<s<4 um	Clay <4 um	USGS Classification
Soil 1	0.0%	100.0%	0.0%	0.0%	Sand
Soil 2	0.0%	19.9%	5.8%	74.3%	Clay
Soil 3	0.0%	82.3%	1.3%	16.4%	Sand
Soil 4	7.4%	19.1%	36.6%	36.9%	Silty clay with gravel
Soil 5	1.2%	57.6%	21.5%	19.7%	Silty Sand
Soil 6	17.6%	48.2%	20.6%	13.5%	Gravelly silty sand

The sieve analysis was conducted on all six soils. This type of particle-size analysis is universally used in the engineering classification of soils. The analysis in this research was strictly executed according to the ASTM method D421 and D422. The finest sieve used in the mechanical separation is sieve No. 200, whose opening diameter is 0.075 mm.

Particle sizes smaller than 75 μm (retained in the pan) were analyzed by applying the hydrometer analysis. The hydrometer analysis is also based on the ASTM method D421 and D422. It is a widely used method of obtaining an estimate of the distribution of soil particles from the No. 200 (0.075mm) sieve to around 0.001 mm, and it is usually used together with the sieve analysis. The hydrometer analysis is based on Stokes' Law which gives the relationship among the velocity of fall of spheres in a fluid, the diameter of the sphere, the specific weights of the sphere and of the fluid, and the fluid viscosity.

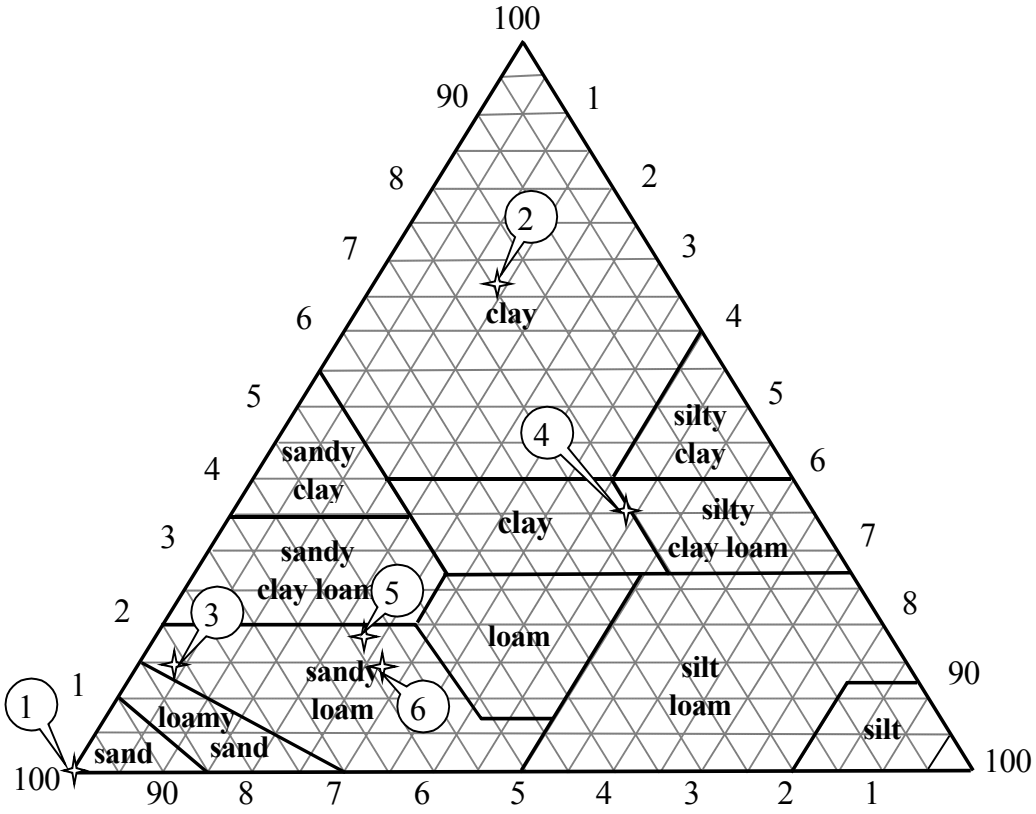

Figure 3-1. Triangular Plot of USDA Soil Classification System.

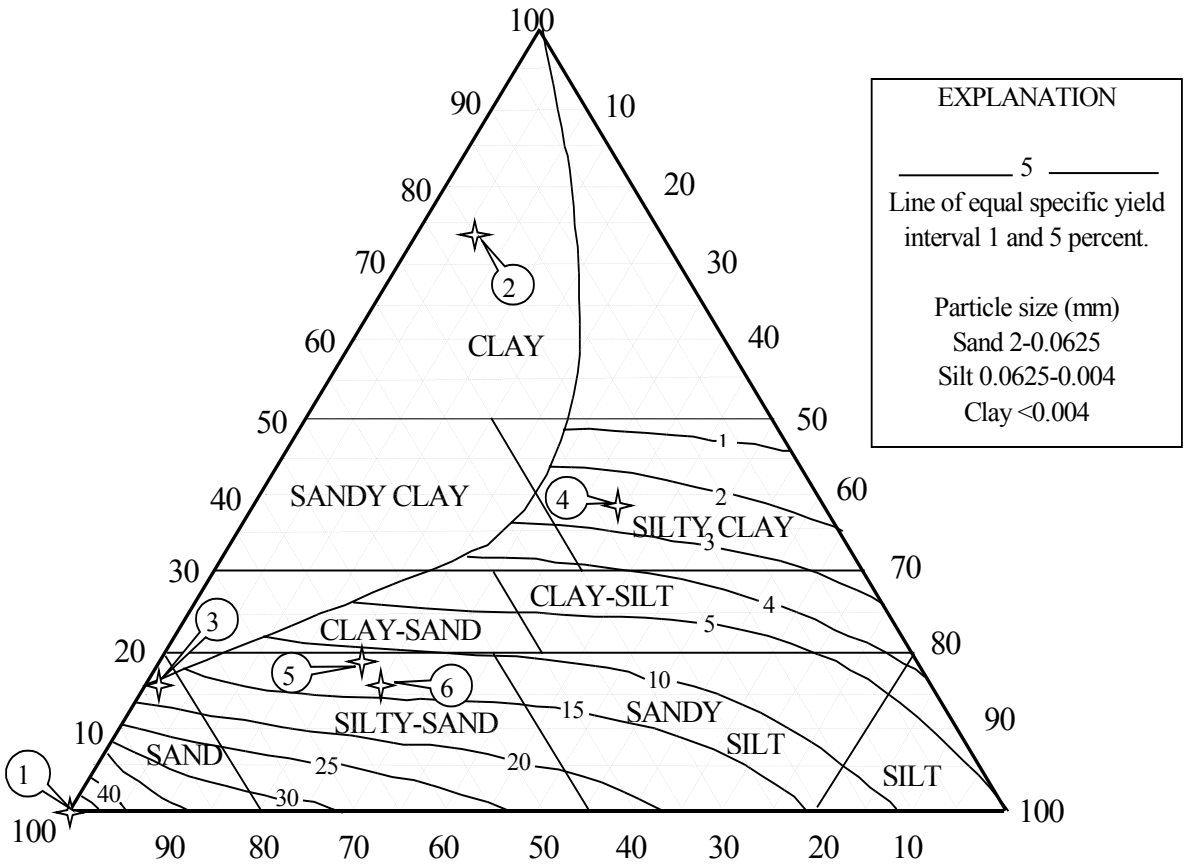

Figure 3-2. Triangular Plot of USGS Soil Classification System.

3.3 SELECTION OF EXPERIMENTAL VARIABLES

3.3.1 Properties of Rainfall

Rainfall intensity and duration are selected as variables in this research because they are the most important characteristics of rainfall in terms of soil erosion. Meyer (1988) pointed out that rainfall intensities between 0.2 and 2 mm/min (12 to 120 mm/h) are usually of the greatest importance in natural rainfalls. Because very low intensities are generally not of major interest for erosion and hydrologic studies, and very high

intensities are so rare, they may be of limited interest. Table 3-3 shows the hourly rainfall intensity data measured in Texas since 1941 (EarthInfo Inc. 1995). More than 95% of the rainfall in Texas in recent 55 years had the intensity less than 12.7 mm/h (0.5 inch/h). About 0.01% of rainfall was heavier than 101.6 mm/h (4 inch/h) in Texas. Therefore, five representative rainfall intensities have been chosen as the experimental variables in this research. The intensities are 12.7, 25.4, 50.8, 76.2 and 102 mm/h (0.5, 1, 2, 3 and 4 inch/hour).

Table 3-3. Measured Rainfall Intensities in Texas

Rainfall Intensity, (inch)	0.01-0.49	0.50-0.99	1.00-1.99	2.00-2.99	3.00-3.99	4-12	Total
No. of Rainfall	1,548,678	58,032	17,456	1,910	387	235	1,626,698
Percentage	95.20	3.57	1.07	0.12	0.02	0.01	100.00

To compare the result of this study with prior research, the rainfall duration used in the experiment was thirty minutes. Wischmeier and Smith (1958) found that EI_{30}, the product of kinetic energy (E) and the maximum 30 minute intensity (I_{30}), was the best single rainfall parameter for prediction of soil loss. The USLE, RUSLE and WEPP all use I_{30} as one of their predictors, thus a 30-minute duration allows some comparison of this research and prior work.

3.3.2 Properties of Soil

Antecedent soil shear strength, antecedent soil compressive strength, soil slope steepness have been chosen as the measured soil variables. All these soil properties and rainfall properties described above are relatively easy to measure in the field.

Soil particle size could be treated as another variable of soil properties, but not in this study. The reason is that there should be a unique correlation between the dependent and the independent variable. More than 30 experiments were conducted on every soil in this research, and each soil has a fixed soil particle size distribution. There is no unique correlation between the erosion amount and the soil particle size and distribution.

Kung (1984) believed that particle size distribution is not important among physical parameters of the soil in terms of erosion. Finkel (1986) pointed out that the amount of soil rolling at the bottom of surface flow increases with the velocity of the stream and decreases with the soil particle size. Chow and Rees (1994) studied the effect of content and size of soil coarse fragments on soil erosion. The minimum diameter of coarse fragment used in their study was 10 mm, and the volume ratio of coarse fragments ranges from 7% to 25%. The runoff and soil loss were found to decrease with increasing size and content of coarse fragments. Bradford and Foster (1996) reported that under transport-limiting conditions, sediment size will influence sediment yield and the splash process seems to be size selective. No soil used in this research has coarse fragment more than 1%. The soil surface is flattened before every experiment and the residue from previous experiment is removed. Thus, soil grain size distribution is expected to remain the same for all experiments for the same soil. Therefore, the soil grain size distribution is not considered a variable in this research.

3.3.2.1 Soil shear strength

Flaxman (1962) pointed out that soils of low strength are easily susceptible to erosion in channel flow whereas those of high strength resist hydraulic stresses of considerable magnitude. Al-Durrah and Bradford (1981) introduced a force-resistance relationship to describe the following relationship between the soil shear stress and the kinetic energy of the raindrop,

$$D = a + b(KE / \tau_f), \qquad \text{Eq. [3-1]}$$

where

D = the amount of soil detached (mg/drop),
KE = raindrop kinetic energy (J),
τ_f = soil shear strength (kPa),
a, b = empirical constants.

Al-Durrah and Bradford (1982a, b) observed that the shape, angle and speed of the raindrop splash are highly correlated with soil shear strength. The amount of soil detached is determined not only by the magnitude of soil deformation that took place in the earlier stages of cavity development, but also by the shear stress of soil resisting the shear stresses of the radial flow acting on the bottom and sides of the cavity.

Luk (1983) suggested that soil shear strength is one of the inherent variables indicate the soil loss. Fan (1987) highlighted that for compacted and fully (or nearly fully) saturated soils, the soil erodibility factor decreases with critical shear stress. McCool, et al. (1987) suggested that shear stress of runoff must exceed a critical shear stress value for the particular soil condition before the flow begins to detach sediment.

Tan (1989b) and Nearing (1991) pointed out that the interaction between shear stress of flow and soil played an important role in the soil erosion caused by overland flow. Wang et al. (1994) revealed that shear strength has an inverse relationship with erodibility of loess soils in terms of interrill and rill erosion processes in the hilly loess region.

Like prior researchers, this dissertation considers the soil shear stress to be an important parameter in terms of soil erosion by water. Researchers suggested that soil shear stress acts as the resisting force to the erosion agent, e.g., the shear stress of raindrop and overland flow for both raindrop detachment and overland flow entrainment. Therefore, we chose soil shear strength as one of our research variables.

The shear strength was chosen as a soil property because it can be measured directly. If a correlation exists then shear strength could be a useful erosion predictor. The K factor from USLE is a value that only depends on the particle size distribution, shape, organic matter concentration and permeability of soil. Although these values can all be measured, they are not direct measurements of a soil's resistance to erosion, and furthermore the measurements are complicated. Soil shear strength on the other hand is easily measured by a cone penetrometer or a vane shear tester.

3.3.2.2 Soil compressive strength

No reported relationship between compressive strength and erosion was found in the literatures reviewed. Soil compressive strength has not been considered as a factor that

affects the soil erosion. However, soil compaction by rollers is frequently used in construction sites as a storm water pollution prevention strategy and for dust control. Compaction is also used in construction to increase the soil compressive strength, thereby increasing the bearing capacity of facilities constructed over them. In this research, the compressive strength was chosen as a variable to reflect the practice of roller compaction as a erosion control method. Compressive strength was measured during all the experiments using a penetrometer.

3.3.2.3 Soil slope steepness

Slope steepness is one of the most important variables in the soil erosion estimation. Numerous prior researches had used it as the key parameter in erosion prediction. In the USLE and its derivatives, the S factor is the least modified parameter. The steepness affects the flow velocity as well as the rainfall impact angle and its importance is related to these two detachment agents.

Because this research is focused on soil erosion phenomenon at highway construction site, the slopes of those highways and the sites are the main concern. In highway construction, there are three different slopes. The first one, named the Vertical Alignment (Grade), is the slope steepness along the road. The second one is the longitudinal gradient, which is introduced specifically to achieve longitudinal drainage in the side ditches. The third one is the embankment of the road. In this research, the soil erosion from the embankment of the road is not studied, although it is a significant

contribution to the soil erosion. Our concern is only on vertical alignment and longitudinal gradient.

In terms of the design of the highway, satisfactory drainage is obtained with slope of 0.35-0.3% or even lower (Oglesby, 1982; O'Flaherty, 1986). Much of the terrain in the southern US is very flat, and the vertical alignment of highways in these states could have a very low grade. Therefore, the minimum slope angle of our research is chosen as 0.1%. The highway engineering design guidelines have suggested that grades of up to about 7% have little effect upon the speeds of passenger cars. However, the speeds of commercial vehicles are reduced when long gradients, with grades in excess of about 2%, are features of the highway profile (Sherrard, 1958; Oglesby, 1982 and O'Flaherty, 1986). Therefore, 7% grade can be used in highway design, however, the distance of this grade should be strictly limited. A 2% grade is not considered a problem in the highway profile for all traffic.

A survey was conducted by contacting the Departments of Transportation of various states in southern US. The Departments of Transportation of Arizona, Colorado, Florida, Louisiana and Texas responded. Among these five states, most of them do not correlate their road mileage to the grade. However, according to the design engineers and the highway design guidelines of these states, the highway grade is generally less than 4% except for mountain terrain. In the state of Colorado, the maximum grades for some mountain passes are less than 5%. The Department of Transportation of Florida organized a data-base about centerline miles by grade and functional classification for the

highway performance monitoring system. According to their statistics, 95.6% of their major road have the grade less than 0.4%, and 99.9% of their major roads have grade less than 4.4%. Therefore, the slope steepnesses for soil in this research have been chosen as: 0.1, 0.5, 1.0, 4.0, and 6.0%. These slope steepness values probably represent 99% or more of the highway miles in the southern US. The experimental design selected 0.1% and 0.5% to represent the major low-grade roads. For example, this grade range can represent about 95.6% of the highways in Florida. The 1.0% slope is used to represent the medium grade roads. The 4.0% and 6.0% slopes are selected to represent the high end of road grades. Appendix A is a brief summary of the highway grades survey conducted in several states in southern US.

3.3.2.4 Soil moisture content

Luk and Hamilton (1986) pointed out that measured soil loss is significantly related to antecedent moisture. Measured soil loss may differ by as much as 800 times if the full range of antecedent soil moisture is considered. The influence of antecedent moisture on soil erosion is complex because it involves the interactive effects of factors pertaining to the force of and resistance to erosion. Other researchers also pointed out that the soil shear strength is greatly influenced by moisture content (Le Bissonnais et al. 1992 and Wang et al. 1994). As we know, high shear strength does help soil resist the water erosion.

Soil compaction is the densification of soil by removal of air, which requires mechanical energy. The degree of compaction of a soil is measured in terms of its dry unit weight. The moisture content at which the maximum dry unit weight is attained is generally referred to as the optimum moisture content. In the condition of optimum moisture content, there is no air in the void spaces-that is, when the soil is completely saturated. Maximum compaction can only be achieved when the soil is at the optimum moisture content (Das, B. M., 1994). After the proper compaction, both shear strength and compressive strength increase, and the moisture content approaches to the optimum moisture content. Because we have to study the soil erosion behavior in highway construction sites, it is necessary to choose soil moisture content as a variable in our research.

3.3.3 Properties of Overland Flow

3.3.3.1 Flow velocity

Flow velocity is important in the study of soil erosion. Most researchers measured flow velocity of rills because it is easy (Nearing et al. 1997). Researchers also measured velocity of interrill flow. They generally use fluorescent dye or salt as the indicator of flow velocity. Few researchers measured the flow velocity with the rainfall applying simultaneously because the raindrops will severely affect the flow pattern of both the interrill and rill flow and create turbulence.

In this study the average flow velocity was approximated during rainfall application. In order to minimize the disturbances generated by the raindrops, a dense liquid tracer was selected to be an indicator of water flow. The indicator was made by mixing of Meriam 295 Red Fluid and corn oil in 1:3 volume ratio. The Meriam 295 Red Fluid was chosen because it has dark red color. Its specific gravity is 2.95, so the corn oil was added to adjust the density closer to that of water. The resulting indicator has a bright red color and its specific gravity is 1.39. The indicator drops are held on the water surface because of the effect of water tension force acting on the oil. If there is no raindrop hit directly on the drops of indicator, by measuring the time elapsed while these indicator drops pass a certain distance, the flow velocity could be calculated. If the raindrops hit the drops of indicator directly, the largest droplet remaining on the surface after the hit was traced as if it was the original drop of indicator. Velocities were estimated from several different fixed locations on the soil surface during every soil erosion experiment. The average of these velocities is reported as the mean flow velocity of this experiment.

3.3.3.2 Flow depth

Flow depth is important in calculating various important hydraulic properties. In this study, the flow depth was measured by using a miniature staff gage (small metal ruler). Twenty-five fixed points were selected on the soil surface, and the flow depth of a simulation was taken as the arithmetic mean of these 25 measured values.

3.4 CONFIGURATION OF EXPERIMENTAL EQUIPMENT

The experimental equipment consists of a nozzle-type rainfall simulator, a water flume and water supply and drainage system. Figure 3-3 is a schematic diagram of the configuration of experimental equipment.

3.4.1 Rainfall Simulator

A nozzle-type rainfall simulator was built for the experiments. The rainfall simulator consists of a wooden frame and a group of 1.27cm diameter PVC pipes with small holes of 0.08 cm in diameter drilled upward every 2.54cm. It is suspended from the ceiling of the lab. It covers an area of 0.81 m^2 (94.7 cm x 86.4 cm) and produces simulated rainfall with intensity as high as 250 mm/h. The soil block directly under the rainfall simulator has an area of 0.66 m^2. A 50 Hz shaker is operated to vibrate the simulator during the tests to help ensure a uniformly distributed drop pattern. The water supply is controlled by a valve and monitored by a flowmeter.

The uniformity of the drop pattern was tested and adjusted. Thirty-six, six hundred-milliliter beakers were placed in the flume at the same location of soil block to collect raindrops while different rainfall intensities were applied. The volume of water in those beakers was measured and recorded, and the simulator was repeatedly adjusted until water volumes in each beaker were identical. The flowmeter reading was calibrated directly to rainfall intensity. As shown in Figure 3-4, 39 rainfall simulations were

conducted, and all the values of flowmeter readings and the average rain gauge reading were plotted in the figure. A best-fit regression line was also plotted on this correlation plot of flowmeter reading and rainfall intensity (from rain gauge reading). The best fit equation of this line is a straight line and used as the working curve to convert flowmeter reading to simulated rainfall intensity. By adjusting the valve on the water supply hose, the flowmeter reading could be adjusted, thereby, simulated rainfall could be controlled to the designed intensity.

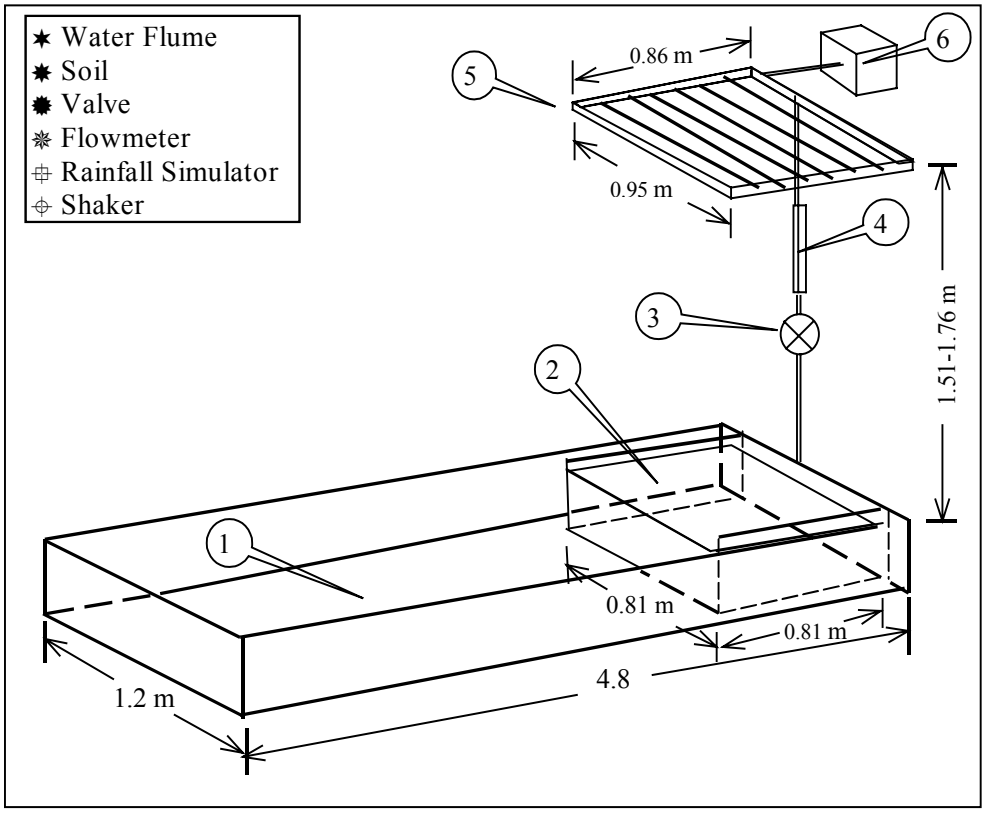

Figure 3-3. Configuration of rainfall simulator

In natural rainfalls, small rain droplets (up to 2mm in diameter) are spherical. As raindrops get larger, they flatten and become shaped like red blood cells. Eventually, they invert and form a parachute shape that causes them to break up into smaller

raindrops (Fraser, 1995 and Learning Kingdom, 1998). The size of natural rainfall drops range from close to zero to about 7 mm in diameter, and the median drop diameter tends to increase with rainfall intensity (Meyer, 1988).

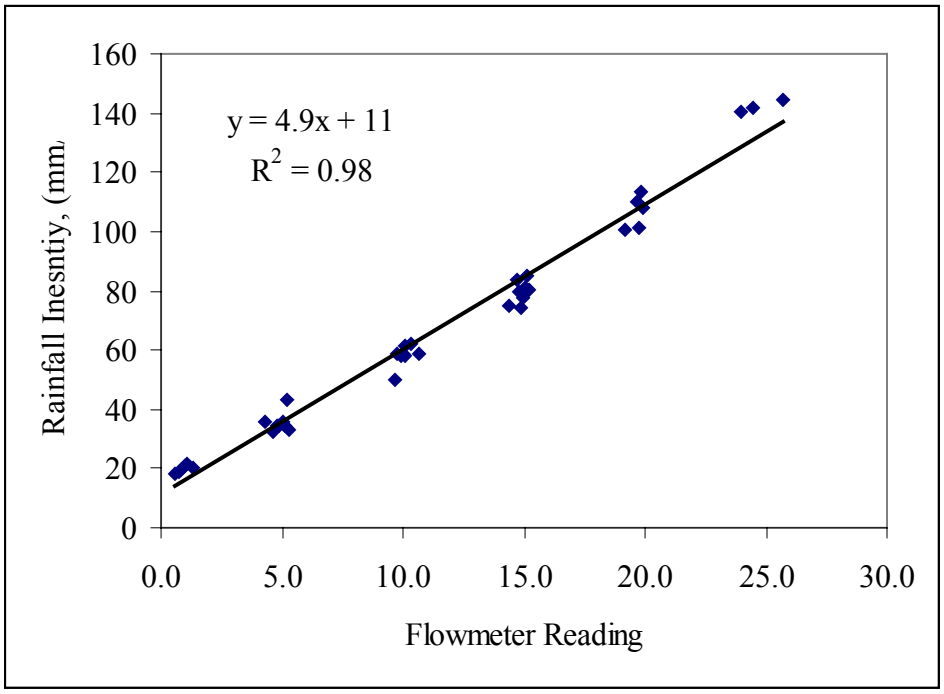

Figure 3-4. Correlation of rainfall intensity and flowmeter reading.

One hundred drops were collected in a graduated jar to estimate the mean raindrop diameter. Assuming spherical drops, the calculated raindrop diameter has a mean value of 6.7 mm, with a standard deviation of 0.5 mm. The mean raindrop diameter was practically invariant over all intensities tested. This result occurs because water flows out of drilled holes, flows downward to the bottom surface of the pipe, then falls down from the pipe surface after overcoming the surface tension force. The raindrop will fall downward only when the gravity force overcomes the surface tension force, therefore, nearly uniform sized raindrops occurred, although the shaker will cause minor accelerations that produce a distribution. The distribution of drops in the present work

was oversized compared to natural rain, but within the range of naturally observed raindrop sizes.

The rainfall simulator was suspended from the ceiling of the lab. The height of the simulator was adjusted to the highest level for increasing the falling velocity of the raindrops. The rainfall simulator was 1.76 m (0.1% slope) to 1.51 m (6% slope) above the soil bed surface, and the average is 1.68 m. To compare the kinetic energy of simulated and natural rainfall, the kinetic energy on one square meter of area and within one second is used in this research. Table 3-3 is a list of calculated energy values for this research. The average velocity of raindrop falling to the soil surface is 5.74 m/s. The kinetic energies of rainfall intensity ranges from 0.2 to 2 mm/min are 0.055 and 0.55 J, respectively. For the natural rainfall at the same intensities, the mean diameters of raindrops are 2.12 and 3.58 mm, respectively (Finkel, 1986). The corresponding terminal velocities are 6.68 and 8.51 m/s, and the kinetic energies are 0.073 and 1.21 J, respectively. Thus, the simulator under-represents the impact forces by 25% at low intensity and by 55% at high rainfall intensity.

Table 3-4. Kinetic energy for simulated rainfall.

Flume Slope	Height of Simulator (m)	Falling Velocity (m/s)	Kinetic Energy for 0.2 mm/min. Rainfall Intensity (J)	Kinetic Energy for 2 mm/min. Rainfall Intensity (J)
0.10%	1.76	5.87	0.058	0.58
0.50%	1.74	5.85	0.057	0.57
1%	1.72	5.81	0.056	0.56
4%	1.60	5.59	0.052	0.52
6%	1.51	5.44	0.049	0.49
Average	**1.68**	**5.74**	**0.055**	**0.55**

3.4.2 Water Flume

A water flume was used to hold the soil and direct the runoff. The flume is 4.8 m long and 1.2 m wide. Soils were carefully put into a smaller square box in the flume, which is 0.66 m^2 (81.3 cm × 81.3 cm) in area. The soil bed was fully covered by the rainfall from the simulator above. The upstream end of flume is mounted on six adjustable supports, allowing the slope of the flume to be adjusted within the range of 0-1.3%. For the higher slopes, a jack has been used to lift up the flume so that the pre-cut supports could be put in to make 4% and 6% stable slopes.

3.5 EXPERIMENTAL PROCEDURE

Soil was first packed loosely in the soil box. For loose packing, the soil was very lightly compacted so that the soil could be evenly distributed in the soil box and the soil surface was trimmed to form a smooth surface. For the compact packing, three layer of soil was put in the soil box separately. After a layer was compacted tightly with a flat surface compaction tool, the next layer was put on top of the previous one and compacted again. The water flume was in the leveling condition while packing the soil and at the beginning of each experiment. Surface of the soil was adjusted to zero slope after the packing and before each experiment. All soils were fully saturated before the experiment so that no swelling would occur during the erosion simulation. There is a possibility that raindrop may compact very loose soil slightly, however, comparing with the compaction executed in this research, the raindrop compaction could be neglected.

The antecedent soil shear strength was measured on the soil surface before the application of rainfall. Nine measurements were conducted for each simulation. The average shear strength value was taken as the shear strength for the simulation. A Torvane^{TM} was used to measure the shear strength. Each reading required only seconds. Following a similar procedure, the antecedent compressive strength of soil was measured by a pocket penetrometer right after the measurement of shear strength. It also took only seconds to get the reading.

After the measurement of the shear strength and compressive strength, a surface soil sample was taken for a moisture content test later in another laboratory. The tests of soil moisture content are conducted according to the ASTM method D2216-90. The soil surface was level again before the flume was adjusted to proper slope. The initial soil level relative to a datum was measured at sixty-four points covering the soil surface. After the flume was adjusted to the designed slope, a selected intensity of rainfall was applied for thirty minutes. Flowmeter readings were taken every three minutes during the test to ensure that the rainfall intensity was applied correctly. If the flowmeter reading was too high or too low, the valve was adjust to maintain the desired flowmeter reading.

Flow depth and velocity were measured after rainfall had been applied for 10 minutes during the experiment. This way, soil surface has been totally wetted and soil had reached equilibrium with rainfall and surface flow in this time. While measuring the velocity, the indicator was injected by syringe at 7 fixed uniformly distributed points perpendicular to the direction of the slope. The distance for indicator to flow through

was 0.50 m. A stopwatch was used to measure the time used by indicator drops to travel through this distance. The arithmetic mean of these 7 values was the flow velocity of that rainfall simulation.

After the simulation, the soil level at each reference point was re-measured. Erosion volume was then determined from the difference of soil level before and after the rainfall event (a cut-and-fill type calculation). The first 222 runs measured only 64 points, which subsequent studies (Section 5.3) show are inadequate to accurately estimate soil loss. The last 15 runs used 225 points, accurately measuring soil erosion.

3.6 DATA ANALYSIS

3.6.1 Regression Analysis

The linear least-square regression analysis was performed to examine how variations in soil erosion amount can be explained by various soil and rainfall properties. The linear least square regression utilizes the relation between two or more quantitative variables so that one variable can be predicted from the other, or others with minimum sum of squared errors of prediction. In my study, the dependent (criterion) variable is the soil erosion amount and the independent (prediction) variables are individual soil and rainfall properties. First, univariate tests are performed to determine the correlation between soil erosion amount and each individual property. Second, a multiple regression analysis was

performed to analyze the relation between the soil erosion amount and all variables of interests.

In the multiple regression analysis, each predictor variable is weighted, the weights denoting their relative contribution to the overall prediction. In calculating the weights, the regression analysis procedure ensures maximal prediction from the set of independent variables in the variate. These weights also facilitate interpretation as to the influence of each variable in making the prediction, although correlation among the independent variables complicates the interpretative process. The computer software, SAS, a statistical data analysis package, was applied to conduct the regression analysis in this research.

3.6.2 Sources of Error

All measurements of physical quantities are subject to uncertainties. It is never possible to measure anything exactly. It is good to make the error as small as possible but it is always there. And in order to draw valid conclusions the error must be indicated and dealt with properly.

There are systematic errors and random errors. Systematic errors are errors tend to shift all measurements in a systematic way so their mean value is displaced. This may be due to such things as incorrect calibration of equipment, consistently improper use of equipment or failure to properly account for some effect. But small systematic errors will always be present. In this research, systematic errors could happen in the measurements

of soil shear strength, compressive strength, rainfall intensity, soil slope, moisture content, flow depth, and flow velocity. Random errors are errors fluctuate from one measurement to the next. They yield results distributed about some mean value. They can occur for a variety of reasons. A good example of "random error" is the statistical error associated with sampling or counting. A major source of “random error” was introduced when soil erosion was estimated using only 64 data points to estimate volume loss. This was corrected for the last phase of the study, but remains a major source of potential error for the study as a whole.

Root mean square deviation, standard deviation, maximum deviation, minimum deviation and significant figures are used in the following chapters to limit the errors occurred in the experiments and data analysis. All these methods are described in detail in the following documents.

3.6.3 Significant Figures

The significant figures of a (measured or calculated) quantity are the meaningful digits in it. Different significant figure digits were encountered in the measurements of the parameters used in this research. The significant figures shown in Table 3-5 were identified based on the measurement range of every equipment and the general rules of significant figure calculation.

Table 3-5. Significant Figures of Measurements

Parameter	Measurement Equipment	Minimum Scale measured	Significant Figures
Shear strength	Torvane®	0.1 lb/in^2	3
Compressive strength	Penetrometer	0.25 lb/in^2	3
Rainfall intensity	Rain Gauge	0.1 in/h	3
Soil slope	Ruler	1 mm	4
Moisture content	Balance	0.01 g	3-5
Flow depth	Ruler	1 mm	2
Flow velocity	Ruler & Stop Watch	1 mm & 0.1 sec	3
Soil surface height change	Ruler	1 mm	3-4
Erosion power	Calculation		2
Soil erosion volume	Calculation		3
Soil erosion weight	Balance	0.01 g	3-5

CHAPTER 4

EXPERIMENTAL RESULTS AND DISCUSSION

Two hundred and thirty-seven rainfall simulations were conducted. All the experimental measurements are shown in Appendix B. Table 4-1 shows the experimental conditions of the all experiments. As shown in Table 4-1, Phase 1, 2 and 3 are general soil erosion simulations. In Phase 4, triplicates of 6% slope and duplicates of 4% slope erosion simulations were conducted to testify the high slope and repeatability of those simulations. In Phase 5, the density of volume measurements was increased to 225 points. The total weight of eroded soils was also measured to verify the reliability of the volume erosion measurements.

Table 4-1. Experimental Conditions

Phase	Condition	Slopes (%)	Rainfall intensities (mm/h)	Soils	Total runs
1	Non- compacted soil	0.1, 0.5 & 1.0	12.7, 25.4, 50.8, & 101.6	1, 2, 3, 4, 5 and 6	72
2	Compacted soil	0.1, 0.5 & 1.0	12.7, 25.4, 50.8, 76.2, & 101.6	1, 2, 3, 4, 5 and 6	90
3	Compacted soil	4.0	12.7, 25.4, 50.8, 76.2, & 101.6	1, 2, 3, 4, 5 and 6	30
4	Compacted soil	4.0 & 6.0	50.8 and 76.2	1, 3, 4 and 5	30
5	Compacted soil	4.0	50.8 and 76.2	1, 4 and 5	15
Total					237

4.1 SOIL PROPERTIES

Figure 4-1 is a plot of the antecedent soil shear strength versus the experiment number for all six soils. The horizontal axis is the experiment number for a particular soil. The first 12 experiments for each soil plotted report the shear strength for loosely packed soils and

the remaining values are for compacted soils. The shear strengths of the artificial soils were all lower than that of the real soils, indicating the real soils are more cohesive than artificial soils in this study. Although the shear strength of artificial soils did not change very much after the compaction, the shear strengths of the real soils were increased. This was especially true of Soil 6, which has a high gravel content (17.6%), and a medium silt and clay content.

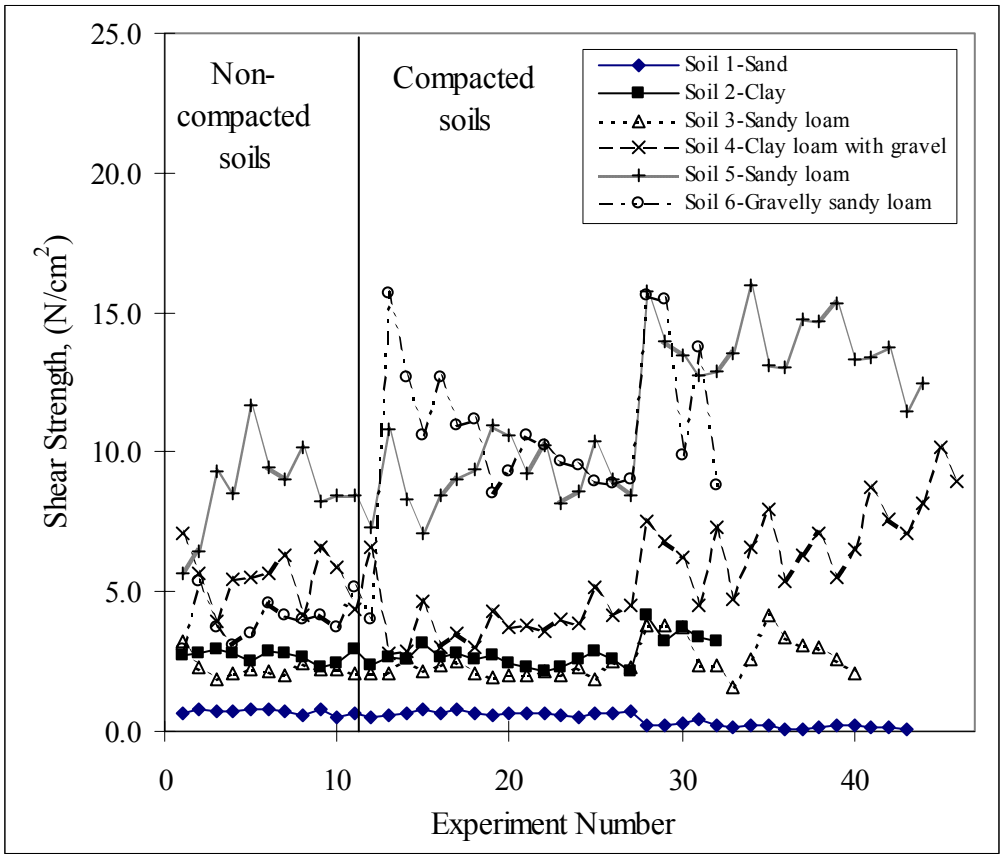

Figure 4-1. Soil shear strength.

The compaction tool used in the research is a flat surfaced heavy tool. While doing the compaction, the tool's flat surface hits the soil and pushes down all the soil particles. This way the soil surface bears the compaction at the same degree. While compacting Soil 6, the gravel was pushed down by this flat surface and compacted the soil particles

underneath them, therefore, the Soil 6 was compacted harder than other soils. This process is the same reason why the sheepsfoot roller is used for the compaction of silty and clayey soils in the construction field. The other reason for increased strength is that while measuring the soil shear strength, Torvane would catch some gravel, therefore, the resistance of turning is increased.

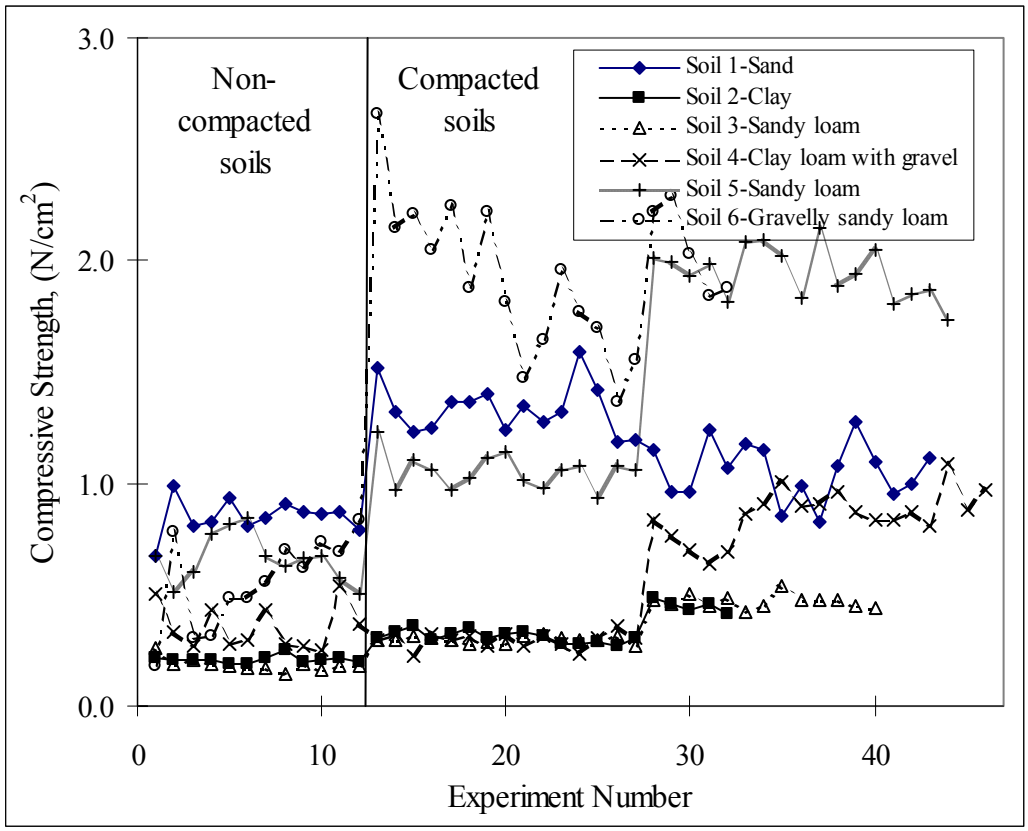

Figure 4-2. Soil compressive strength.

Figure 4-2 is a plot of antecedent soil compressive strength versus experiment number for all six soils. Like in Figure 4-1, first 12 experiments were on loose packed soils. The compressive strength of all soils was increased after the compaction. Soil 2 and 3 showed the lowest compressive strengths, and their compressive strengths remained low after the compaction. The reason is that these two soils had a large amount of clay

minerals and their pore volumes were fully saturated with water. With flat-surface compaction, not much water could be driven out of the pore volume, so their compressive strengths remained low after the compaction. Pure sand is a non-cohesive soil and has grain to grain support mechanism. The compaction condensed the soil's volume and reduced the distance between particles, therefore, its resistance of downward pressure, which is the compressive strength, is increased. Soil 4, 5 and 6 are real soils, and their moisture contents are much lower than that of Soil 2 and 3. After the compaction, most of the air in the pore volume was driven out, so the compressive strength could be increased dramatically.

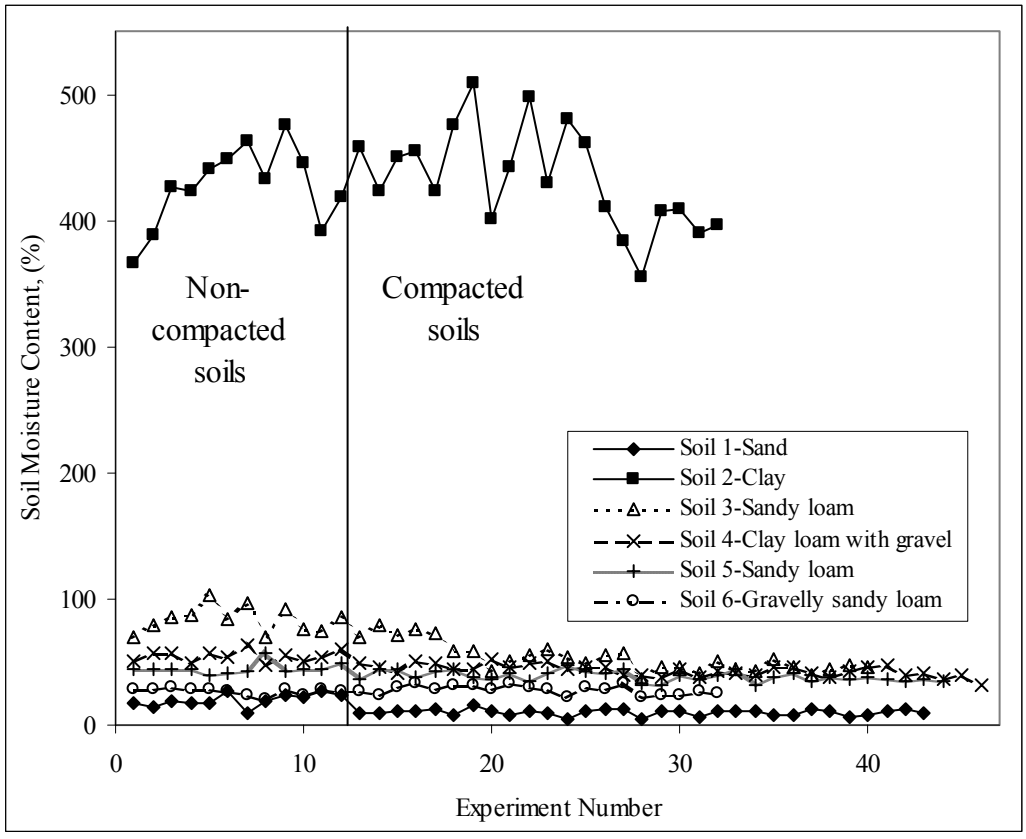

Figure 4-3. Soil moisture content.

Soil moisture content (not corrected for swelling) is plotted on Figure 4-3. The remarkably high moisture content of pure bentonite clay is because this clay swelled to 400% of its dry volume. Soil 3 is also exhibits fairly high moisture content because it has 30% of swelled bentonite. The pure sand has the lowest moisture content because its grain skeleton is a very good drainage system. Only very limited amount of water can be stored in its pore volume.

4.2 SOIL EROSION VS. RAINFALL AND SOIL PROPERTIES

Figure 4-4 is a plot of the unit soil volume loss and rainfall intensity. The unit soil volume loss is defined as the soil loss volume per unit area in 30 minutes. (Please refers to the section 5.3 for the detail of soil volume loss vs. weight loss.) The plot displays a trend indicating that higher rainfall intensity induces more erosion. This result is because higher rainfall intensities have more net kinetic energy to apply to the surface to erode the soil, and the increased runoff volume will transport the eroded soil away from the site.

Figures 4-5 through 4-9 are the plots of the unit soil loss and shear strength at five different rainfall intensities. Results of all 237 simulations are shown in these plots. Each plot represents a series of experimental measurements for different soil samples using the same rainfall intensity. Trends are suggested that soils with high shear strength, on the average, exhibited lower erosion volumes than low strength soils. The linear regression equations and the correlation coefficients are shown in the plots.

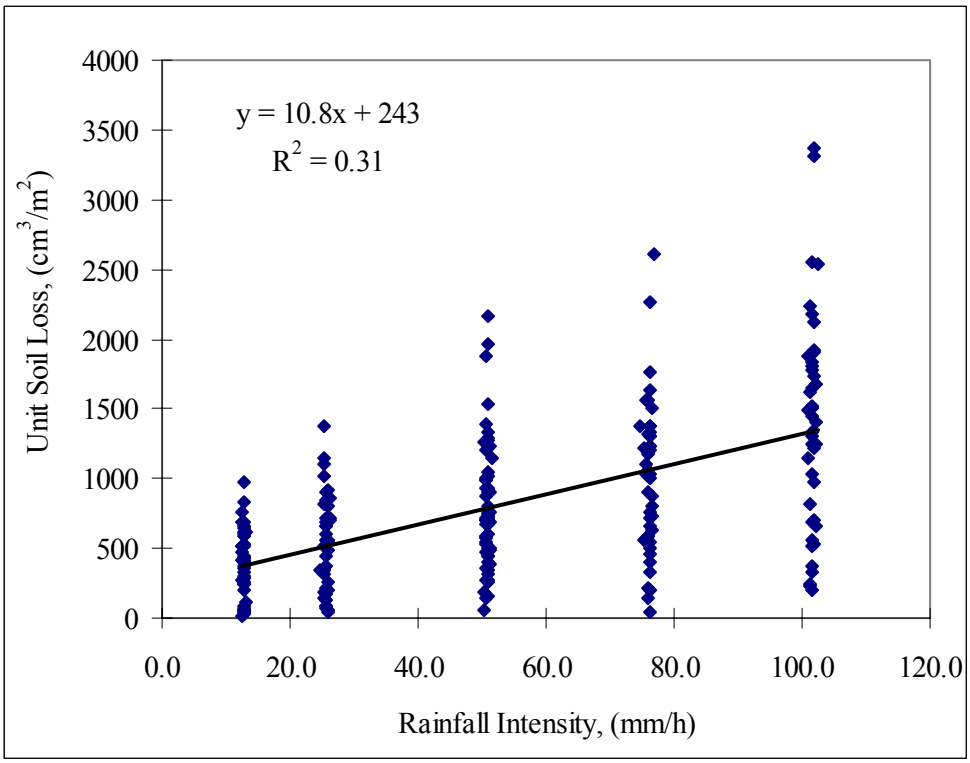

Figure 4-4. Plot of unit soil volume loss and rainfall intensity.

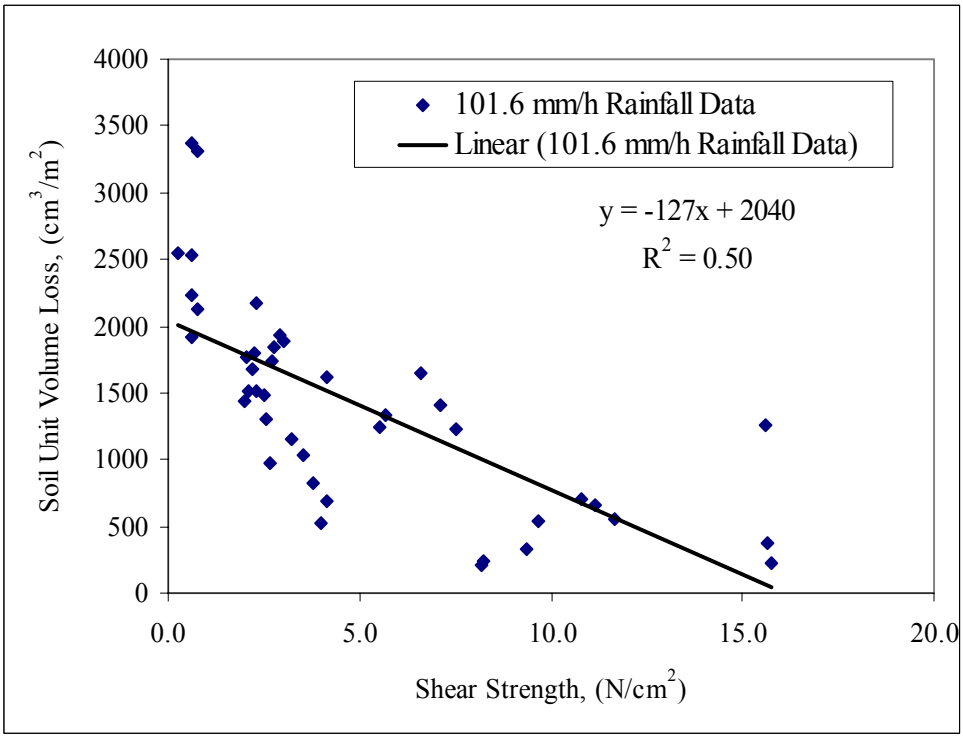

Figure 4-5. Soil unit volume loss vs. soil shear strength in 101.6 mm/h (4.0 in/h) rainfall.

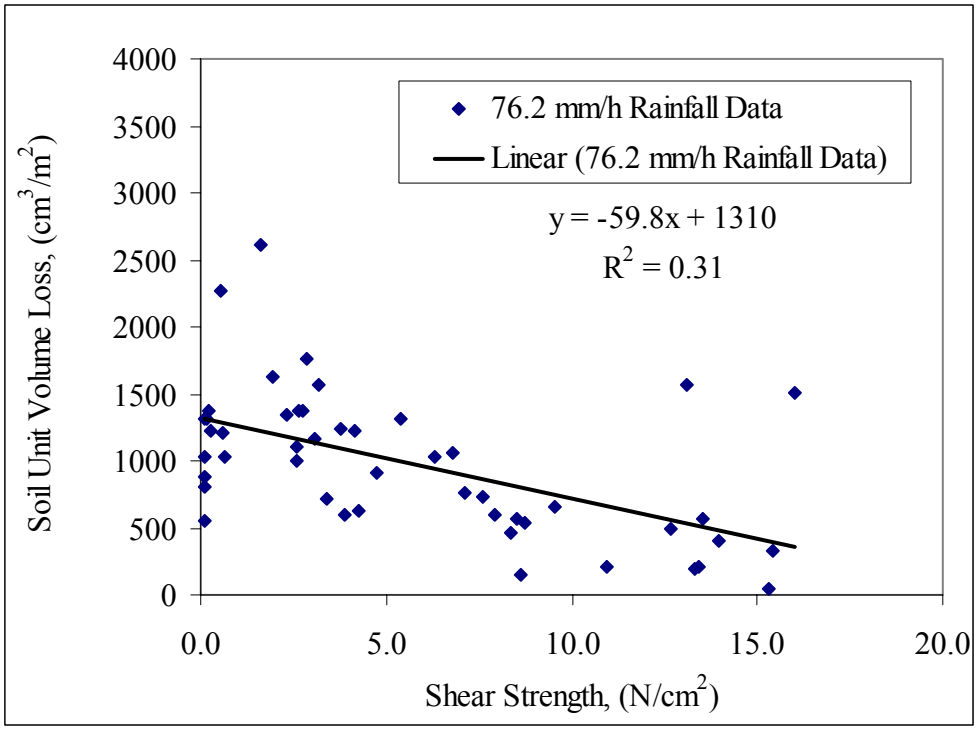

Figure 4-6. Soil unit volume loss vs. soil shear strength in 76.2 mm/h (3.0 in/h) rainfall.

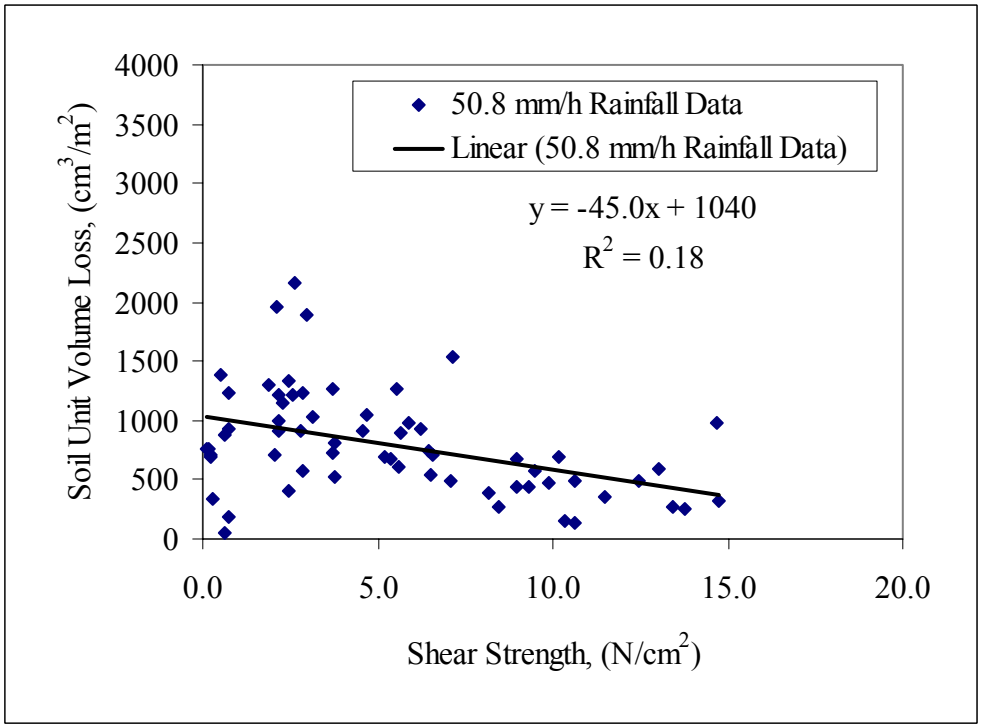

Figure 4-7. Soil unit volume loss vs. soil shear strength in 50.8 mm/h (2.0 in/h) rainfall.

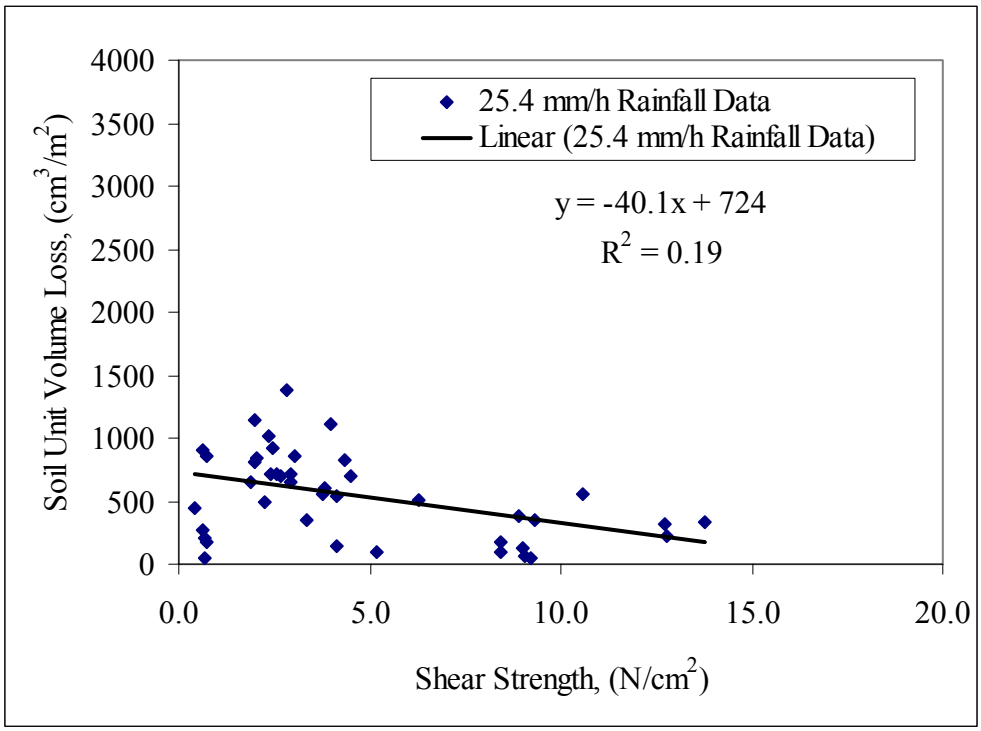

Figure 4-8. Soil unit volume loss vs. soil shear strength in 25.4 mm/h (1.0 in/h) rainfall.

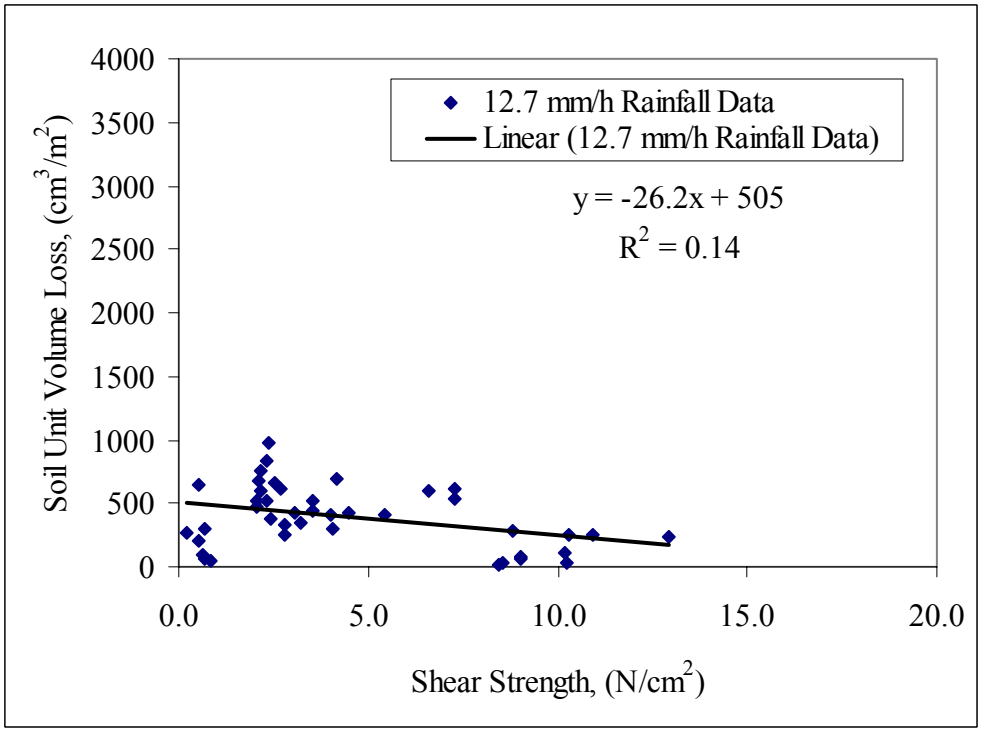

Figure 4-9. Soil unit volume loss vs. soil shear strength in 12.7 mm/h (0.5 in/h) rainfall.

It is known that the soil shear strength is related to the interparticle attractive forces in the soil. The higher the shear strength, the greater the traction stress required to dislodge the particles. Thus higher rainfall intensities are required to produce more soil loss for a given soil strength. However, this figure also indicates that the slopes of the regression lines increase as the rainfall intensity increases. For low rainfall intensity, soil loss is found to be nearly independent of shear strength, while at high intensities the shear strength appears to play some important role in resisting soil loss.

Figures 4-10 through 4-14 show the inverse correlations between unit soil loss and compressive strength at different rainfall intensities. Again, the plots indicate five sets of data collected in the erosion simulations. The linear regression equations for each data set are shown in every plot. Although the correlation coefficients of these regressions are not very high (the best is only about 0.37), there appears to be some correlation between compressive strength and erosion. There is a trend displayed in the plot that the higher the compressive strength, the lower the amount of soil erosion. The slopes of the regression lines are not changed very much in these erosion simulations. The trends also suggest that the effect of compressive strength to soil erosion is independent of the rainfall intensity. This analysis indicates that soil compaction probably does help protect soil from rainfall erosion.

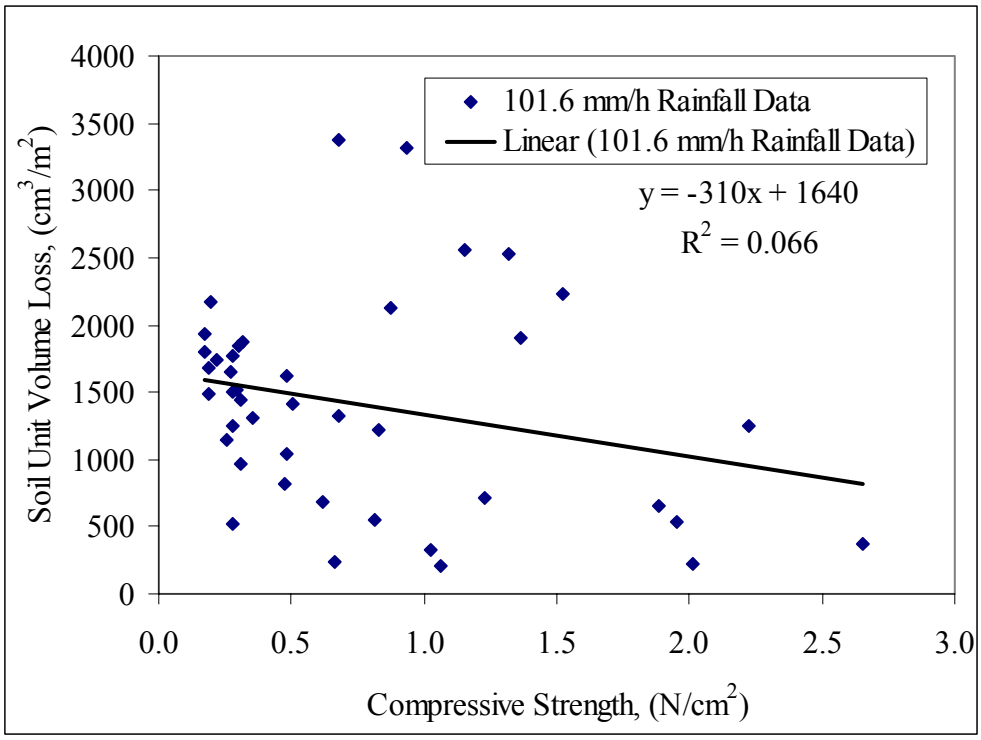

Figure 4-10. Soil unit volume loss vs. compressive strength in 101.6 mm/h rainfall.

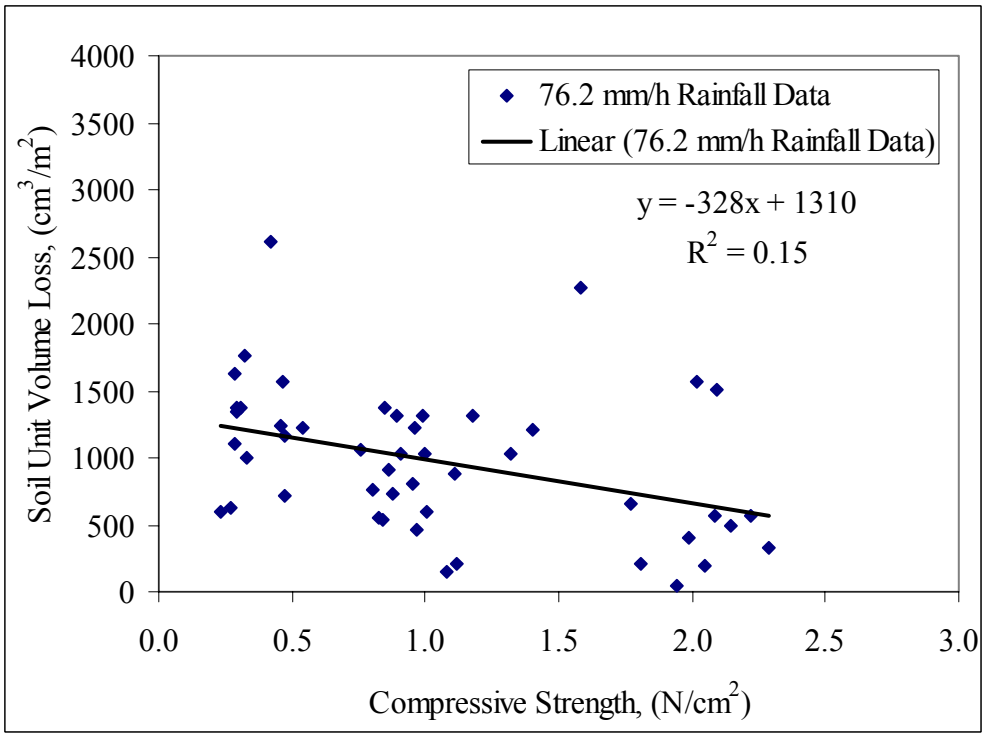

Figure 4-11. Soil unit volume loss vs. compressive strength in 76.2 mm/h rainfall.

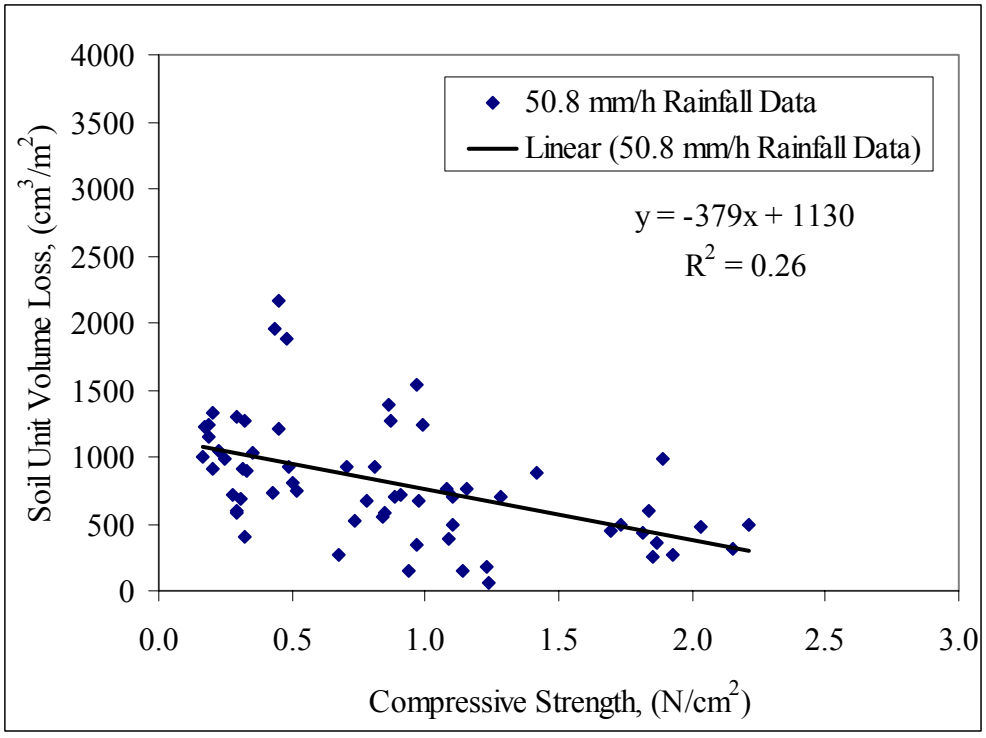

Figure 4-12. Soil unit volume loss vs. compressive strength in 50.8 mm/h rainfall.

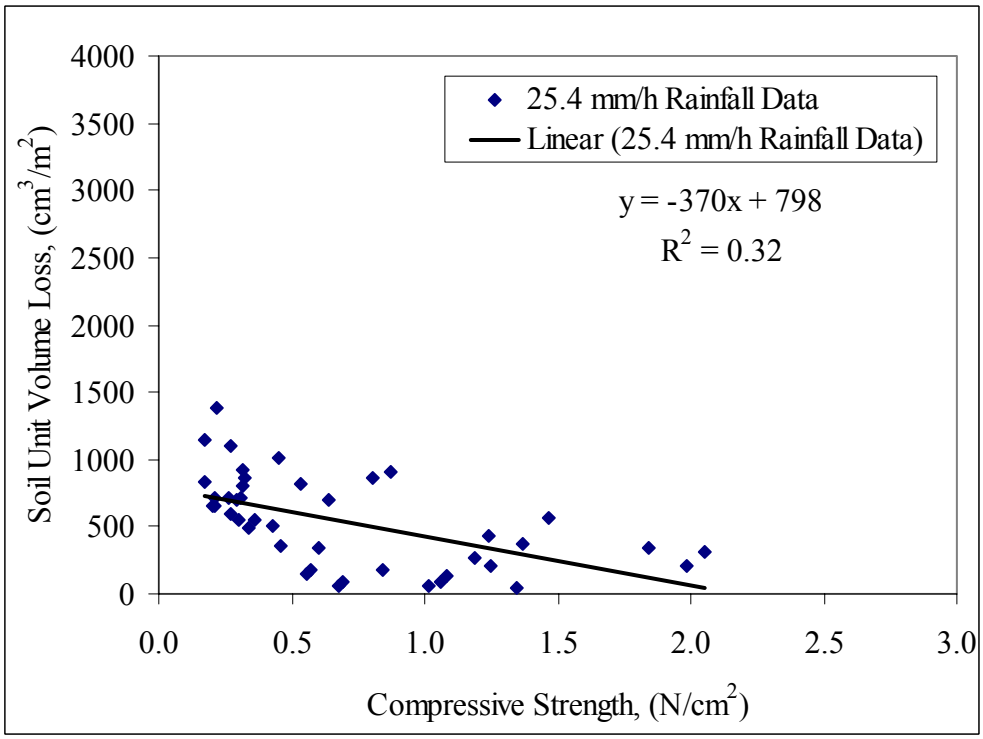

Figure 4-13. Soil unit volume loss vs. compressive strength in 25.4 mm/h rainfall.

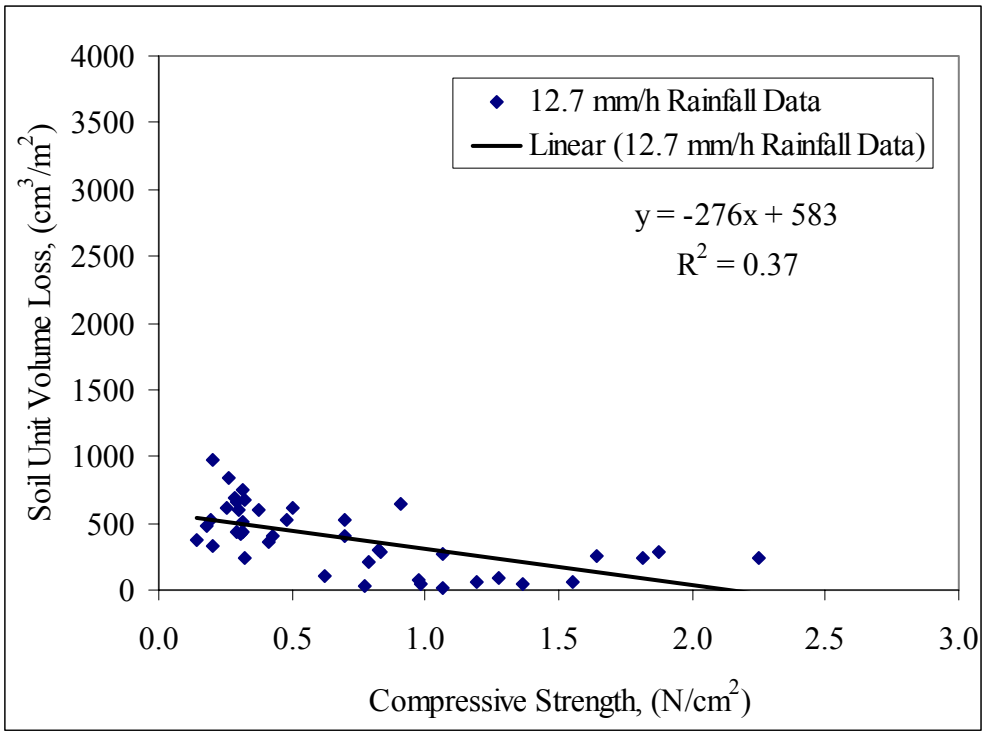

Figure 4-14. Soil unit volume loss vs. compressive strength in 12.7 mm/h rainfall.

Figure 4-15 is a plot of the unit soil volume loss and soil bed slope. No apparent correlation was found between them in our experiments. Although some data sets did show that higher slope cause higher erosion, the main trend did not support this result. However other researchers have found that slope steepness has a positive correlation with soil erosion. A reason for slope effects observed in this study was that the slope range may not be high enough to show the effect in such a small erosion simulation area (0.66 m^2), although five different slopes (0.1% to 6%) were used. For example, the standard slope used in USLE was 9%. Also, manual compaction affected the shear strength and compressive strength of soils, and these two factors are stronger variables than slope. It is possible that the slope length is too short to show the slope length effect. Presumably,

higher slope, like 9% and higher will show the effect of the slope steepness to the soil erosion.

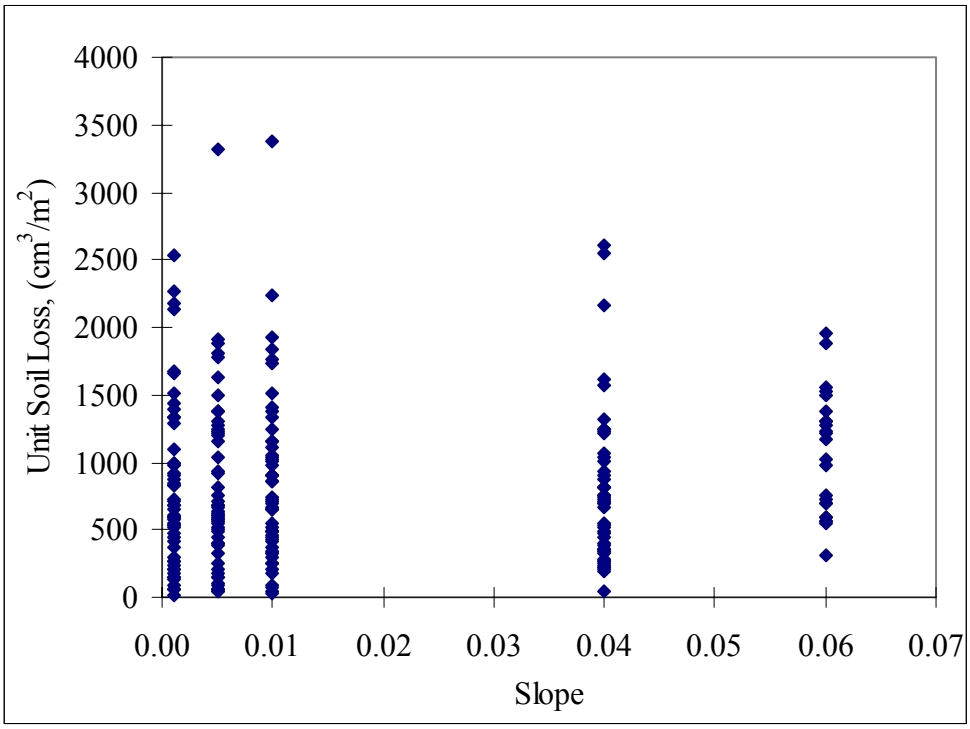

Figure 4-15. Plot of unit soil volume loss and soil slope.

As discussed in Chapter 3, some researchers pointed out that there are complex relationships between the shear strength and moisture content. Unfortunately, there is no such kind of observation in this research. However, as shown in the Figure 4-16, a regression line could be fitted in the plot of moisture content and compressive strength. In this plot the Soil 2 data was excluded because the Soil 2 does not belong to this soil population. Although the correlation coefficient of the regression is not high (only 0.32), it indicates that the soil compressive strength is not totally independent the soil moisture content.

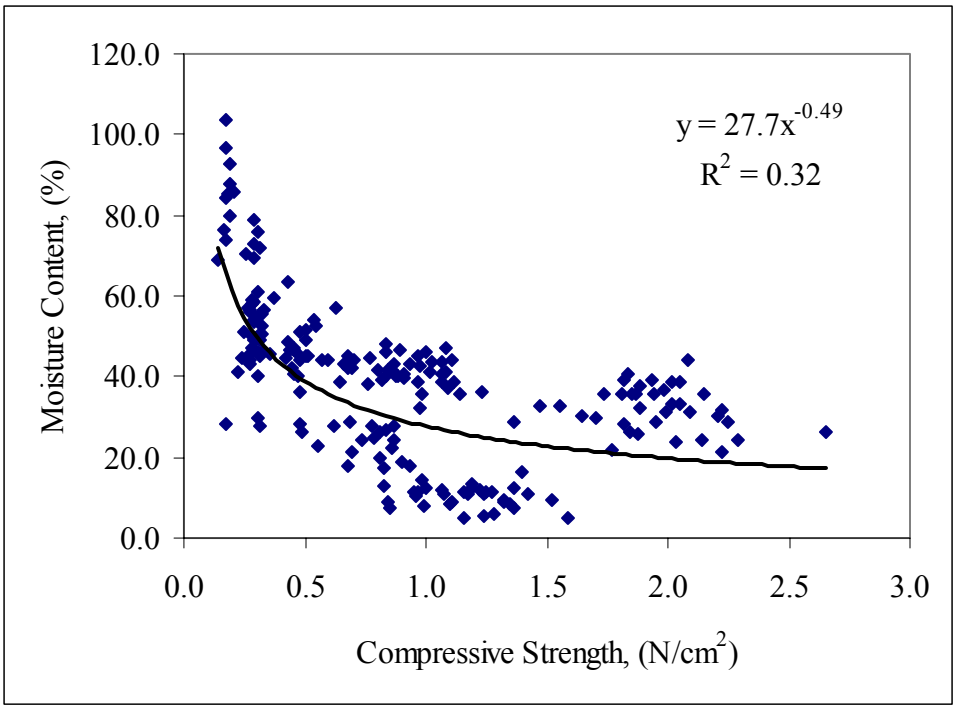

Figure 4-16. Plot of soil moisture content and compressive strength.

4.3 RAINFALL EROSION MODEL

Figure 4-4 through 4-15 suggest that the soil loss depends on the shear strength, compressive strength and rainfall intensity, but is less affected by the bed slope and moisture content. Like prior research, no single variable appeared to be a useful prediction factor to the soil erosion. Therefore, the multiple regression analysis was applied to this research to develop a predictive model between the amount of soil erosion and properties of soil and rainfall.

Limited by the research project, no field test would be conducted to verify the model. Therefore, the multiple regression analysis was conducted using 80% (190) of the total

237 experimental data. The other 20% (47) of data would be used as a substitute for an independent data set to test the applicability of the model. In order to censor the data objectively, forty-seven integers were generated in the range from 1 through 237 by random sampling without replacement. Because the experiments was ordered consecutively, based on data, the experiment whose case number matched with these random integers were censored and set aside to substitute an independent data set to test the prediction result of the model later.

In order to find a model that can predict the soil erosion, several different functional forms were evaluated. Rainfall intensity, soil shear strength, soil compressive strength, bed slope and products of these variables were chosen as possible regression parameters. The moisture content was not used in the multiple regression analysis because it is not completely independent from compressive strength. Unit soil volume loss is the dependent variable used for the regression analysis. Unlike USLE methods, all factors are field measurable and geotechnical parameters.

These variables and various functional combinations were used in a regression analysis to identify a likely prediction model. Correlation coefficients were used as the screening tool to select the best combination of variables. Then, only the best combinations were analyzed again to find out the regression parameter for the predictive model. Appendix C lists the multiple regression results for all the soils, and variable combinations explored.

Two possible predictive models were developed based on the multiple regression analysis results. The first model is a linear additive model and the second is a product model. The additive model can be expressed as

$$U = C_1 + b_1 S + b_2 \tau + b_3 \sigma + b_4 I \qquad \text{Eq. [4-1]}$$

where

U = the 30 minute unit soil volume loss (cm^3/m^2),
S = slope of the soil bed (%),
τ = shear strength (N/cm^2),
σ = compressive strength (N/cm^2),
I = the rainfall intensity (mm/hour),
b_1, b_2, b_3 and b_4 = regression parameters,
C_1 = erosion factor (cm^3/m^2).

The product model is

$$U = C_2 \cdot S^{b_1} \cdot \tau^{b_2} \cdot \sigma^{b_3} \cdot I^{b_4}, \qquad \text{Eq. [4-2]}$$

where

C_2 = erosion factor, and all the other symbols have the same meaning as that of Eq. [4-1].

The product model is structurally similar to USLE and its derivatives, in that it predicts soil loss as the product of various factors.

Figure 4-17 and 4-18 show the unit soil volume loss predicted by the additive and product model. The regression parameters of these two models are listed in Table 4-2. Both the additive and product models use the measured data as the x-coordinate, and the estimated values as the y-coordinate. A 45° line was drawn in both plots to show the ideal prediction result. A perfect prediction would plot all the calculated values along

this line, meaning that the predicted values equal the measured values. The closer the data points to the 45° line, the better the prediction of the model. The data are scattered in the present work. After analysis, Soil 1 (sand) is found to be the soil contributed most of the scattered data points.

To remove the scattered points associated by Soil 1, multiple regressions were conducted again excluding experimental results of Soil 1. Regression parameters are also shown in Table 4-2. Figure 4-19 and 4-20 show the results of these analyses. Data points are much closer to the ideal line than the Soil 1 was included.

The root mean square deviation (RMS), maximum deviation (MaxD) and minimum deviation (MinD) are used in the comparison of estimated data and measured data. For these three parameters, the prediction is better if the values of these parameters are low. The calculation methods of these goodness-of-it measures are shown below:

$$RMS = \frac{\sqrt{\sum_{i=1}^{N} (Estimated - Measured)^2}}{N}, \qquad \text{Eq. [4-3]}$$

$$MaxD = MAX(Estimated - Measured), \text{ and} \qquad \text{Eq. [4-4]}$$

$$MinD = MIN(Estimated - Measured). \qquad \text{Eq. [4-5]}$$

The regression parameters of Figure 4-17, 18, 19 and 20 are also shown in the Table 4-2 for convenient reference. From the caption of these figures, both the additive and product models predicted soil erosion much better if the Soil 1 is not included in the prediction.

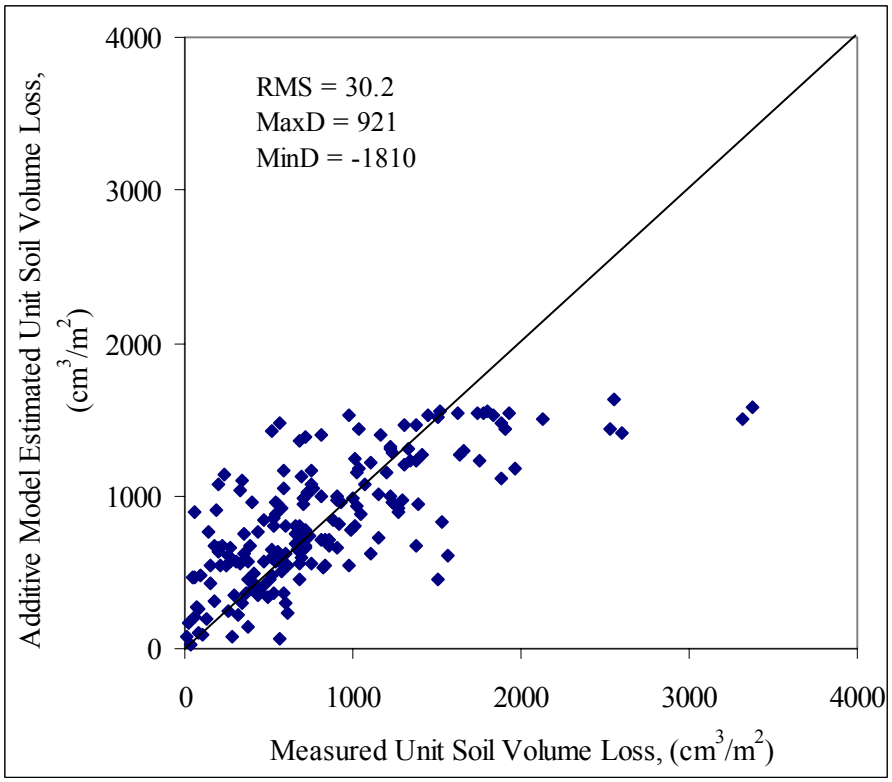

Figure 4-17. Additive model vs. measured unit soil volume loss (all soils tested).

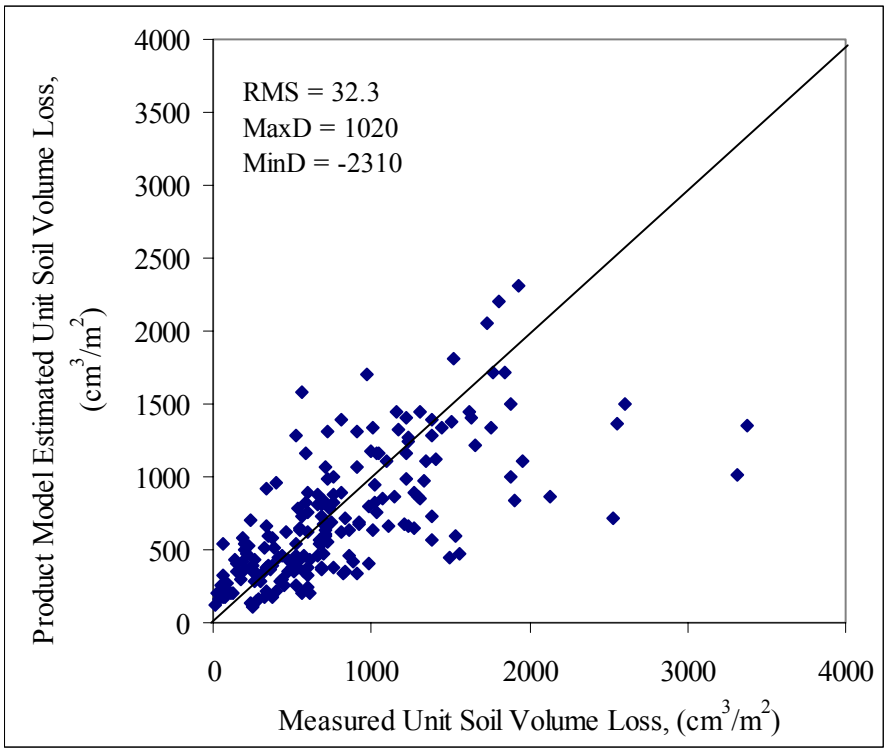

Figure 4-18. Product model vs. measured unit soil volume loss (all soils tested).

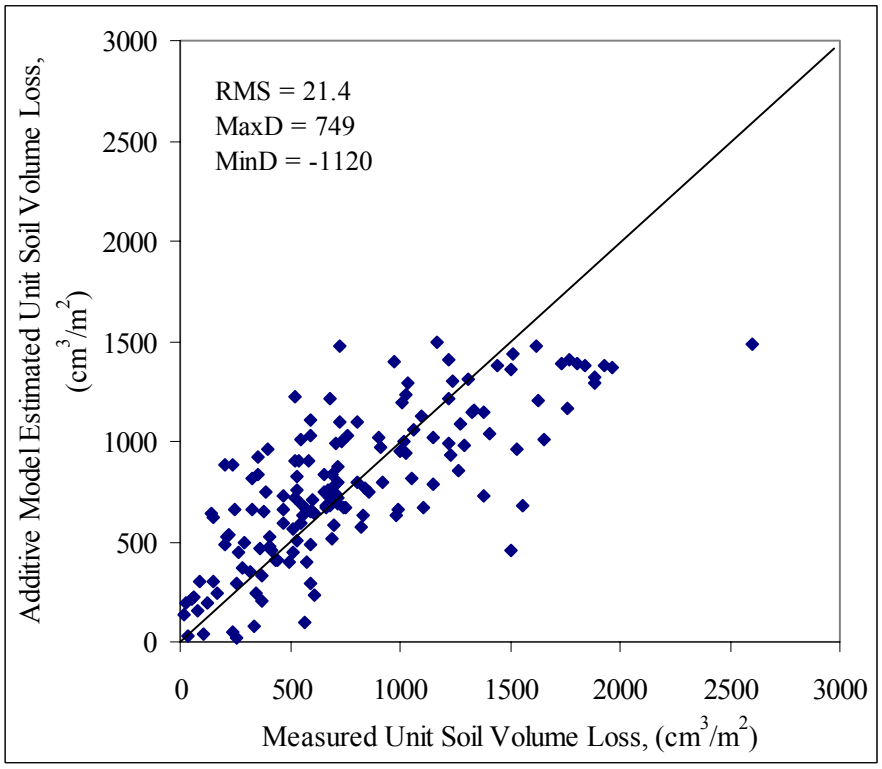

Figure 4-19. Additive model vs. measured unit soil volume loss (Soil 1 excluded).

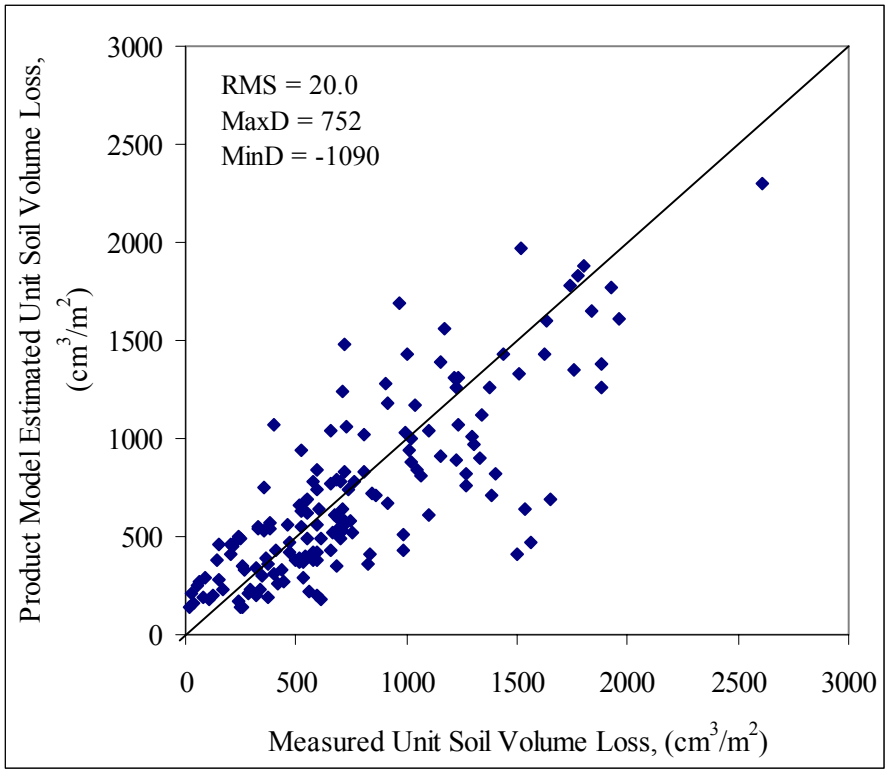

Figure 4-20. Product model vs. measured unit soil volume loss (Soil 1 excluded).

The product model was selected for further study because it is similar in format to earlier models. In addition, at zero rainfall it predicts zero erosion whereas the additive model violated this physically intuitive limit.

Table 4-2. Regression parameters for additive and product models.

Models	C_1	C_2	b_1	b_2	b_3	b_4	R^2
Additive model for all soils, (Figure 4-17)	560		4000	-52	-170	11	0.51
Product model for all soils, (Figure 4-18)		15	0.12	-0.15	-0.57	0.69	0.52
Additive model for Soil 2-6, (Figure 4-19)	710		6900	-80	-7.8	8.1	0.57
Product model for Soil 2-6, (Figure 4-20)		95	0.15	-0.64	-0.19	0.57	0.58

4.4 COMPARISON OF PRODUCT MODEL, MUSLE, AND RUSLE

The Revised Universal Soil Loss Equation (RUSLE) is the soil erosion prediction tool used by USDA. It is also widely used to estimate the soil erosion caused by single rainfall events, despite its limitations introduced in Section 2.3.5. The Texas Department of Transportation (TXDOT)uses a USLE-based soil erosion estimation tool that shares the same origins as RUSLE and thus the same limitations. The RUSLE and the MUSLE used by TXDOT are applied in this research to compare their ability for estimating soil loss during single rainfall events, with the product model.

In using the RUSLE, the R factor was calculated by the equation (2-6) of Renard et al. (1997) as

$$e_m = 0.29 \cdot [1 - 0.72 \cdot \exp(0.05 i_m)], \qquad \text{Eq. [4-6]}$$

where

e_m = unit energy, (MJ/ha-mm)
i_m = rainfall intensity, (mm/h).

The K factor was calculated by the equation [3-5] of Renard et al. (1997) as:

$$K = 7.594\{0.0034 + 0.0405\exp[-\frac{1}{2}(\frac{\log(Dg) + 1.659}{0.7101})^2]\}, \quad \text{Eq. [4-7]}$$

$$Dg = \exp(0.01\sum f_i \ln m_i), \quad \text{Eq. [4-8]}$$

where

Dg = the geometric mean particle diameter (mm),
f_i = the primary particle size fraction (%)
m_i = the arithmetic mean of the particle size limits of that size range (mm), (Shirazi and Boersma 1984).

The LS factor was determined using the table provided by the Renard et al. (1997). The C and P factors are equal to 1. Appendix D shows the RUSLE estimated soil erosion volume by applying the above calculation methods.

From these equations, the RUSLE estimated single rainfall induced soil erosion could be calculated by applying the experimental results obtained in the laboratory. According to the RUSLE, the results are in the unit of ton/acre. For the comparison with the developed product model, the ton/acre unit should be changed to the unit used in our research, the unit soil volume loss, cm^3/m^2. Appendix E lists the unit conversion procedure.

As described in section 2.3.4, the Modified USLE from Farmer and Fletcher (1977) is currently used in the Texas Department of Transportation system. This equation (Eq. 2-21) was applied to estimate the soil erosion behavior under current research condition. According to their paper, all other factors are the same as that of RUSLE except the VM factor, which happened to be 1.0 for bare soil condition according to Vose and Smith

(1993). This way, the calculated results from MUSLE were exactly equal to that of RUSLE. Therefore, the RUSLE results will be used in the comparison between the developed product model, MUSLE and RUSLE.

Figures 4-21 and 4-22 are two plots of the unit soil volume loss predicted by the RUSLE and the developed product model, respectively. Both plots have the same logarithmic scale at the x and y axis because of the estimated values from RUSLE. The unit soil mass loss calculated by RUSLE was converted to unit soil volume loss using the dry density and moisture content of the soils. The measured soil loss is plotted as the x-coordinate, and the predicted soil loss is plotted as the y-coordinate. A perfect prediction would plot all the estimated values along the 45° line drawn on the plot, which means that the predicted values are equal to the measured values. The regression parameters of the product model of Figure 4-22 are the same as that of Figure 4-18.

From the plot, it is very clear that RUSLE estimated soil erosion values distributed in a much bigger area than that of product model, which means that, the prediction accuracy of RUSLE for the current laboratory rainfall simulation situation is not good. The over-predicted results are much more than under-predicted results in this logarithmic plot. Because this plot is on a logarithmic scale, the over-prediction and the under-prediction effects are very significant.

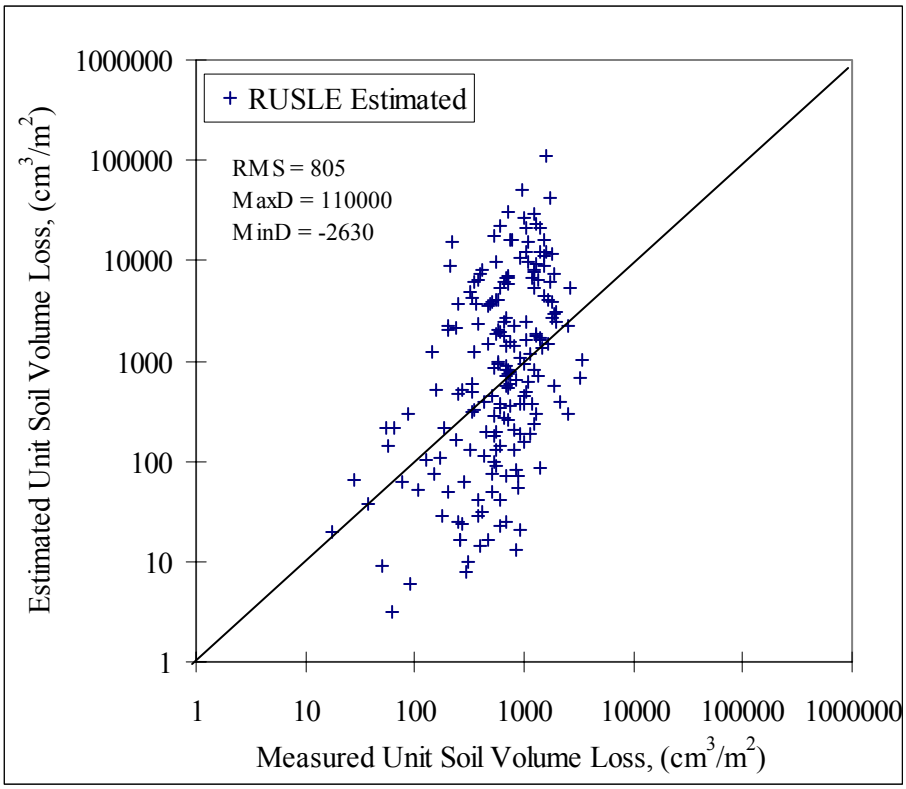

Figure 4-21. RUSLE prediction of unit soil loss (all soils tested).

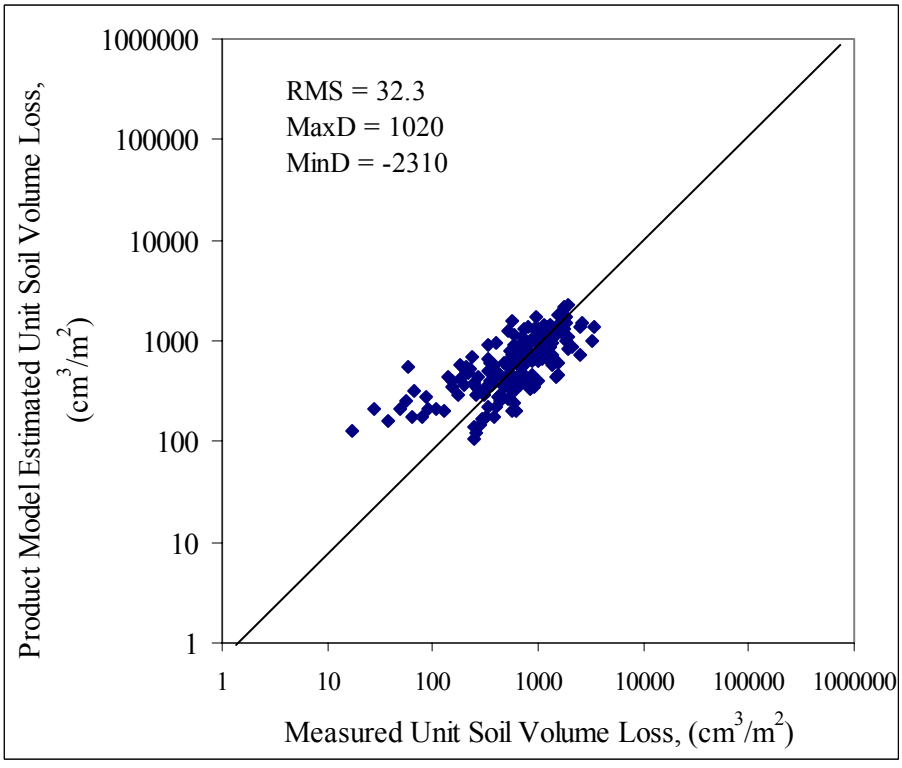

Figure 4-22. Product model prediction of unit soil loss (all soils tested).

The kinetic energy of the current simulated rainfall is about 25 to 55% lower than that of the natural rainfall as illustrated in Section 3.4.1. However, the prediction result distribution of the developed product model is still much closer and concentrated to the 45 degree line than that of the RUSLE and MUSLE.

In the present work, the data are also scattered, with the most scattering observed for Soil 1, the pure sand. Figures 4-23 is a plot showing the results of the same kind of comparison by excluding Soil 1. In this figure, the data points are less scattered than that of Figure 4-21. And the regression parameters of the product model vs. RUSLE prediction are the same as that of the product model vs. measured soil loss (Figure 4-20).

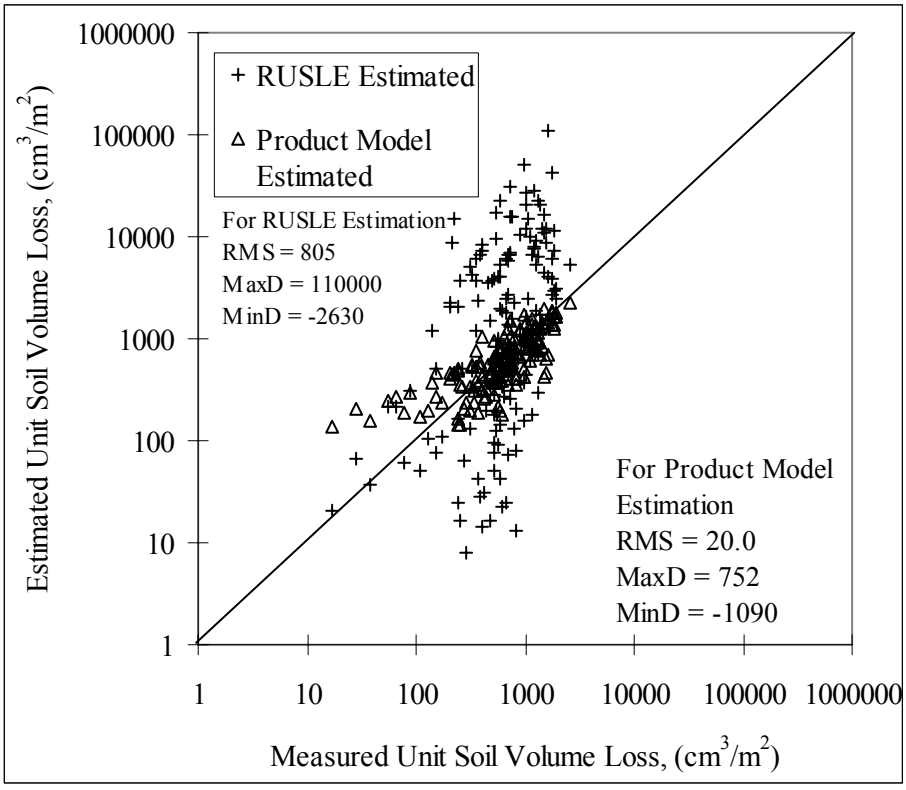

Figure 4-23. Product model vs. RUSLE prediction of unit soil loss (Soil 1 excluded).

In all cases showed above, the RUSLE method performed less accuracy on soil erosion estimation than that of developed product model in this research. The RMS of RUSLE and MUSLE estimations is more than 25 times higher than that of the developed product model. The RUSLE over-predicts the soil erosion under most of the situation significantly.

CHAPTER 5

EROSION POWER DEVELOPMENT AND MODEL VERIFICATION

5.1 EROSION POWER DEVELOPMENT

In terms of erosion, only the kinetic energy of raindrop and energy of water flow are the energies related to the soil erosion and transportation. Velocity of raindrop hitting the soil surface is difficult to measure in experiments. Therefore, by neglecting friction, potential energy of raindrop equals to the kinetic energy of the raindrop hitting the soil surface. Stream power has been used by many hydrologists as one of the most important parameters in estimating sediment load in water channels since the introduction by Bagnold in 1966. Stream power is defined as

$$\omega = \tau \cdot v = \rho \cdot g \cdot q \cdot S\,, \qquad \text{Eq. [5-1]}$$

where

ω = stream power (kg/s^3),
τ = shear strength of flow (N/m^2),
v = flow velocity (m/s),
ρ = density of water, (kg/m^3),
g = gravitational constant (m/s^2),
q = unit discharge of water (m^2/s),
S = slope (%).

Govers and Rauws (1986) found that the shear velocity and stream power of overland flow had direct influence to the erosion and transportation of soil particles. Most current models rely on a gross characteristic of flow, most commonly either hydraulic shear stress or stream power, to characterize the capability of the flow to detach soil, e.g.,

Foster, (1982) and Rose, (1985). Also, hydrologists used stream power to develop other parameters, such as unit stream power (Yang, 1972, 1979, 1984 and 1987; Yang and Molinas, 1982) and effective stream power (Govers, 1990) to estimate sediment erosion and transportation. Hussein (1996) and Nearing, et al. (1997) both stated that stream power is a consistent and appropriate predictor for unit sediment load for the rill erosion. The flow erosion power is the product of stream power and the soil area.

The erosion power developed in this study consists of two parts. One is the rainfall erosion power, which is based upon the potential energy of raindrops. The other is the flow erosion power, based on the concept of stream power. The equation of rainfall erosion power is

$$P_r = I \cdot A \cdot \rho \cdot h \cdot g\,, \qquad \text{Eq. [5-2]}$$

where

P_r = rainfall erosion power (w),
I = rainfall intensity (m/s),
A = area of the eroded soil (m^2),
h = height from the soil surface to the rainfall simulator (m).

The equation of the flow erosion is defined as

$$P_f = \tau \cdot v \cdot A = \rho \cdot g \cdot R \cdot S \cdot v \cdot A\,, \qquad \text{Eq. [5-3]}$$

where

P_f = flow erosion power (w),
R = hydraulic radius (m), which equals to water depth for shallow flow.

The water erosion power (P_e) is derived as

$$P_e = P_r + P_f = I \cdot A \cdot \rho \cdot g \cdot h + \rho \cdot g \cdot R \cdot S \cdot v \cdot A = \rho \cdot g \cdot A(I \cdot h + R \cdot S \cdot v)$$, Eq. [5-4]

Based on the concept developed above and measured data of flow depth and velocity, the erosion power was calculated for each experiment. Figure 5-1 is a plot of the erosion power versus the amount of soil lost. The pattern is very similar to that of Figure 4-4, i.e. the unit soil loss vs. the rainfall intensity, which suggests that soil properties cannot be ignored.

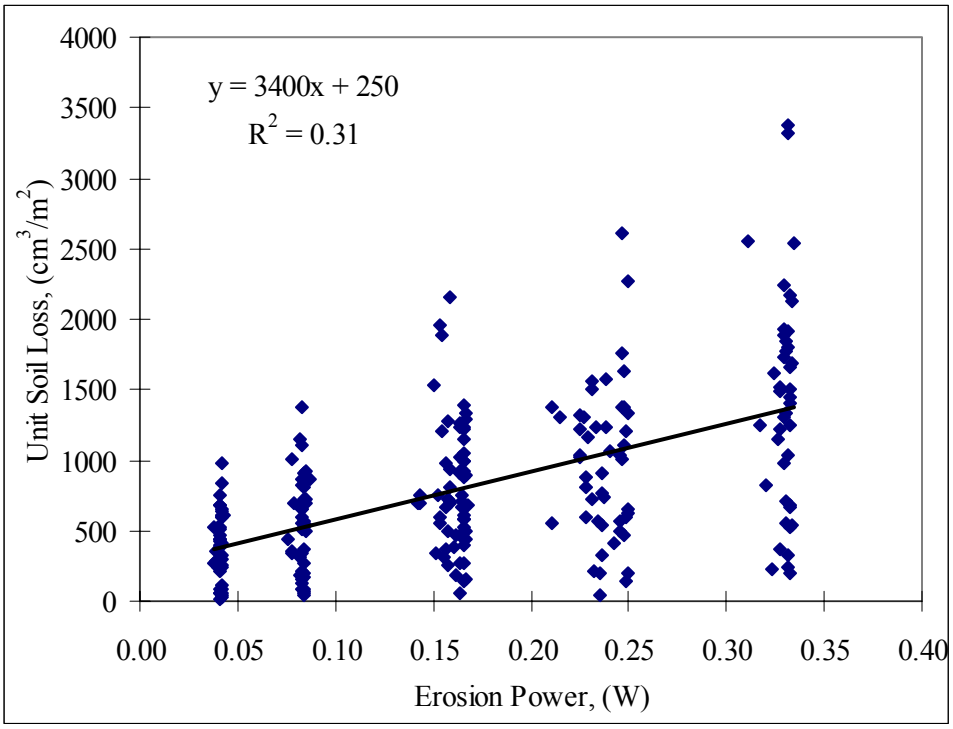

Figure 5-1. Plot of unit soil volume loss and erosion power.

However, the correlation coefficient is not very high. As other variables discussed in Chapter 4, the erosion power cannot predict soil erosion accurately enough solely. Therefore, multiple regression analysis was also conducted by using the erosion power instead of the rainfall intensity. Appendix F shows the correlation coefficients of the

analysis conducted for the situations of erosion power. Only the results of product model showed.

From the data tables showed in Appendix F, the correlation coefficients of models with erosion power are slightly lower than that of models with rainfall intensities. Statistically, the erosion power is almost as important as that of rainfall intensity, however, the rainfall intensity is still going to be used in the product model developed in this research as one of the key factors. The reason is that the rainfall intensity is a field measuable property and the erosion power is a derived theoretical concept. The rainfall intensity is more practical in the field application. However, erosion power is an important factor to express the properties of rainfall and surface flow. Further study is necessary.

5.2 MODEL VERIFICATION

Within the total 237 experimental data points, 20% of them had been randomly selected out to test the model for its prediction accuracy. The model discussed in the above chapters and sections was developed from 80% of experimental data. This model is shown as

$$U = 6.5 \cdot S^{0.12} \cdot \tau^{-0.15} \cdot \sigma^{-0.57} \cdot I^{0.69}, \qquad \text{Eq. [5-5]}$$

where

U = the 30 minute unit soil volume loss (cm^3/m^2);
6.5 = erosion factor ($h^{0.69} N^{0.72} m^{-1.13}$);
S = slope of the soil bed (%);
τ = shear strength (N/cm^2);

σ = compressive strength (N/cm^2);
I = the rainfall intensity, (mm/hour).

As the model we have, this equation was used to predict the amount of soil loss for the data left for testing. The testing was conducted by applying the experimental measurements of those censored data to this equation so that we have the estimated soil erosion amount. Then the estimated erosion amount and measured erosion amount were plotted together to find out the distribution of data points. The model shown above is the model for all soils because the censored data could include sand data.

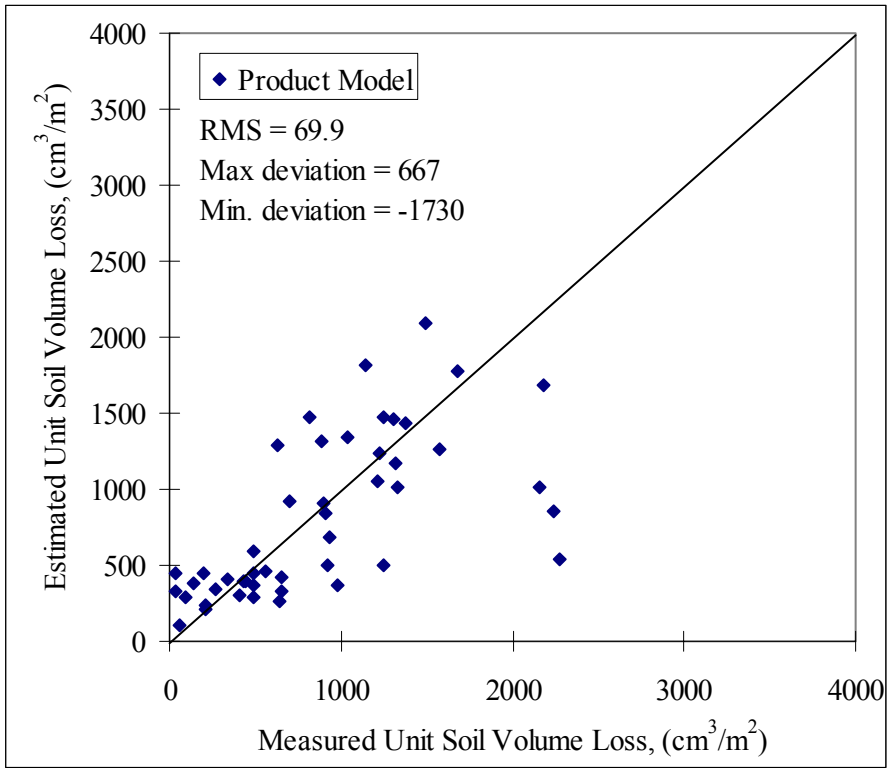

Figure 5-2. Test of product model on censored data.

Figure 5-2 is the plot of the testing. Eq. [5-2] is used to calculate the y coordinates, i.e. the estimated soil loss. Same as before, the measured soil erosion data was used as the x

coordinates and the estimated data was plotted to the y coordinates. The perfect match with measured data should be the plotted 45º line on the plot. As the plot shows, the estimated erosion values were all plotted close to the 45º line. This way, it shows that the model can predict unit soil loss fairly well.

5.3 VOLUME METHOD VS. WEIGHT METHOD

Most prior researchers use weight to measure the soil erosion during their studies. The reason is that the soil particles could be easily collected because the experimental area is small, the slope is high and no other easy ways to measure the soil erosion. In using the weight method, the key point is to collect all the soil particles.

A volume method was applied in this research. The disadvantage of volume method is that there must be a reference datum to measure the volume change, and the datum is not easy to be referenced in the field condition. Radke, et al (1981) introduced a micro-processor controlled rillmeter which can measure the soil surface topography with the vertical resolution of 1 mm over a 25 cm range. It could measure 300 surface elevations in less than 1 minute and be driven by battery. The measurement could be automatically recorded. This is a very good tool to measure the volume change of the soil erosion. The disadvantage of this rillmeter was that it had to be mounted on two paralleled tracks, and the distance between the two tracks limited the area it could cover. No further information was available about this rillmeter and no literature about soil erosion addressed the application of this tool.

A datum was used to measure the height difference before and after the rainfall simulation in this research. For the simulation area, 64 points were initially measured. To verify the volume method, the weight method was also used in the experiments together with the volume method in the Phase 4 and 5. During the erosion simulation, the eroded soil particles left on the flume were washed into a large vessel, which collected all the runoff from the simulation at the end of flume. The runoff and eroded soil mixture in the bucket was sampled and evaporated to measure the total weight to verify the relationship between the volume and weight. In Phase 4, experiments were conducted with 4% and 6% slope and weight measurement. Triplicate experiments of 6% slope and duplicate 4% slope experiments were designed to test the repeatability of soil erosion and the volume-weight correlation. The test results of soil erosion are listed in Appendix G.

From the Appendix G, the standard deviations of soil volume loss are generally much higher than that of soil weight loss. The main reason for these high standard deviations is that the soil surface was adjusted before every experiment, so that the soil surface could be kept for the designed slope. But, the adjustment also changed the soil shear strength and compressive, which was shown very clearly in the Appendix F. However, the standard deviation of weight loss is small. Therefore, the repeatability of soil erosion is good for real heterogeneous soils were used in the research. But, the measurements of soil volume is not accurate enough because of the high standard deviations.

To verify the correlation of volume loss and weight loss, four figures were plotted for three soils. Figure 5-3, 5-4, 5-5 and 5-6 show there is no correlation between soil

volume loss and weight loss using the coarse grid measurements. Therefore, Phase 5 was designed to increase the volume change measurement points from 64 to 225 on the same soil surface area. The experiments were conducted on 3 soils and solely on 4% slope in triplicate.

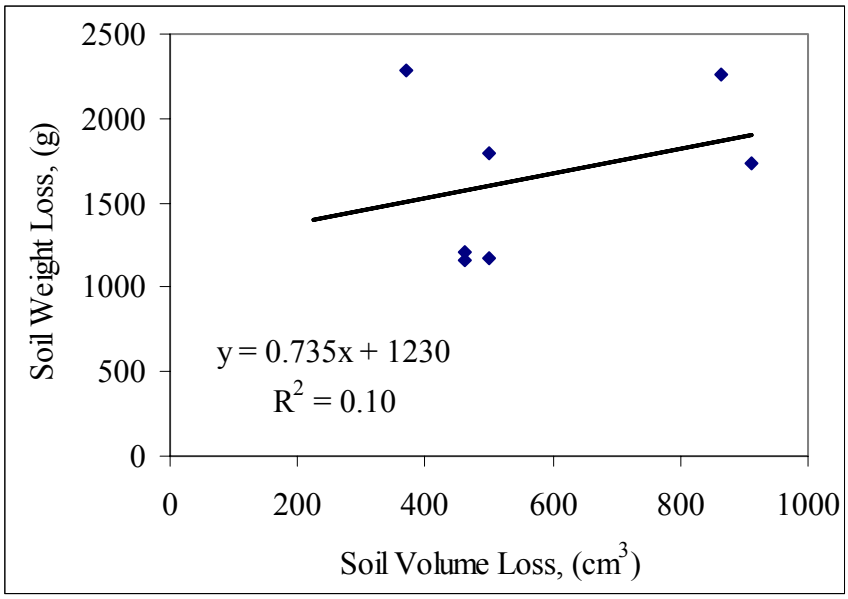

Figure 5-3. Weight Vs. Volume Method, (Soil 1, coarse grid measurement)

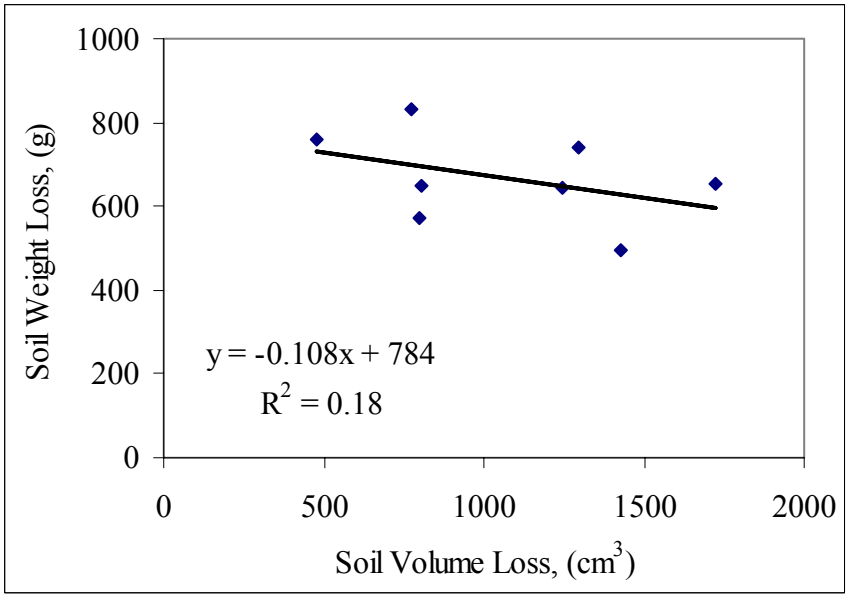

Figure 5-4. Weight Vs. Volume Method, (Soil 3, coarse grid measurement)

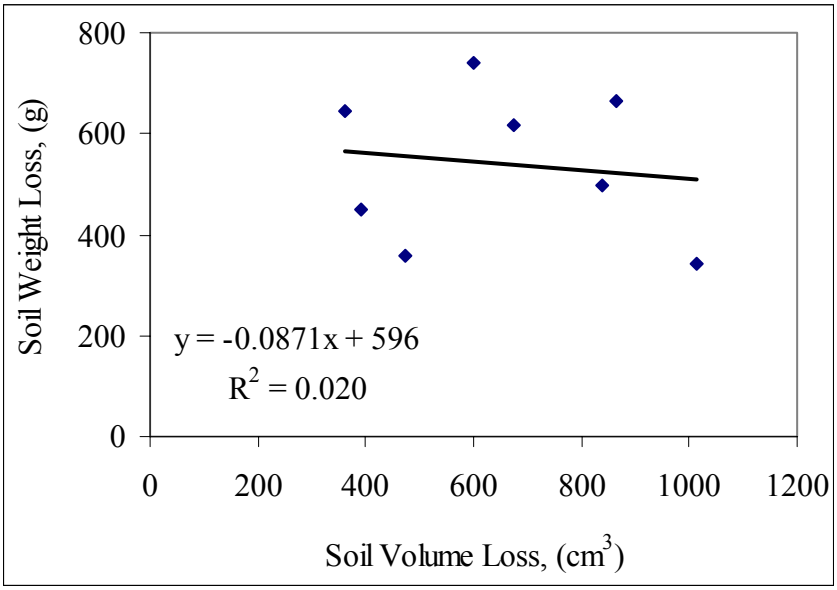

Figure 5-5. Weight Vs. Volume Method, (Soil 4, coarse grid measurement)

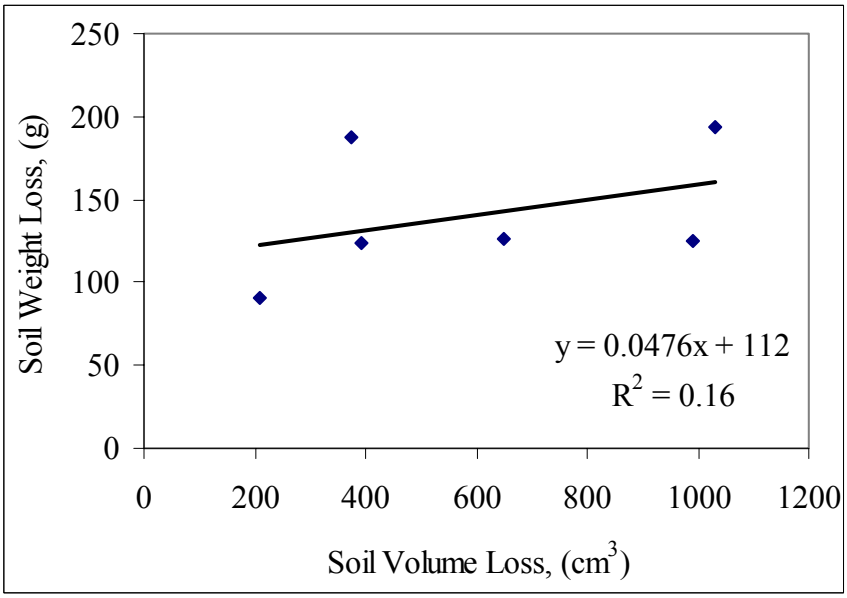

Figure 5-6. Weight Vs. Volume Method, (Soil 5, coarse grid measurement)

The experimental results are shown in Appendix H. It can be seen from Appendix H that the standard deviation is dramatically decreased, demonstrates that the repeatability of

soil erosion is very good. The standard deviation of weight loss is about the same as the results from Appendix G.

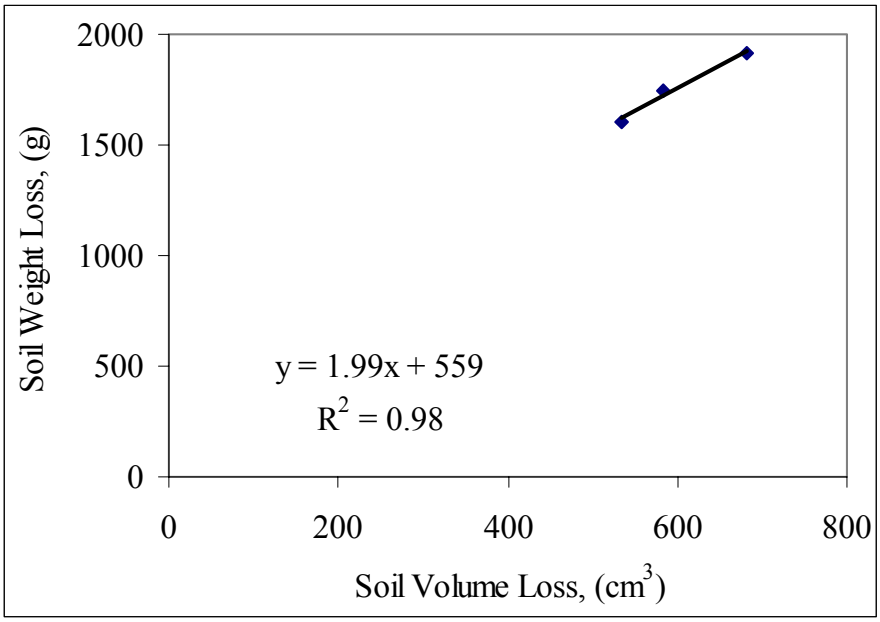

Figure 5-7. Weight Vs. Volume, (Soil 1, fine grid measurement).

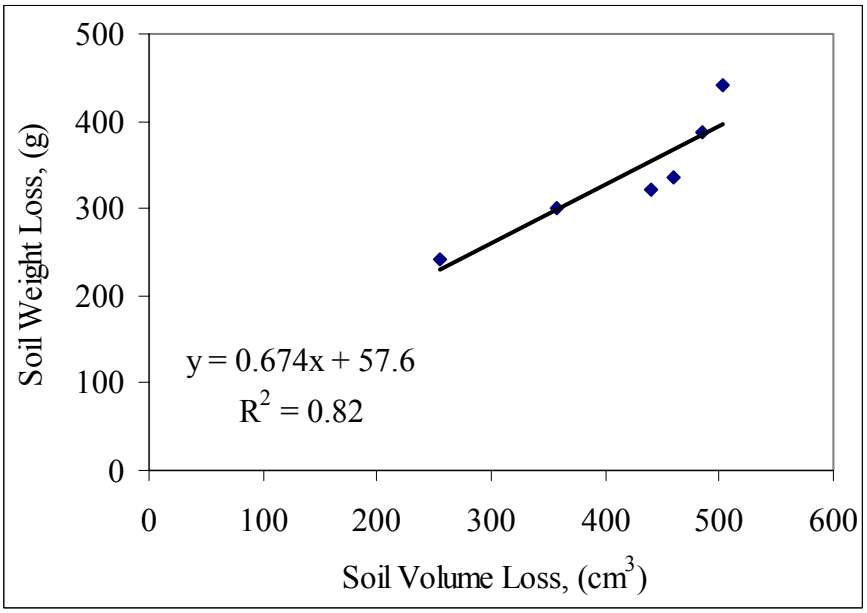

Figure 5-8. Weight Vs. Volume, (Soil 4, fine grid measurement).

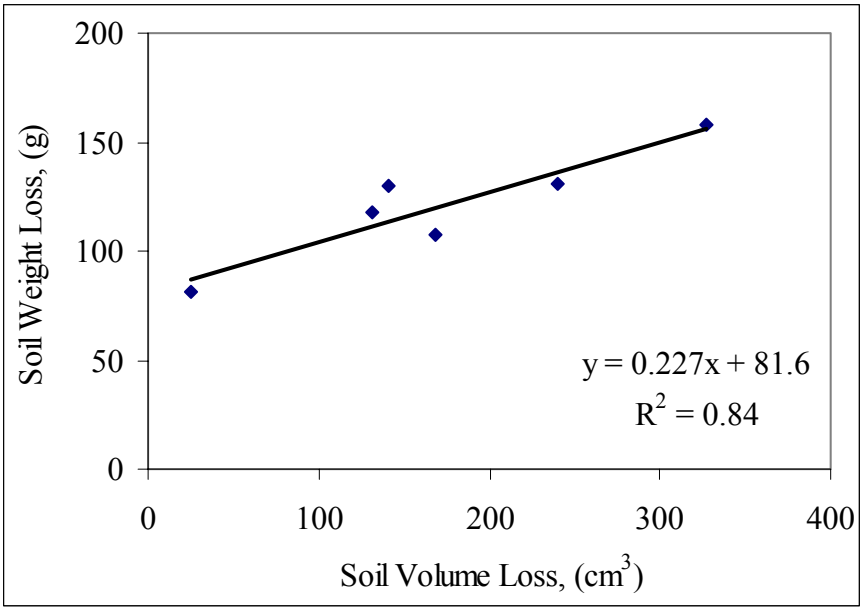

Figure 5-9. Weight Vs. Volume, (Soil 5).

From Figure 5-7, 5-8 and 5-9, it is very clear that there is a positive linear correlation between the soil volume loss and weight loss after using the increased number of measurements. The volume-weight correlation is different for different soil. Therefore, from the experiments of Phase 5, the volume method applied is as accuracy as that of weight method when using the 225 measuring points. Unfortunately, these results indicate there is a major source of error in the data collected and the results derived from the first 4 phases of the study. In the future, the volume measurement should be as intensive as possible to accurately estimate soil erosion.

CHAPTER 6

CONCLUSIONS

Two hundred and thirty seven rainfall-induced soil erosion simulations were conducted to assist in predicting soil loss and subsequent increase in total suspended solids leaving a highway construction site during a rainfall event. A rainfall simulator and an inclined, 4.8 m-long and 1.2 m-wide water flume are the major equipment for the research**.** Soil shear strength, compressive strength, rainfall intensity, soil bed slope and water erosion power were treated as variables during the simulation. Rainfall duration is fixed to 30 minutes to compare with other researcher' work.

The results of this study confirmed that higher rainfall intensity produced more erosion. The soil with higher shear strength, on the average, exhibited lower soil erosion, but soil loss appears to be independent of shear strength at low rainfall intensity. Compressive strength is a predictor of resistance to soil erosion. Lower soil loss could be expected for the cohesive soil if the compressive strength is high. In the situation of low slope steepness and short slope length, soil loss is independent to the slope steepness. A water erosion power concept was developed but is not good enough to predict the amount of soil erosion solely, in part because it neglects soil properties.

Multiple regression analysis was used to incorporate soil and rainfall properties into a single prediction equation. An additive model and a product model were developed. The product model was selected because it is similar to earlier models, and at zero rainfall it

predicts zero erosion whereas the additive model violates this intuitive limit. The magnitude of the product model exponents can be interpreted in a factor analysis fashion suggesting that the importance of predictive variables decreases in the following order for cohesive soils (ignoring the parameter of intercept): shear strength, rainfall intensity, compressive strength, and slope. The ranking when sand is included is: rainfall intensity, compressive strength, shear strength and slope.

As indicated in the literature, the RUSLE is not suitable for estimating soil erosion caused by single rainfall event. Thus, it is a poor tool for estimating soil loss over short construction periods (less than 1 year). Also, the MUSLE, which is currently used by TXDOT, will probably overestimate the soil erosion during rainstorm events. Engineers will oversize the erosion control devices according to the results from MUSLE. In the current study, the soil erosion predicted by MUSLE happened to be the same as that of RUSLE. The distribution of soil erosion results predicted by RUSLE and MUSLE at the bare soil condition are much more scattered than the developed product model. Most of the estimation are over-estimations. The rainfall kinetic energy simulated by this research is 25% to 55% lower than that of natural rainfall. However, if the simulated rainfall kinetic energy could be adjusted to the same as that of natural rainfall, the distribution of the product model prediction result is still much more closer to the measured results than the results predicted by the RUSLE and MUSLE.

Most of the volume change data collected in this study to estimate soil volume loss was too widely spaced to accurately determine the actual amount of soil loss. It was only

when the density of sampling points was increased almost 4-fold that the volume-based measurement became a good approximation of weight-based soil loss measurement. Weight-based soil loss estimates are widely used by other researchers, however, the volume method could have extreme value in the highway construction conditions. With the continual improvements of Global Positioning Systems, the volume change at a field scale, especially over large areas, could be accurately measured. Also, with the development of computer image analyzing technology, every pixel of photograph taken on the landscape could be analyzed, so that, large areas of soil volume change could be recorded easily. This way, the approach used in this research, and similar work in the future could be applied in the field without difficulties associated with collecting and weighing solids.

The validity of the empirical equations developed in this study is limited by the potential error introduced by using low density soil sampling to estimate soil erosion. Nonetheless, the general approach and conclusion should remain valid.

The approach presented in this work should be applicable to bare soils whose textures are comparable to soils tested in this study. In highway construction planning, such a model could be applied directly to a homogeneous slope to estimate the possible soil erosion. The advantage of this approach is that the use of directly measurable properties of the soils reduces the need to rely upon non-measurable properties such as erosion control factors, cover and management factors, and support practice factors in predicting soil erosion.

CHAPTER 7

FUTURE WORK

- Volume measurement points should be increased to allow soil loss to be accurately measured. In particular, Phase 1-4 of this study should be re-run with a high density volume grid to improve the predictability of the soil loss model.
- More texturally varied soils need to be examined to expand the applicability of the model to more soils.
- Field scale test is necessary to expand the model to highway construction sites.
- Computer controlled measurement tool would be developed to eliminate the tedious manual measurement and measurement errors.
- Future research should expand the current research to the side slopes of the highway.

REFERENCES

Al-Durrah, M. M. and J. M. Bradford, 1981. New methods of studying soil detachment due to waterdrop impact. *Soil Science Society of America Journal*, 45, 949-953.

Al-Durrah, M. M. and J. M. Bradford, 1982a. Parameters for describing soil detachment due to single waterdrop impact, *Soil Science Society of America Journal*, 46, 4, 836-840.

Al-Durrah, M. M. and J. M. Bradford, 1982b. The mechanism of raindrop splash on soil surfaces, *Soil Science Society of America Journal*, 46, 5, 1086-1090.

Bagnold, R. A., 1966. An approach to the sediment transport problem from general physics, *United States Geological Survey Professional Paper*, *422-I.*

Bomboi, M.T., and A. Hernandez, 1991. Hydrocarbons in Urban Runoff: Their Contribution to the Wastewaters, *Water Research*, 25, 5, 557-565.

Bryan, R. B. 1974. Water erosion by splash and wash and the erodibility of Albertan Soils, *Geografiska Annaler*, 56A, 3-4, 159-181.

Cooley, K. R. and Williams, J. R., 1985. Applicability of the universal soil loss equation (USLE) and modified USLE to Hawaii, In *International Conference on Soil Erosion and Conservation, "Malama Aina 83",* 509-522.

Das, B. M., 1994. Chapter 4, Soil compaction, In *Principles of Geotechnical Engineering*, 3rd ed. PWS Publishing Company, Boston. 88-128.

Driver, N. E. and M. H. Mustard, 1984. U. S. Geological Survey urban-hydrology data base for 22 metropolitan areas throughout the United States. American Geophysical Union, 1984 Fall meeting. San Francisco, CA, United States. Dec. 3-7, 1984. *Eos, Transactions, American Geophysical Union*.65; 45, 885.

EarthInfo Inc., 1996. NCDC Hourly and 15 minute Precipitation.

Ekern, P. C., Jr., and R. J. Muchenhirn, 1947. Waterdrop impact as a force in transporting sand. *Soil Science Society of America*, 12, 441-444.

EPA, 1983. Results of the Nationwide Urban Runoff Program: Volume I - Final Report, Water Planning Division, United States Environmental Protection Agency, National Technical Information Service, Publication Number PB84-185552.

EPA, 1998. National Pollutant Discharge Elimination System--Proposed Regulations for Revision of the Water Pollution Control Program Addressing Storm Water Discharges. *Federal Register*, Vol. 63, No. 6, January 9, 1998/Proposed Rules. 1535-1643.

Fan, J. C., 1987. Measurements of Erosion on Highway Slopes and Use of the Universal Soil Loss Erosion Equation. Doctoral Degree Dissertation, Purdue University, West Lafayette, IN, US. Pages: 390.

Farmer, E. E. and J. E. Fletcher, 1977. Highway Erosion Control Systems: An Evaluation Based on the Universal Soil Loss Equation In *Soil Erosion: Prediction and Control*. Soil Conservation Society of America. Ankeny, IA. 12-21.

Finkel, H. J., 1986. Chapter 3. The Soil erosion process, In *Semiarid Soil and Water Conservation*, 27-37.

Flaxman, E. M., 1962. A method of determining the erosion potential of cohesive soils. *I. A. S. H. Commission of Land Erosion,* 59, 114-123.

Foster, G. R., 1982. Chapter 8. Modeling the erosion process. In *Hydrologic Modeling of Small Watersheds*. ASAE Monograph, 5, 297-380.

Fraser, A. B. Bad Meteorology: Raindrops are shaped like teardrops. http://www.ems.psu.edu/~fraser/Bad/BadRain.html

Fullerton, M. J. and L. B. Fullerton, 1973. Rill formation in a homogeneous medium and its relationship to slope angle, *Abstracts with Programs for 1973,* 316.

Gabriels, D. and M. De Boodt, 1975. A rainfall simulator for soil erosion studies in the laboratory, *Pedologie,* 25, 2, 80-86.

Govers, G., 1990. Empirical relationships for the transport capacity of overland flow: Erosion, transport, and deposition process, *IAHS Publ*., 189, 45-63.

Govers, G., and G. Rauws, 1986. Transporting capacity of overland flow on plane and on irregular beds, *Earth Surface Processes and Landforms,* 11, 515-524.

Hairsine, P. B. and C. W. Rose, 1992a. Modeling water erosion due to overland flow using physical principles, 1, Sheet flow. *Water Resources Research,* 28, 237-243.

Hairsine, P. B. and C. W. Rose, 1992b. Modeling water erosion due to overland flow using physical principles, 2, Rill flow. *Water Resources Research,* 28, 245-250.

Haji, G, H., B. Hussain, and O. N. Wakhlu, 1988. Soil erosion; a function of shear resistance, In *Evaluation and Applications in Geotechnical Engineering*. 455-459.

Hall, M. J., 1970. A critique of methods of simulating rainfall, *Water Resources Research,* 6, 1104-1114.

Huang, C. and J. M. Bradford, 1993. An empirical analysis of slope and runoff factors for Soil erosion, In American Society of Agronomy, Crop Science Society of America

and Soil Science Society of America; 1993 annual meetings; *Agronomy Abstracts*. 85; 317.

Hussein, M. H., 1996. Analysis of rainfall, runoff and erosion in the low rainfall zone of northern Iraq. *Journal of Hydrology*. 181, 1-4, 105-126.

Kamalu, C., 1992. Soil erosion on road shoulders-The effects of slope length and on the separate and combined actions of rainfall and runoff (Part 1), In *The Environment Is Our Future*, 369-370.

Kung, S. K. J., 1984. Soil Erosion By Raindrop Impact. Doctoral Dissertation. Cornell University.

Learning Kingdom, 1998. Falling rain. http://mitk.learningkingdom.com/coolfact/2-4-98.html

Le Bissonnais, Y., M. J. Singer and J. M. Bradford, 1992. Assessment of soil erodibility: the relationship between soil properties, erosion processes and susceptibility to erosion, In *Farm land erosion: Temperate Plains Environment and Hills*. 87-96.

Le Bissonnais, Y., B. Renaux and H. Delouche, 1995. Interactions between soil properties and moisture content in crust formation, runoff and interrill erosion from tilled loess soils," *Catena*, 25, 1, 33-46.

Line, D. E. and L. D. Meyer, 1988. Comparing erodibilities of three soils of different textures, Paper no. 88-2594. ASAE, St. Joseph, MI.

Loch, R. J., 1984. Field rainfall simulator studies on two clay soils of the Darling Downs, Queensland; III, An evaluation of current methods for deriving soil erodibilities (K factors). *Australian Journal of Soil Research*, 22, 4, 401-412.

Luk, S. H., 1983. Effect of aggregate size and microtopography on rainwash and rainsplash erosion, *Zeitschrift fuer Geomorphologie*. 27, 3, 283-295.

Luk, S. H. and H. Hamilton, 1986. Experimental effects of antecedent moisture and soil strength on rainwash erosion of two Luvisols, Ontario. *Geoderma*. 37; 1, 29-43.

McCool, D. K., L. C. Brown, G. R. Foster, C. K. Mutchler and, L. D. Meyer, 1987. Revised slope steepness factor for the Universal Soil Loss Equation, *Transactions of the ASAE*, 30, 1387-1396.

McCool, D. K., G. R. Foster, C. K. Mutchler and L. D. Meyer, 1989. Revised slope length factor in the Universal Soil Loss Equation, *Transactions of the ASAE,* 30, 1571-1576.

Merritt, E., 1984. The identification of four stages during micro-rill development, *Earth Surface Processes and Landforms*, 9, 493-496.

Meyer, L. D., 1981. How rain intensity affects interrill erosion, *Trans. ASAE*, 24, 1472-1475.

Meyer, L. D., 1988. Chapter 4, Rainfall simulators for Soil conservation research, In *Soil Erosion Research Methods*, 75-95.

Meyer, L. D. and W. C. Harmon, 1989. How row-sideslope length and steepness affect sideslope erosion, *Trans. ASAE,* 32, 639-644.

Meyer, L. D. and D. L. McCune, 1958. Rainfall simulator for runoff plots. *Agricultural Engineering*, 39, 10, 644-648.

Miller, W. P., 1987. Infiltration and soil loss of three gypsum-amended ultisols under sikulated rainfall. *Soil Science Society of America Journal,* 51, 5, 1314-1320.

Montoya, D. R. and K. W. Brown, 1984. Erodibility of strip-mine spoils. *Soil Science*, 138, 5, 365-373.

Mutchler, C. K. and Hermsmeier, L. F., 1965. A Review of Rainfall Simulators, *Transactions of the ASAE*, 8, 67-68.

Mutchler, C. K. and Moldenhauer, W. C., 1963. Applicator for laboratory rainfall simulator. *Transactions of the ASAE*, 6, 3, 220-222.

Mutchler, C. K. and Murphree, C. E. Jr., 1985. Experimentally derived modification of the USLE, *Proceedings of the International Conference on Soil Erosion and Conservation, "Malama Aina 83",* 523-527.

Nearing, M. A., 1991. A probabilistic model of soil detachment by shallow turbulent flow. *Transactions of the ASAE ,* 34, 81-85.

Nearing, M. A., G. R. Foster, L. J. Lane and S. C. Finkner, 1989. A process-based soil erosion model for USDA-Water Erosion Prediction Project Technology. *Transactions of the ASAE,* 32, 5, 1587-1593.

Nearing, M. A., L. J. Lane, E. E. Alberts and J. M. Laflen, 1990. Prediction technology for soil erosion by water: Status and research needs. *Soil Science Society of America, Journal of,* 54, 1702-1711.

Nearing, M. A., L. D. Norton, D. A. Bulgakov, G. A. Larionov, L. T. West and K. M. Dontsova, 1997. Hydraulics and erosion in eroding rills. *Water Resources Research*, 33, 4, 865-876.

Neibling, W. H., G. R. Foster, R. A. Nattermann, J. D. Nowlin and P. V. Holbert, 1981. Laboratory and field testing of a programmable plot-sized rainfall simulator, In *Erosion and Sediment Transport Measurement (Proceedings of the Florence Symposium)*, 405-414.

Novotny, V. and G. Chesters, 1989. Delivery of sediment and pollutants from nonpoint sources: A water quality perspective." *Journal of Soil and Water Conservation*, 44(6), 568-576.

O'Flaherty, C. A., 1986. In *Highways, Vol. 1, Traffic planning and engineering*, 3rd ed. 390-392.

Oglesby, C. H. and R. G. Hicks, 1982. In *Highway Engineering*, 4th ed. John Wiley & Sons, 311-312.

Onstad, C. A., J. K. Radke and R. A. Young, 1981. An outdoor portable rainfall erosion laboratory, In *Erosion and Sediment Transport Measurement (Proceedings of the Florence Symposium,* 415-422.

Parsons, D. A., 1943. Discussion of "The application and measurement of artificial rainfall on Types FA and F infiltrometer." *American Geophysical Union*, *Transactions,* 24, 485-487.

Pechacek, L. D., 1993. Urban stormwater runoff based on singular landuse activity and particle size distribution, Masters Thesis, Department of Civil and Environmental Engineering, University of Houston, Houston, Texas.

Proffitt, A. P. B. and C. W. Rose, 1991. Soil erosion processes; I, The relative importance of rainfall detachment and runoff entrainment. *Australian Journal of Soil Research*, 29; 5, 671-683.

Radke, J. K., M. A. Otterby, R. A. Young and C. A. Onstad, (1981). A microprocessor automated rillmeter. *Transactions of American Society of Agriculture Engineers*. 24,

Rauws, G. and G. Govers, 1988. Hydraulic and soil mechanical aspects of rill generation on agricultural soils. *Journal of Soil Science*, 39, 111-124.

Renard, K. G., G. R. Foster, G. A. Weesies and J. P. Porter, 1991. RUSLE Revised universal soil loss equation, *Journal of Soil and Water Conservation*, 46, 30-33.

Renard, K G., G. R. Foster, D. C. Yoder and D. K. McCool, 1994. RUSLE revisited: Status, questions, answers, and the future. *Journal of Soil & Water Conservation*, 49, 3, 213-220.

Renard, K. G., G. R. Foster, G. A. Weesies, D. K. Cool, and D. C. Yoder. 1997. In *Predicting Soil Erosion by Water: A Guide to Conservation Planning with the Revised*

Universal Soil Loss Equation (RUSLE). USDA-ARS, Agriculture Handbook Number 703.

Rose, C. W., J. R. Williams, G. C. Sander and D. A. Barry, 1983a. A mathematical model of soil erosion and deposition processes, I, Theory for a plane land element. *Soil Sci. Soc. Am. J., 47.* 991-995.

Rose, C. W., J. R. Williams, G. C. Sander and D. A. Barry, 1983b. A mathematical model of soil erosion and deposition processes, II, Application to data from an arid-zone catchment, *Soil Sci. Soc. Am. J., 47*, 996-1000, 1983.

Rose, C. W., 1985. Developments in erosion and deposition models. In *Advances in Soil Science*, Vol. 2, ed. B. A. Stewart, 1-63.

Sander, G. C., , P. B. Hairsine, C. W. Rose, D. D. Cassidy, J. Y. Parlange, W. L. Hogarth and I. G. Lisle, 1996. Unsteady soil erosion model, analytical solutions and comparison with experimental results, *Journal of Hydrology*, 178, 1-4, 351-367.

Schroeder, S. A., 1987. Slope gradient effect on erosion of reshaped spoil, *Soil Science Society of America Journal*, 51, 2, 405-409.

Sherrard, H. M., 1958. In *Australian Road Practice; an Introduction to Highway Engineering*. Melbourne University Press, 248-350.

Singer, M. J. and J. Blackard, 1982. Slope angle-interrill soil loss relationships for slopes up to 50%, *Soil Science Society of America Journal,* 46; 6, 1270-1273.

Singer, M. J. and P. H. Walker, 1983. Rainfall-runoff in soil erosion with simulated rainfall, overland flow and cover, *Australian Journal of Soil Research*, 21, 2, 109-122.

Slattery, M. C. and R. B. Bryan, 1992. Hydraulic conditions for rill incision under simulated rainfall; a laboratory experiment, *Earth Surface Processes and Landforms,* 17, 2, 127-146.

Smith, D. D. and W. H. Wischmeier, 1957. Factors affecting sheet and rill erosion, *Transactions, American Geophysical Union*, 38, 6, 889-896.

Swanson, N., 1965. Rotating-boom rainfall simulator. *Transactions of the ASAE*. 8, 71-72.

Tan, S. K., 1989a. Erosion by raindrops, In *Proceedings of the International Symposium on River Sedimentation*, 4, 192-199.

Tan, S. K., 1989b. Erosion of clays by rainfall, In *Hydraulics and the environment; proceedings of the XXIII congress of the International Association for Hydraulic Research*; 23, B547-B554.

Truman, C. C. and J. M. Bradford, 1993. Relationships between rainfall intensity and the interrill Soil loss-slope steepness ratio as affected by antecedent water content, *Soil Science*, 156, 6, 405-413.

Turner, A. K., T. A. McMahon and R. Srikanthan, 1985. Rainfall intensity and overland flow in relation to soil erosion studies for tropical lands, In *Soil Erosion Management*. (ACIAR Proceedings Series). 24-31.

ULI, ASCE and NAHB, 1978. In *Residential Erosion and Sediment Control: Objectives, Principles and Design Considerations*, pages 21-29.

USDA-NRCS, 1996. Soil Loss Equation Federal Register Notice, *Federal Register*, Vol. 61, No. 108, June 4, 1996/Rules and Regulations.

Vice, R. B., Guy, H. P., and Fergnson, G. E., 1969. Sediment movement in an area of suburban highway construction, Scott Run Basin, Fairfax Co., Virginia, 1961-1964. *U. S. Geological Survey Water Supply Paper 1591-E*.

Vipulanandan, C., R. J. Krizek and M. L. Wilkey, 1982. Erosion Model for Reclamation Areas. *Proceedings of the 1982 Symposium on Surface Mining Hydrology, Sedimentology and Reclamation. 339-348.*

Vose Jr., W. O. and P. N. Smith, 1993. In *TXDOT Storm Water Management Guidelines for Construction Activities*. Division of Bridges and Structures, Hydraulics Section for Storm Water Management Task Force.

Wang, G. P., Z. P. Wei, and Z. G. Zhang, 1994. Soil shear strength; an indicator for erodibility of the loess Soils, *International Journal of Sediment Research,* 9; 1, 77-91.

Weggel, J. R. and R. Rustom, 1992. Soil Erosion by Rainfall and Runoff -- State of the Art, *Geotextiles and Geomembranes,* 11, 4-6, 551-572.

Wheeler, F. F., 1976. Soil Survey of Harris County, Texas. By USDA-Soil Conservation Service, Texas Agricultural Experiment Station and the Harris County Flood Contral District.

Williams, J. R. 1975. Sediment-yield prediction with universal equation using runoff energy factor, In: Present and Prospective Technology for Predicting Sediment Yield and Sources. USDA, ARS-S-40, 244-252.

Winslow and Associates, and McClelland Engineers, 1985. Barker Reservoir watershed sedimentation study, Final report to Harris County Flood Control District, Houston, Texas.

Wischmeier, H. H., 1976. Use and misuse of the universal soil loss equation, *Journal of Soil and Water Conservation*, 31, 1, 5-9.

Wischmeier, W. H, 1977. Soil erodibility by rainfall and runoff, In *Erosion; Research Techniques, Erodibility and Sediment Delivery*. Pages, 45-56.

Wischmeier, W. H. and D. D. Smith, 1958. Rainfall energy and its relationship to soil loss, *Transactions, American Geophysical Union*, 39, 285-291.

Wischmeier, W. H. and D. D. Smith, 1978. Predicting rainfall erosion losses, A Guide to Conservation Planning, Handbook. No. 537, USDA, Washington, D. C., 1978.

Wischmeier, W. H., D. D. Smith and R. E. Uhland, 1958. Evaluation of Factors in the Soil Loss Equation, *Agricultural Engineering*, 39, 458-462, 474.

Xanthopoulos, C., and A. Augustin, 1992. Input and Characterization of Sediments in Urban Sewer Systems, *Water Science and Technology*, 25, 8, 21-28.

Yang, C. T., 1972. Unit stream power and sediment transport, *Journal of the Hydraulics Division,* ASCE, 18, HY10, 1805-1826.

Yang, C. T., 1979. Unit stream power equations for total load, *Journal of Hydrology*, 40, 123-138.

Yang, C. T., 1984. Unit stream power equation for gravel, *Journal of the Hydraulics Engineering,* ASCE, 110, HY12, 1783-1797.

Yang, C. T., 1987. Chapter 8, Sediment transport and unit stream power, In *Water Resources Environmental*, ed P. N. Cheremisinoff, N. P. Cheremisinoff and S. L. Cheng, 265-289.

Yang, C. T. and A. Molinas, 1982. Sediment transport and unit stream power function, *Journal of the Hydraulics Division,* ASCE*,* 108, HY6, 774-793.

Young, R. A. and J. L. Wiersma, 1973. The role of rainfall impact in soil detachment and transport, *Water Resource Research*, 9, 6, 1629-1636.

Zhang, X. C., M. A. Nearing, L. M. Risse and K. C. McGregor, 1996. Evaluation of WEPP runoff and soil loss predictions using natural runoff plot data. *Transactions of the ASAE*, 39, 3, 855-863.

Zingg, A. W., 1940. Degree and length of land slope as it affects soil loss in runoff, *Agricultural Engineering*, 21, 59-64.

Appendix A

Survey Of Highway Grades in the States Of Florida, Louisiana, Texas, Arizona, and Colorado

The survey of highway grades and the relative centerline mileage was conducted in several states in southern US. The Departments of Transportation (DOT) of Florida, Louisiana, Texas, Arizona, and Colorado had been contacted. They all replied to the survey and provided relative information. Most of the DOTs do not organize the grades and its relative centerline mileage together except Florida DOT. However, they provided the highway design criteria enforced in their state.

Florida

The highway performance monitoring system of the Florida DOT has sample sections on the state highway system. The total sample data represents about 20% of the total mileage of the Florida highway. Table A-1 from Florida DOT provided the statistical information of their highway grades and related centerline mileage.

Table A-1. Centerline Miles of Major Florida Roads

Functional Classification	Class A 0.0-0.4%	Class B 0.5-2.4%	Class C 2.5-4.4%	Class D 4.5-6.4%	Class E 6.5-8.4%	Class F 8.5 & up	Sample Length
Rural Interstate	343.6	8.1	5.2	0.0	0.5	0.0	356.7
Rural Other Principal Arterial	740.3	30.5	10.4	0.8	0.0	0.0	783.7
Rural Minor Arterial	309.2	15.4	4.0	1.6	0.0	0.0	331.5
Urban Interstate	215.5	10.0	1.1	0.0	0.0	0.0	226.4
Urban Freeways	112.9	5.7	1.8	0.4	0.0	0.0	121.1
Urban Other Principal Arterial	520.2	9.9	6.9	0.0	0.3	1.2	525.2
Total for Sample	2,241.7	79.5	29.4	2.7	0.8	1.2	2,344.6
% of Total	95.6%	3.4%	1.3%	0.1%	0.0%	0.0%	100%

Louisiana

Louisiana DOT conducted a similar survey of highway grades and relative centerline mileage. However, they couldn't locate the report of that survey. Mr. Nick Kalivoda remembered that from the report that about 99% of the highway in Louisiana has a grade lower than 1%. A summary of their highway design standard is shown in Table A-2.

Table A-2. Design Standard of Grades for Louisiana Highway

Items	Type	Design Speed, (km/h)	Pavement Cross Slope (m/m)	Maximum Grade (%)
Freeways	F-1	80	0.025	4
	F-2	100	0.025	3
	F-3	120	0.025	3
Arterial Roads and Streets	Rural	100-110	0.025	3
	Urban	60-70	0.025	7-6
Collector Roads and Streets	Rural	100	0.025	7-5
	Urban	50-70	0.025	9-8
Local Roads and Streets	Rural	50-80	0.025	9-8
	Urban	30-50	0.025	10-9

Texas

Texas Department of Transportation (TxDot) does not arrange their database in the form of highway grades and related centerline mileage. However, they provided the highway design guideline. A summary of TxDot highway design standard is shown in Table A-3.

Table A-3. Design Standard of Maxiumu Grades for Texas Highway

Functional Classification		Type of Terrain	Design Speed, mph				
			30	40	50	60	70
Urban	Local	All	<15	<15			
	Collector	Level	7	7	6	-	-
		Rolling	9	8	7	-	-
	Arterial	Level	7	7	6	5	-
		Rolling	9	8	7	6	-
	Freeway	Level	-	-	4	3	3
		Rolling	-	-	5	4	4
Rural	Local	Level	7	7	6	5	-
		Rolling	10	9	8	6	-
	Collector	Level	7	7	6	5	-
		Rolling	9	8	7	6	-
	Arterial	Level	-	-	-	3	3
		Rolling	-	-	-	4	4
	Freeway	Level	-	-	4	3	3
		Rolling	-	-	5	4	4

Arizona

Like Texas, Arizona Department of Transportation does not arrange their database in the form of highway grades and related centerline mileage, either. They provided the highway design guideline. A summary of Arizona DOT highway design standard is shown in Table A-4.

Table A-4. Design Standard of Maxiumu Grades for Arizona Highway

Conditions		Design Speed (km/h)							
		50	60	70	80	90	100	110	120
Controlled Access Highways	Level Terrain						3%	3%	3%
	Rolling Terrain					4%	4%		
	Mountainous Terrain		6%	6%	6%	6%	5%		
	Urban/Fringe Urban Areas		4%	3%	3%				
Rural Divided Highways	Level Terrain					3%	3%	3%	
	Rolling Terrain			5%	4%	4%			
	Mountainous Terrain		7%	7%	6%				
Rural Non-Divided Highways	Level Terrain					3%	3%	3%	
	Rolling Terrain			4%	4%	4%			
	Mountainous Terrain		7%	7%	6%				
Urban/Fringe Urban Highways Arterial Streets	Level Terrain		8%	7%	6%	6%	5%		
	Rolling Terrain	9%	8%	7%	7%	6%			
	Mountainous Terrain	11%	10%	9%	9%	8%			

Colorado

Colorado Department of Transportation does not publish a list of grades for the state highway system. A mountain passes list for travelers were provided representing the maximum grades of highways in Colorado. Table A-5 shows this list.

Table A-5. Mountain Passes with Settpest Grades Above 3% in Colorado Highways

Pass	Elevation, feet	State Highway	Steepest Grade above 3%
Berthoud Pass	11,315	U.S. 40	North side 6.1%, South 6%
Cumbres	10,022	S.H. 17	6.30%
Fremont	11,318	S.H. 91	5.70%
Hoosier	11,541	S.H. 9	North side 8%
Independence	12,095	S.H. 82	6%
Kenosha	10,001	U.S. 285	East side, 5.3%
La Manga	10,230	S.H. 17	5.20%
Lizard Head	10,222	S.H. 145	4.10%
Loveland	11,992	U.S. 6	6%
Milner	10,758	U.S. 34	West side, 5.4%
Molas Divide	10,910	U.S. 550	7% and greater
Monarch	11,312	U.S. 50	6.40%
Cochetopa	10,149	S.H. 114	6%
Red Mountain	11,018	U.S. 550	7% and greater
Slumgullion	11,361	S.H. 149	North side 9.4%, South 7.9%
Spring Creek	10,901	S.H. 149	7.5%
Tennessee	10,424	U.S. 24	6%
Trail Ridge High Point	12,183	U.S. 34	West side, 5.4%
Vail	10,666	I-70	7%
Wolf Creek	10,850	U.S. 160	6.80%

Appendix B

General Data Table Of Experimental Data

Soil	Case Number	Slope	Shear Strength (N/cm^2)	Compressive Strength (N/cm^2)	Rainfall Intensity (mm/h)	Moisture Content (%)	Flow Depth (mm)	Flow Velocity (m/s)	Erosion Power (w)	Soil Loss (cm^3)	U. Soil Loss in 0.5 hour (cm^3/m^2)	Weight (g)
	S12	0.001	5.21E-01	7.88E-01	1.27E+01	24.5	0.7	2.00E-03	4.1E-02	1.36E+02	2.06E+02	
	S87	0.001	6.91E-01	1.19E+00	1.28E+01	13.3	0.7	2.00E-03	4.2E-02	4.13E+01	6.25E+01	
	S11	0.001	6.27E-01	8.71E-01	2.56E+01	27.6	1.1	2.00E-03	8.4E-02	6.01E+02	9.09E+02	
	S86	0.001	6.38E-01	1.19E+00	2.58E+01	12.4	1.1	2.00E-03	8.4E-02	1.73E+02	2.62E+02	
	S10	0.001	5.00E-01	8.61E-01	5.07E+01	22.1	1.2	4.00E-03	1.7E-01	9.16E+02	1.39E+03	
	S85	0.001	6.27E-01	1.42E+00	5.06E+01	10.7	1.2	4.00E-03	1.7E-01	5.81E+02	8.80E+02	
	S84	0.001	5.21E-01	1.59E+00	7.63E+01	5.0	1.7	2.00E-02	2.5E-01	1.50E+03	2.27E+03	
	S9	0.001	7.76E-01	8.71E-01	1.02E+02	24.4	2.7	3.70E-02	3.3E-01	1.40E+03	2.13E+03	
	S83	0.001	5.96E-01	1.32E+00	1.02E+02	9.4	2.7	3.70E-02	3.4E-01	1.67E+03	2.53E+03	
	S8	0.005	5.53E-01	9.04E-01	1.28E+01	18.8	0.8	2.00E-03	4.2E-02	4.22E+02	6.39E+02	
	S82	0.005	6.17E-01	1.27E+00	1.29E+01	11.3	0.8	2.00E-03	4.2E-02	5.88E+01	8.90E+01	
	S6	0.005	7.23E-01	8.41E-01	2.52E+01	8.8	0.8	2.00E-03	8.2E-02	1.20E+02	1.81E+02	
	S81	0.005	6.70E-01	1.35E+00	2.60E+01	8.5	0.8	2.00E-03	8.4E-02	2.68E+01	4.06E+01	
Soil 1	S7	0.005	7.66E-01	8.08E-01	5.06E+01	26.2	1.4	7.00E-03	1.6E-01	6.12E+02	9.26E+02	
Sand	S80	0.005	6.17E-01	1.24E+00	5.04E+01	10.8	1.4	7.00E-03	1.6E-01	3.82E+01	5.78E+01	
	S79	0.005	6.06E-01	1.40E+00	7.63E+01	16.3	2.0	2.70E-02	2.5E-01	7.95E+02	1.20E+03	
	S5	0.005	7.66E-01	9.34E-01	1.02E+02	18.1	1.9	2.70E-02	3.3E-01	2.19E+03	3.32E+03	
	S78	0.005	6.27E-01	1.37E+00	1.02E+02	7.5	1.9	2.70E-02	3.3E-01	1.26E+03	1.91E+03	
	S4	0.010	6.81E-01	8.28E-01	1.28E+01	17.5	0.8	2.00E-03	4.1E-02	1.99E+02	3.02E+02	
	S77	0.010	8.19E-01	1.36E+00	1.27E+01	12.3	0.8	2.00E-03	4.1E-02	3.30E+01	5.00E+01	
	S3	0.010	7.34E-01	8.08E-01	2.58E+01	19.7	1.0	3.00E-03	8.3E-02	5.71E+02	8.64E+02	
	S76	0.010	6.70E-01	1.25E+00	2.61E+01	11.4	1.0	3.00E-03	8.4E-02	1.33E+02	2.02E+02	
	S2	0.010	7.66E-01	9.87E-01	5.10E+01	14.6	1.3	4.00E-03	1.6E-01	8.18E+02	1.24E+03	
	S75	0.010	7.55E-01	1.23E+00	5.03E+01	11.9	1.3	4.00E-03	1.6E-01	1.21E+02	1.83E+02	
	S74	0.010	6.27E-01	1.32E+00	7.62E+01	9.1	1.9	1.80E-02	2.5E-01	6.84E+02	1.04E+03	
	S1	0.010	6.38E-01	6.78E-01	1.02E+02	17.7	2.5	3.10E-02	3.3E-01	2.23E+03	3.37E+03	

S73	0.010	5.96E-01	1.52E+00	1.01E+02	9.3	2.5	3.10E-02	3.3E-01	1.48E+03	2.24E+03	
S167	0.040	2.34E-01	1.07E+00	1.26E+01	11.8	0.0	1.67E-03	3.7E-02	1.80E+02	2.72E+02	
S166	0.040	4.25E-01	1.24E+00	2.56E+01	5.6	0.4	2.78E-03	7.6E-02	2.89E+02	4.37E+02	
S165	0.040	2.77E-01	9.64E-01	5.08E+01	11.3	0.8	4.47E-03	1.5E-01	2.25E+02	3.41E+02	
S200	0.040	1.81E-01	1.15E+00	5.12E+01	11.4	0.8	1.36E-03	1.5E-01	4.99E+02	7.56E+02	1.79E+03
S164	0.040	2.45E-01	9.61E-01	7.64E+01	10.7	1.1	2.39E-02	2.3E-01	8.12E+02	1.23E+03	
S199	0.040	1.60E-01	1.18E+00	7.59E+01	10.7	0.9	1.68E-03	2.3E-01	8.67E+02	1.31E+03	1.02E+03
S224	0.040	1.17E-01	9.51E-01	7.66E+01	11.4	1.1	2.73E-03	2.3E-01	5.35E+02	8.09E+02	1.61E+03
S225	0.040	1.17E-01	1.00E+00	7.57E+01	12.5	1.2	2.48E-03	2.3E-01	6.83E+02	1.03E+03	1.91E+03
S226	0.040	9.57E-02	1.11E+00	7.65E+01	9.1	1.6	3.34E-03	2.3E-01	5.82E+02	8.81E+02	1.75E+03
S163	0.040	2.34E-01	1.15E+00	1.02E+02	5.0	1.6	2.38E-02	3.1E-01	1.68E+03	2.55E+03	
S196	0.060	1.38E-01	1.08E+00	5.11E+01	10.9	0.2	8.33E-04	1.4E-01	4.98E+02	7.55E+02	1.17E+03
S197	0.060	2.45E-01	1.28E+00	5.11E+01	6.1	0.3	9.67E-04	1.4E-01	4.61E+02	6.98E+02	1.21E+03
S198	0.060	2.23E-01	1.10E+00	5.07E+01	8.4	0.3	1.14E-03	1.4E-01	4.63E+02	7.01E+02	1.16E+03
S193	0.060	2.13E-01	8.51E-01	7.48E+01	7.3	0.5	1.13E-03	2.1E-01	9.11E+02	1.38E+03	1.73E+03
S194	0.060	1.06E-01	9.90E-01	7.64E+01	8.1	0.1	8.33E-04	2.1E-01	8.65E+02	1.31E+03	2.26E+03
S195	0.060	1.06E-01	8.28E-01	7.52E+01	12.9	0.1	8.33E-04	2.1E-01	3.69E+02	5.59E+02	2.29E+03
S24	0.001	2.38E+00	1.99E-01	1.29E+01	418.6	2.6	3.00E-03	4.2E-02	6.48E+02	9.81E+02	
S102	0.001	2.17E+00	3.02E-01	1.27E+01	384.0	2.6	3.00E-03	4.1E-02	3.91E+02	5.92E+02	
S23	0.001	2.91E+00	2.13E-01	2.56E+01	391.3	3.1	4.00E-03	8.4E-02	4.72E+02	7.14E+02	
S101	0.001	2.55E+00	2.66E-01	2.58E+01	409.8	3.1	4.00E-03	8.4E-02	4.76E+02	7.20E+02	
S22	0.001	2.47E+00	2.06E-01	5.10E+01	445.3	3.5	7.00E-03	1.7E-01	8.79E+02	1.33E+03	
S100	0.001	2.84E+00	2.89E-01	5.07E+01	460.8	3.5	7.00E-03	1.7E-01	3.84E+02	5.81E+02	
S99	0.001	2.61E+00	2.83E-01	7.58E+01	480.2	3.3	1.10E-02	2.5E-01	7.28E+02	1.10E+03	
S21	0.001	2.30E+00	1.99E-01	1.02E+02	474.8	3.7	1.30E-02	3.3E-01	1.44E+03	2.18E+03	
S98	0.001	2.30E+00	2.83E-01	1.02E+02	429.2	3.7	1.30E-02	3.3E-01	9.95E+02	1.51E+03	
S20	0.005	2.67E+00	2.53E-01	1.31E+01	433.4	2.3	3.00E-03	4.2E-02	4.04E+02	6.11E+02	
S97	0.005	2.17E+00	3.12E-01	1.26E+01	497.5	2.3	3.00E-03	4.1E-02	4.99E+02	7.56E+02	
S19	0.005	2.82E+00	2.16E-01	2.54E+01	463.5	2.6	5.00E-03	8.3E-02	9.12E+02	1.38E+03	

Soil 2 Clay	S96	0.005	2.28E+00	3.36E-01	2.61E+01	442.0	2.6	5.00E-03	8.5E-02	3.26E+02	4.94E+02	
	S18	0.005	2.87E+00	1.89E-01	5.11E+01	449.0	2.8	7.00E-03	1.7E-01	8.15E+02	1.23E+03	
	S95	0.005	2.46E+00	3.26E-01	5.11E+01	401.6	2.8	7.00E-03	1.7E-01	2.62E+02	3.97E+02	
	S94	0.005	2.74E+00	3.06E-01	7.62E+01	509.1	2.9	9.00E-03	2.5E-01	9.11E+02	1.38E+03	
	S17	0.005	2.49E+00	1.86E-01	1.01E+02	440.9	3.0	7.00E-03	3.3E-01	9.85E+02	1.49E+03	
	S93	0.005	2.55E+00	3.52E-01	1.02E+02	474.7	3.0	7.00E-03	3.3E-01	8.64E+02	1.31E+03	
	S16	0.010	2.79E+00	2.06E-01	1.30E+01	423.1	1.8	5.00E-03	4.2E-02	2.18E+02	3.30E+02	
	S92	0.010	2.81E+00	3.26E-01	1.27E+01	423.2	1.8	5.00E-03	4.1E-02	1.63E+02	2.47E+02	
	S15	0.010	2.95E+00	2.09E-01	2.56E+01	427.1	2.5	6.00E-03	8.3E-02	4.34E+02	6.58E+02	
	S91	0.010	2.68E+00	2.96E-01	2.61E+01	454.3	2.5	6.00E-03	8.4E-02	4.61E+02	6.98E+02	
	S14	0.010	2.81E+00	2.06E-01	5.08E+01	388.7	2.1	9.00E-03	1.6E-01	6.02E+02	9.11E+02	
	S90	0.010	3.12E+00	3.56E-01	5.08E+01	450.3	2.1	9.00E-03	1.6E-01	6.76E+02	1.02E+03	
	S89	0.010	2.60E+00	3.32E-01	7.63E+01	423.3	2.7	1.30E-02	2.5E-01	6.65E+02	1.01E+03	
	S13	0.010	2.71E+00	2.19E-01	1.02E+02	366.8	3.0	1.70E-02	3.3E-01	1.15E+03	1.74E+03	
	S88	0.010	2.64E+00	3.09E-01	1.02E+02	458.7	3.0	1.70E-02	3.3E-01	6.42E+02	9.72E+02	
	S172	0.040	3.23E+00	4.12E-01	1.28E+01	396.3	1.6	2.98E-03	3.9E-02	2.33E+02	3.53E+02	
	S171	0.040	3.34E+00	4.55E-01	2.52E+01	389.8	1.9	6.85E-03	7.8E-02	2.33E+02	3.53E+02	
	S170	0.040	3.72E+00	4.29E-01	5.09E+01	409.4	2.0	1.28E-02	1.6E-01	4.81E+02	7.28E+02	
	S169	0.040	3.20E+00	4.62E-01	7.58E+01	406.7	2.1	2.46E-02	2.4E-01	1.04E+03	1.57E+03	
	S168	0.040	4.13E+00	4.85E-01	1.01E+02	354.8	2.6	3.73E-02	3.2E-01	1.07E+03	1.62E+03	
	S36	0.001	2.04E+00	1.83E-01	1.26E+01	85.2	0.9	3.00E-03	4.1E-02	3.13E+02	4.73E+02	
	S117	0.001	2.32E+00	2.66E-01	1.28E+01	56.8	2.0	4.00E-03	4.2E-02	5.51E+02	8.34E+02	
	S35	0.001	2.05E+00	1.76E-01	2.58E+01	74.0	1.6	5.00E-03	8.4E-02	5.54E+02	8.39E+02	
	S116	0.001	2.48E+00	3.16E-01	2.58E+01	55.4	2.0	7.00E-03	8.4E-02	6.06E+02	9.17E+02	
	S34	0.001	2.19E+00	1.63E-01	5.07E+01	76.4	2.0	9.00E-03	1.7E-01	6.59E+02	9.98E+02	
	S115	0.001	1.88E+00	2.96E-01	5.10E+01	49.3	2.0	1.10E-02	1.7E-01	8.54E+02	1.29E+03	
	S114	0.001	2.30E+00	2.92E-01	7.63E+01	53.8	1.9	1.90E-02	2.5E-01	8.85E+02	1.34E+03	
	S33	0.001	2.21E+00	1.86E-01	1.02E+02	92.6	2.9	1.20E-02	3.3E-01	1.11E+03	1.68E+03	
	S113	0.001	2.00E+00	3.09E-01	1.02E+02	61.0	2.6	2.20E-02	3.3E-01	9.53E+02	1.44E+03	

	S32	0.005	2.41E+00	1.43E-01	1.27E+01	69.1	2.0	4.00E-03	4.1E-02	2.51E+02	3.80E+02	
	S112	0.005	2.12E+00	3.19E-01	1.26E+01	55.7	0.9	3.00E-03	4.1E-02	4.50E+02	6.81E+02	
	S31	0.005	2.01E+00	1.73E-01	2.52E+01	96.7	2.0	7.00E-03	8.2E-02	7.60E+02	1.15E+03	
	S111	0.005	2.01E+00	3.16E-01	2.59E+01	50.8	1.6	5.00E-03	8.4E-02	5.34E+02	8.08E+02	
Soil 3	S30	0.005	2.17E+00	1.70E-01	5.11E+01	84.4	2.0	1.10E-02	1.7E-01	8.06E+02	1.22E+03	
Sandy	S110	0.005	2.03E+00	2.76E-01	5.07E+01	43.0	2.0	9.00E-03	1.6E-01	4.70E+02	7.11E+02	
Loam	S109	0.005	1.94E+00	2.86E-01	7.62E+01	58.4	1.6	1.50E-02	2.5E-01	1.08E+03	1.63E+03	
	S29	0.005	2.25E+00	1.76E-01	1.02E+02	103.6	2.6	2.20E-02	3.3E-01	1.19E+03	1.80E+03	
	S108	0.005	2.04E+00	2.83E-01	1.02E+02	59.0	2.9	1.20E-02	3.3E-01	1.17E+03	1.77E+03	
	S28	0.010	2.06E+00	1.93E-01	1.26E+01	87.8	1.8	5.00E-03	4.1E-02	3.43E+02	5.19E+02	
	S107	0.010	2.53E+00	2.92E-01	1.28E+01	73.1	1.8	5.00E-03	4.2E-02	4.33E+02	6.56E+02	
	S27	0.010	1.87E+00	2.06E-01	2.57E+01	85.6	2.0	4.00E-03	8.3E-02	4.32E+02	6.55E+02	
	S106	0.010	2.38E+00	3.09E-01	2.62E+01	75.9	2.0	4.00E-03	8.4E-02	4.75E+02	7.19E+02	
	S26	0.010	2.27E+00	1.86E-01	5.14E+01	79.8	2.1	8.00E-03	1.7E-01	7.62E+02	1.15E+03	
	S105	0.010	2.18E+00	3.16E-01	5.08E+01	71.8	2.1	8.00E-03	1.6E-01	5.98E+02	9.05E+02	
	S104	0.010	2.65E+00	2.92E-01	7.64E+01	78.9	2.6	1.20E-02	2.5E-01	9.06E+02	1.37E+03	
	S25	0.010	3.20E+00	2.59E-01	1.01E+02	70.3	2.9	1.60E-02	3.3E-01	7.59E+02	1.15E+03	
	S103	0.010	2.11E+00	2.92E-01	1.02E+02	69.5	2.9	1.60E-02	3.3E-01	1.00E+03	1.52E+03	
	S177	0.040	2.34E+00	4.82E-01	1.26E+01	51.1	1.6	1.68E-03	3.8E-02	3.45E+02	5.22E+02	
	S176	0.040	2.36E+00	4.52E-01	2.53E+01	40.5	2.1	5.48E-03	7.8E-02	6.70E+02	1.01E+03	
	S175	0.040	3.75E+00	5.05E-01	5.10E+01	45.2	2.2	1.27E-02	1.6E-01	5.34E+02	8.08E+02	
	S208	0.040	2.61E+00	4.49E-01	5.11E+01	42.3	1.7	1.58E-02	1.6E-01	1.43E+03	2.16E+03	4.97E+02
	S174	0.040	3.76E+00	4.59E-01	7.63E+01	46.5	2.1	2.20E-02	2.4E-01	8.17E+02	1.24E+03	
	S207	0.040	1.60E+00	4.19E-01	7.70E+01	44.6	2.1	3.33E-02	2.5E-01	1.72E+03	2.61E+03	6.53E+02
	S173	0.040	3.81E+00	4.79E-01	1.01E+02	36.0	2.2	3.54E-02	3.2E-01	5.43E+02	8.22E+02	
	S204	0.060	2.98E+00	4.79E-01	5.05E+01	44.0	1.7	1.99E-02	1.5E-01	1.24E+03	1.88E+03	6.45E+02
	S205	0.060	2.56E+00	4.52E-01	5.06E+01	47.0	1.9	1.72E-02	1.5E-01	7.99E+02	1.21E+03	5.72E+02
	S206	0.060	2.10E+00	4.39E-01	5.09E+01	46.4	1.6	1.60E-02	1.5E-01	1.30E+03	1.96E+03	7.40E+02
	S201	0.060	4.14E+00	5.42E-01	7.54E+01	52.8	1.8	1.80E-02	2.2E-01	8.08E+02	1.22E+03	6.49E+02

	S202	0.060	3.38E+00	4.72E-01	7.63E+01	45.4	2.0	2.30E-02	2.3E-01	4.78E+02	7.23E+02	7.62E+02
	S203	0.060	3.07E+00	4.72E-01	7.59E+01	40.0	1.8	2.27E-02	2.3E-01	7.72E+02	1.17E+03	8.29E+02
	S48	0.001	6.62E+00	3.72E-01	1.27E+01	59.5	1.8	5.00E-03	4.2E-02	3.94E+02	5.97E+02	
	S132	0.001	4.51E+00	3.09E-01	1.24E+01	40.0	1.8	5.00E-03	4.0E-02	2.77E+02	4.19E+02	
	S47	0.001	4.34E+00	5.35E-01	2.54E+01	53.8	2.0	1.10E-02	8.3E-02	5.44E+02	8.23E+02	
	S131	0.001	4.15E+00	3.59E-01	2.60E+01	45.5	2.0	1.10E-02	8.5E-02	3.60E+02	5.45E+02	
	S46	0.001	5.89E+00	2.49E-01	5.07E+01	51.0	2.1	1.40E-02	1.7E-01	6.52E+02	9.87E+02	
	S130	0.001	5.19E+00	3.06E-01	5.13E+01	46.0	2.1	1.40E-02	1.7E-01	4.52E+02	6.84E+02	
	S129	0.001	3.87E+00	2.36E-01	7.60E+01	44.7	2.7	1.60E-02	2.5E-01	3.90E+02	5.91E+02	
	S45	0.001	6.62E+00	2.69E-01	1.02E+02	55.9	3.1	2.10E-02	3.3E-01	1.09E+03	1.65E+03	
	S128	0.001	4.00E+00	2.79E-01	1.02E+02	50.3	3.1	2.10E-02	3.3E-01	3.44E+02	5.20E+02	
	S44	0.005	4.19E+00	2.83E-01	1.27E+01	47.3	1.7	1.00E-03	4.1E-02	4.54E+02	6.87E+02	
	S127	0.005	3.55E+00	3.16E-01	1.28E+01	48.9	1.7	1.00E-03	4.1E-02	3.40E+02	5.14E+02	
	S43	0.005	6.29E+00	4.32E-01	2.53E+01	63.6	2.0	9.00E-03	8.3E-02	3.37E+02	5.11E+02	
	S126	0.005	3.81E+00	2.69E-01	2.56E+01	45.4	2.0	9.00E-03	8.3E-02	3.95E+02	5.98E+02	
Soil 4	S42	0.005	5.63E+00	2.92E-01	5.08E+01	53.9	2.2	1.20E-02	1.7E-01	3.98E+02	6.03E+02	
Clay	S125	0.005	3.70E+00	3.22E-01	5.04E+01	52.4	2.2	1.20E-02	1.6E-01	8.37E+02	1.27E+03	
Loam	S124	0.005	4.28E+00	2.73E-01	7.66E+01	43.9	2.3	1.90E-02	2.5E-01	4.13E+02	6.25E+02	
With	S41	0.005	5.52E+00	2.83E-01	1.02E+02	57.8	2.7	2.90E-02	3.3E-01	8.24E+02	1.25E+03	
Gravel	S123	0.005	3.04E+00	3.16E-01	1.01E+02	44.9	2.7	2.90E-02	3.3E-01	1.24E+03	1.88E+03	
	S40	0.010	5.41E+00	4.29E-01	1.28E+01	48.8	1.8	5.00E-03	4.2E-02	2.71E+02	4.11E+02	
	S122	0.010	3.53E+00	2.92E-01	1.27E+01	48.8	1.8	5.00E-03	4.1E-02	2.89E+02	4.37E+02	
	S39	0.010	3.97E+00	2.69E-01	2.53E+01	56.4	1.7	2.30E-02	8.3E-02	7.30E+02	1.10E+03	
	S121	0.010	3.02E+00	3.22E-01	2.63E+01	50.5	1.7	2.30E-02	8.7E-02	5.70E+02	8.62E+02	
	S38	0.010	5.65E+00	3.29E-01	5.13E+01	56.7	1.9	2.30E-02	1.7E-01	5.94E+02	9.00E+02	
	S120	0.010	4.68E+00	2.26E-01	5.08E+01	41.3	1.9	2.30E-02	1.7E-01	6.95E+02	1.05E+03	
	S119	0.010	2.85E+00	3.22E-01	7.62E+01	46.0	2.1	2.50E-02	2.5E-01	1.16E+03	1.76E+03	
	S37	0.010	7.13E+00	5.02E-01	1.02E+02	51.3	2.7	3.20E-02	3.3E-01	9.29E+02	1.41E+03	
	S118	0.010	2.78E+00	2.99E-01	1.02E+02	49.1	2.7	3.20E-02	3.3E-01	1.22E+03	1.84E+03	

S182	0.040	7.27E+00	6.95E-01	1.27E+01	42.3	1.8	4.93E-03	4.0E-02	3.50E+02	5.30E+02	
S181	0.040	4.49E+00	6.41E-01	2.55E+01	38.6	1.7	7.69E-03	7.9E-02	4.58E+02	6.94E+02	
S180	0.040	6.25E+00	7.01E-01	5.09E+01	43.9	1.9	1.61E-02	1.6E-01	6.15E+02	9.31E+02	
S216	0.040	6.56E+00	9.11E-01	5.08E+01	39.8	1.9	1.56E-02	1.6E-01	4.72E+02	7.14E+02	3.58E+02
S231	0.040	8.15E+00	1.09E+00	5.11E+01	36.9	1.7	1.94E-02	1.6E-01	2.55E+02	3.85E+02	2.41E+02
S232	0.040	1.02E+01	8.84E-01	5.06E+01	40.4	1.7	1.92E-02	1.6E-01	4.61E+02	6.97E+02	3.37E+02
S233	0.040	8.98E+00	9.74E-01	5.09E+01	32.1	1.6	1.22E-02	1.6E-01	4.41E+02	6.67E+02	3.22E+02
S179	0.040	6.80E+00	7.61E-01	7.60E+01	38.1	2.0	2.80E-02	2.4E-01	7.04E+02	1.07E+03	
S215	0.040	4.72E+00	8.61E-01	7.60E+01	41.7	2.0	2.24E-02	2.4E-01	6.00E+02	9.08E+02	7.39E+02
S227	0.040	8.75E+00	8.38E-01	7.61E+01	48.1	1.6	2.45E-02	2.4E-01	3.58E+02	5.41E+02	3.01E+02
S228	0.040	7.59E+00	8.74E-01	7.64E+01	39.9	1.9	2.13E-02	2.4E-01	4.84E+02	7.33E+02	3.87E+02
S229	0.040	7.12E+00	8.04E-01	7.63E+01	41.5	1.9	2.12E-02	2.4E-01	5.03E+02	7.61E+02	4.42E+02
S178	0.040	7.51E+00	8.31E-01	1.02E+02	40.4	2.5	4.02E-02	3.3E-01	8.07E+02	1.22E+03	
S212	0.060	7.13E+00	9.64E-01	5.10E+01	38.6	1.5	1.17E-02	1.5E-01	1.01E+03	1.53E+03	3.42E+02
S213	0.060	5.54E+00	8.71E-01	5.09E+01	43.2	1.9	1.93E-02	1.6E-01	8.39E+02	1.27E+03	4.99E+02
S214	0.060	6.51E+00	8.38E-01	5.07E+01	46.2	1.8	1.50E-02	1.5E-01	3.61E+02	5.47E+02	6.46E+02
S209	0.060	7.93E+00	1.00E+00	7.60E+01	46.3	1.7	2.17E-02	2.3E-01	3.91E+02	5.92E+02	4.48E+02
S210	0.060	5.38E+00	8.94E-01	7.63E+01	46.4	1.9	1.68E-02	2.3E-01	8.65E+02	1.31E+03	6.66E+02
S211	0.060	6.29E+00	9.07E-01	7.60E+01	40.8	1.5	1.85E-02	2.2E-01	6.76E+02	1.02E+03	6.19E+02
S60	0.001	7.30E+00	5.05E-01	1.29E+01	49.2	1.7	5.00E-03	4.2E-02	4.04E+02	6.11E+02	
S147	0.001	8.47E+00	1.06E+00	1.26E+01	43.9	1.7	5.00E-03	4.1E-02	1.14E+01	1.72E+01	
S59	0.001	8.46E+00	5.72E-01	2.56E+01	44.3	2.0	1.00E-02	8.4E-02	1.14E+02	1.72E+02	
S146	0.001	9.02E+00	1.08E+00	2.55E+01	41.2	2.0	1.00E-02	8.3E-02	8.36E+01	1.27E+02	
S58	0.001	8.47E+00	6.78E-01	5.07E+01	45.0	2.4	1.50E-02	1.7E-01	1.76E+02	2.67E+02	
S145	0.001	1.04E+01	9.37E-01	5.11E+01	43.0	2.4	1.50E-02	1.7E-01	1.02E+02	1.55E+02	
S144	0.001	8.61E+00	1.08E+00	7.60E+01	47.1	2.7	1.10E-02	2.5E-01	9.39E+01	1.42E+02	
S57	0.001	8.21E+00	6.61E-01	1.01E+02	43.0	3.1	2.50E-02	3.3E-01	1.59E+02	2.41E+02	
S143	0.001	8.19E+00	1.06E+00	1.02E+02	40.9	3.1	2.50E-02	3.3E-01	1.35E+02	2.05E+02	
S56	0.005	1.02E+01	6.25E-01	1.30E+01	56.8	1.5	3.00E-03	4.2E-02	7.12E+01	1.08E+02	

	S142	0.005	1.02E+01	9.80E-01	1.28E+01	35.6	1.5	3.00E-03	4.1E-02	2.48E+01	3.75E+01	
	S55	0.005	9.06E+00	6.75E-01	2.57E+01	42.2	2.0	6.00E-03	8.3E-02	4.33E+01	6.56E+01	
	S141	0.005	9.22E+00	1.01E+00	2.59E+01	41.0	2.0	6.00E-03	8.4E-02	3.61E+01	5.47E+01	
Soil 5	S54	0.005	9.49E+00	8.44E-01	5.07E+01	41.7	2.2	1.50E-02	1.7E-01	3.80E+02	5.75E+02	
Sandy	S140	0.005	1.06E+01	1.14E+00	5.07E+01	35.7	2.2	1.50E-02	1.7E-01	9.39E+01	1.42E+02	
Loam	S139	0.005	1.10E+01	1.12E+00	7.64E+01	38.7	2.6	2.70E-02	2.5E-01	1.35E+02	2.05E+02	
	S53	0.005	1.17E+01	8.14E-01	1.01E+02	39.3	2.7	2.40E-02	3.3E-01	3.66E+02	5.55E+02	
	S138	0.005	9.36E+00	1.03E+00	1.02E+02	43.7	2.7	2.40E-02	3.3E-01	2.18E+02	3.30E+02	
	S52	0.010	8.53E+00	7.71E-01	1.30E+01	44.6	1.5	6.00E-03	4.2E-02	1.86E+01	2.81E+01	
	S137	0.010	9.02E+00	9.74E-01	1.27E+01	42.7	1.5	6.00E-03	4.1E-02	5.16E+01	7.81E+01	
	S51	0.010	9.30E+00	5.98E-01	2.54E+01	44.3	1.6	1.30E-02	8.3E-02	2.26E+02	3.42E+02	
	S136	0.010	8.44E+00	1.06E+00	2.55E+01	38.7	1.6	1.30E-02	8.3E-02	5.78E+01	8.75E+01	
	S50	0.010	6.48E+00	5.15E-01	5.09E+01	45.0	2.1	1.60E-02	1.7E-01	4.92E+02	7.45E+02	
	S135	0.010	7.08E+00	1.10E+00	5.11E+01	44.0	2.1	1.60E-02	1.7E-01	3.24E+02	4.91E+02	
	S134	0.010	8.34E+00	9.67E-01	7.63E+01	45.0	2.3	2.50E-02	2.5E-01	3.08E+02	4.66E+02	
	S49	0.010	5.67E+00	6.78E-01	1.02E+02	43.7	2.7	3.00E-02	3.3E-01	8.78E+02	1.33E+03	
	S133	0.010	1.08E+01	1.23E+00	1.02E+02	36.1	2.7	3.00E-02	3.3E-01	4.67E+02	7.08E+02	
	S187	0.040	1.29E+01	1.81E+00	1.28E+01	39.1	1.2	6.32E-03	4.0E-02	1.60E+02	2.42E+02	
	S186	0.040	1.28E+01	1.99E+00	2.55E+01	36.6	1.6	1.70E-02	8.2E-02	1.42E+02	2.16E+02	
	S185	0.040	1.35E+01	1.93E+00	5.08E+01	39.4	2.0	2.48E-02	1.6E-01	1.78E+02	2.69E+02	
	S237	0.040	1.38E+01	1.85E+00	5.10E+01	35.6	1.5	1.48E-02	1.6E-01	1.68E+02	2.54E+02	1.07E+02
	S238	0.040	1.15E+01	1.87E+00	5.07E+01	35.9	1.4	1.55E-02	1.6E-01	2.40E+02	3.63E+02	1.30E+02
	S239	0.040	1.24E+01	1.73E+00	5.09E+01	35.6	1.9	1.33E-02	1.6E-01	3.27E+02	4.96E+02	1.58E+02
	S184	0.040	1.40E+01	1.99E+00	7.62E+01	31.0	2.3	2.84E-02	2.4E-01	2.68E+02	4.06E+02	
	S234	0.040	1.53E+01	1.94E+00	7.62E+01	35.9	1.9	1.90E-02	2.4E-01	2.53E+01	3.82E+01	8.16E+01
	S235	0.040	1.33E+01	2.05E+00	7.63E+01	38.6	1.9	1.92E-02	2.4E-01	1.31E+02	1.98E+02	1.18E+02
	S236	0.040	1.34E+01	1.81E+00	7.59E+01	35.9	1.9	1.48E-02	2.3E-01	1.41E+02	2.13E+02	1.30E+02
	S183	0.040	1.57E+01	2.01E+00	1.01E+02	33.1	2.2	4.03E-02	3.2E-01	1.48E+02	2.23E+02	
	S220	0.060	1.30E+01	1.83E+00	5.07E+01	40.5	1.7	1.72E-02	1.5E-01	3.91E+02	5.92E+02	1.24E+02

	S221	0.060	1.47E+01	2.15E+00	5.08E+01	35.5	1.7	1.94E-02	1.6E-01	2.08E+02	3.16E+02	9.10E+01
	S222	0.060	1.47E+01	1.89E+00	5.07E+01	37.6	2.0	1.80E-02	1.6E-01	6.49E+02	9.83E+02	1.26E+02
	S217	0.060	1.35E+01	2.08E+00	7.59E+01	44.0	2.0	2.80E-02	2.3E-01	3.73E+02	5.64E+02	1.87E+02
	S218	0.060	1.60E+01	2.09E+00	7.65E+01	31.3	1.6	2.63E-02	2.3E-01	9.92E+02	1.50E+03	1.25E+02
	S219	0.060	1.31E+01	2.02E+00	7.56E+01	38.6	2.1	2.29E-02	2.3E-01	1.03E+03	1.56E+03	1.93E+02
Soil 6 Gravelly Sandy Loam	S72	0.001	4.04E+00	8.31E-01	1.28E+01	26.6	1.6	3.00E-03	4.2E-02	1.93E+02	2.92E+02	
	S162	0.001	9.00E+00	1.55E+00	1.27E+01	32.7	1.6	3.00E-03	4.1E-02	4.02E+01	6.09E+01	
	S71	0.001	5.16E+00	6.88E-01	2.55E+01	29.0	2.0	8.00E-03	8.3E-02	5.78E+01	8.75E+01	
	S161	0.001	8.91E+00	1.37E+00	2.56E+01	28.6	2.0	8.00E-03	8.4E-02	2.48E+02	3.75E+02	
	S70	0.001	3.75E+00	7.38E-01	5.07E+01	24.1	2.2	9.00E-03	1.7E-01	3.49E+02	5.28E+02	
	S160	0.001	8.96E+00	1.70E+00	5.10E+01	29.6	2.2	9.00E-03	1.7E-01	2.94E+02	4.45E+02	
	S159	0.001	9.55E+00	1.77E+00	7.62E+01	21.6	2.3	1.60E-02	2.5E-01	4.34E+02	6.58E+02	
	S69	0.001	4.14E+00	6.18E-01	1.02E+02	27.8	2.4	1.60E-02	3.3E-01	4.52E+02	6.84E+02	
	S158	0.001	9.67E+00	1.95E+00	1.02E+02	28.9	2.4	1.60E-02	3.3E-01	3.53E+02	5.34E+02	
	S68	0.005	4.02E+00	6.98E-01	1.27E+01	21.2	1.5	5.00E-03	4.1E-02	2.66E+02	4.03E+02	
	S157	0.005	1.03E+01	1.64E+00	1.28E+01	30.3	1.5	5.00E-03	4.2E-02	1.68E+02	2.55E+02	
	S67	0.005	4.13E+00	5.55E-01	2.53E+01	23.0	1.3	1.00E-02	8.2E-02	9.91E+01	1.50E+02	
	S156	0.005	1.06E+01	1.47E+00	2.59E+01	32.6	1.3	1.00E-02	8.4E-02	3.72E+02	5.62E+02	
	S66	0.005	4.56E+00	4.89E-01	5.09E+01	26.4	1.8	1.10E-02	1.7E-01	6.07E+02	9.19E+02	
	S155	0.005	9.30E+00	1.81E+00	5.10E+01	28.1	1.8	1.10E-02	1.7E-01	2.89E+02	4.37E+02	
	S154	0.005	8.51E+00	2.22E+00	7.56E+01	31.7	2.0	1.90E-02	2.5E-01	3.79E+02	5.73E+02	
	S65	0.005	3.52E+00	4.82E-01	1.02E+02	28.4	2.3	2.70E-02	3.3E-01	6.83E+02	1.03E+03	
	S153	0.005	1.12E+01	1.88E+00	1.02E+02	32.5	2.3	2.70E-02	3.3E-01	4.37E+02	6.61E+02	
	S64	0.010	3.06E+00	3.12E-01	1.28E+01	27.9	1.3	3.00E-03	4.1E-02	2.86E+02	4.33E+02	
	S152	0.010	1.09E+01	2.25E+00	1.29E+01	28.5	1.3	3.00E-03	4.2E-02	1.63E+02	2.47E+02	
	S63	0.010	3.75E+00	3.02E-01	2.56E+01	29.5	1.6	7.00E-03	8.2E-02	3.65E+02	5.53E+02	
	S151	0.010	1.27E+01	2.05E+00	2.54E+01	33.3	1.6	7.00E-03	8.2E-02	2.11E+02	3.19E+02	
	S62	0.010	5.36E+00	7.80E-01	5.07E+01	27.8	2.0	1.80E-02	1.6E-01	4.45E+02	6.73E+02	
	S150	0.010	1.06E+01	2.21E+00	5.13E+01	30.3	2.0	1.80E-02	1.7E-01	3.27E+02	4.95E+02	

S149	0.010	1.27E+01	2.14E+00	7.61E+01	24.5	1.7	2.00E-02	2.5E-01	3.27E+02	4.95E+02	
S61	0.010	2.90E+00	1.76E-01	1.02E+02	28.1	2.1	2.30E-02	3.3E-01	1.27E+03	1.93E+03	
S148	0.010	1.57E+01	2.66E+00	1.01E+02	26.3	2.1	2.30E-02	3.3E-01	2.47E+02	3.73E+02	
S192	0.040	8.83E+00	1.87E+00	1.27E+01	25.7	0.7	7.78E-03	3.9E-02	1.85E+02	2.80E+02	
S191	0.040	1.38E+01	1.84E+00	2.48E+01	26.5	1.2	1.36E-02	7.8E-02	2.24E+02	3.39E+02	
S190	0.040	9.89E+00	2.03E+00	5.07E+01	23.7	1.6	2.65E-02	1.6E-01	3.12E+02	4.72E+02	
S189	0.040	1.54E+01	2.29E+00	7.63E+01	24.1	1.5	2.85E-02	2.4E-01	2.20E+02	3.33E+02	
S188	0.040	1.56E+01	2.22E+00	1.01E+02	21.5	1.7	3.90E-02	3.2E-01	8.27E+02	1.25E+03	

Appendix C

Multiple Regression Analysis Results

Abbreviations used in Multi-Variable Regression Analysis

UNITLOSS = Unit soil volume loss
RAINFALL = Rainfall intensity
SHEAR = Soil shear strength
COMP = Soil compressive strength
SLOPE = Soil bed slope
SHCOMP = Product of shear strength and compressive strength
LNSLOPE = ln(soil bed slope)
LNSHEAR = ln(Soil shear strength)
LNCOMP = ln(Soil compressive strength)
LNRAIN = ln(Rainfall intensity)
LNSHCOMP = ln(Product of shear strength and compressive strength)

Table C-1. Multi-Variable Regression-Additive Model Analysis

Six Soils Regression Models for Dependent Variable: UNITLOSS

Number in Model	R-square	Variables in Model
1	0.30592657	RAINFALL
1	0.14875425	SHEAR
1	0.07430466	COMP
1	0.00921274	SLOPE
2	0.48205035	SHEAR RAINFALL
2	0.41335739	COMP RAINFALL
2	0.30661887	SLOPE RAINFALL
2	0.17670453	SLOPE SHEAR
2	0.15126794	SHEAR COMP
2	0.10967755	SLOPE COMP
3	0.49202983	SLOPE SHEAR RAINFALL
3	0.49097128	SHEAR COMP RAINFALL
3	0.43007712	SLOPE COMP RAINFALL
3	0.18579453	SLOPE SHEAR COMP
4	0.50709028	SLOPE SHEAR COMP RAINFALL

Table C-2. Multi-Variable Regression-Additive Model Analysis

Six Soils Regression Models for Dependent Variable: UNITLOSS

Number in Model	R-square	Variables in Model
1	0.30592657	RAINFALL
1	0.09417964	SHCOMP
1	0.00921274	SLOPE
2	0.43499612	SHCOMP RAINFALL
2	0.30661887	SLOPE RAINFALL
2	0.12700402	SLOPE SHCOMP
3	0.44929315	SLOPE SHCOMP RAINFALL

Table C-3. Multi-Variable Regression-Productive Model Analysis

Six Soils Regression Models for Dependent Variable: LNUNLOSS

Number in Model	R-square	Variables in Model
1	0.26822425	LNRAIN
1	0.13173210	LNCOMP
1	0.06649280	LNSHEAR
1	0.01577122	LNSLOPE
2	0.45085996	LNCOMP LNRAIN
2	0.33196406	LNSHEAR LNRAIN
2	0.27080203	LNSLOPE LNRAIN
2	0.19412060	LNSLOPE LNCOMP
2	0.17413692	LNSHEAR LNCOMP
2	0.08166428	LNSLOPE LNSHEAR
3	0.48688326	LNSHEAR LNCOMP LNRAIN
3	0.48540949	LNSLOPE LNCOMP LNRAIN
3	0.33434254	LNSLOPE LNSHEAR LNRAIN
3	0.23080026	LNSLOPE LNSHEAR LNCOMP
4	0.51768504	LNSLOPE LNSHEAR LNCOMP LNRAIN

Table C-4. Multi-Variable Regression-Productive Model Analysis

Six Soils Regression Models for Dependent Variable: LNUNLOSS

Number in Model	R-square	Variables in Model
1	0.26822425	LNRAIN
1	0.15160522	LNSHCOMP
1	0.01577122	LNSLOPE
2	0.44251086	LNRAIN LNSHCOMP
2	0.27080203	LNSLOPE LNRAIN
2	0.18659144	LNSLOPE LNSHCOMP
3	0.45529282	LNSLOPE LNRAIN LNSHCOMP

Table C-5. Regression Parameter Analysis of Additive Model for All Soils

Model: Additive MODEL
Soil: SIX SOILS
Dependent Variable: UNITLOSS

Analysis of Variance

Source	DF	Sum of Squares	Mean Square	F Value	Prob>F
Model	4	33926804.27	8481701.0676	47.581	0.0001
Error	185	32978055.34	178259.75859		
C Total	189	66904859.61			

Root MSE	422.20819	R-square	0.5071
Dep Mean	808.29947	Adj R-sq	0.4964
C.V.	52.23413		

Parameter Estimates

Variable	DF	Parameter Estimate	Standard Error	T for H0: Parameter=0	Prob > |T|
INTERCEP	1	558.846008	73.82171524	7.570	0.0001
SLOPE	1	3970.954816	1614.4464783	2.460	0.0148
SHEAR	1	-52.145989	9.69920746	-5.376	0.0001
COMP	1	-169.220331	71.17563467	-2.378	0.0185
RAINFALL	1	11.022637	1.00376220	10.981	0.0001

The developed equation of this analysis is shown as follows.

$$U = 559 + 3970 \cdot S - 52.1 \cdot \tau - 169 \cdot \sigma + 11.0 \cdot I \,, \qquad \text{Eq. [C-1]}$$

where

U = the 30 minute unit soil volume loss (cm^3/m^2),
S = slope of the soil bed (%),
τ = shear strength (N/cm^2),
σ = compressive strength (N/cm^2),
I = the rainfall intensity, (mm/hour).

Table C-6. Regression Parameter Analysis of Product Model for All Soils

Model: PRODUCT MODEL
Soil: SIX SOILS
Dependent Variable: LNUNLOSS

Analysis of Variance

Source	DF	Sum of Squares	Mean Square	F Value	Prob>F
Model	4	81.43836	20.35959	49.642	0.0001
Error	185	75.87420	0.41013		
C Total	189	157.31256			

Root MSE	0.64041	R-square	0.5177
Dep Mean	6.37787	Adj R-sq	0.5073
C.V.	10.04120		

Parameter Estimates

Variable	DF	Parameter Estimate	Standard Error	T for H0: Parameter=0	Prob > |T|
INTERCEP	1	4.290715	0.31876919	13.460	0.0001
LNSLOPE	1	0.119536	0.03477686	3.437	0.0007
LNSHEAR	1	-0.148834	0.04230054	-3.518	0.0005
LNCOMP	1	-0.565688	0.06745665	-8.386	0.0001
LNRAIN	1	0.687510	0.06553975	10.490	0.0001

The developed equation of this analysis is shown as follows.

$$U = 73 \cdot S^{0.12} \cdot \tau^{-0.15} \cdot \sigma^{-0.57} \cdot I^{0.69}, \qquad \text{Eq. [C-2]}$$

where

U = the 30 minute unit soil volume loss (cm^3/m^2),
S = slope of the soil bed (%),
τ = shear strength (N/cm^2),
σ = compressive strength (N/cm^2),
I = the rainfall intensity, (mm/hour).

Table C-7. Regression Parameter Analysis of Additive Model for Five Soils

Model: Additive MODEL
Soil: FIVE SOILS
Dependent Variable: UNITLOSS

Analysis of Variance

Source	DF	Sum of Squares	Mean Square	F Value	Prob>F
Model	4	22313522.782	5578380.6954	51.341	0.0001
Error	152	16515255.885	108652.99924		
C Total	156	38828778.667			

Root MSE	329.62554	R-square	0.5747
Dep Mean	768.25605	Adj R-sq	0.5635
C.V.	42.90569		

Parameter Estimates

Variable	DF	Parameter Estimate	Standard Error	T for H0: Parameter=0	Prob > |T|
INTERCEP	1	711.412907	65.54050724	10.855	0.0001
SLOPE	1	6913.697241	1439.1670894	4.804	0.0001
SHEAR	1	-79.865926	15.29933483	-5.220	0.0001
COMP	1	-7.780208	98.94184628	-0.079	0.9374
RAINFALL	1	8.125779	0.85955696	9.453	0.0001

The developed equation of this analysis is shown as follows.

$$U = 711 + 6910 \cdot S - 79.9 \cdot \tau - 7.78 \cdot \sigma + 8.13 \cdot I \,, \qquad \text{Eq. [C-3]}$$

where

U = the 30 minute unit soil volume loss (cm^3/m^2),
S = slope of the soil bed (%),
τ = shear strength (N/cm^2),
σ = compressive strength (N/cm^2),
I = the rainfall intensity, (mm/hour).

Table C-8. Regression Parameter Analysis of Product Model for Five Soils

Model: PRODUCT MODEL
Soil: FIVE SOILS
Dependent Variable: LNUNLOSS

Analysis of Variance

Source	DF	Sum of Squares	Mean Square	F Value	Prob>F
Model	4	65.67891	16.41973	52.235	0.0001
Error	152	47.77989	0.31434		
C Total	156	113.45880			

Root MSE	0.56066	R-square	0.5789
Dep Mean	6.37423	Adj R-sq	0.5678
C.V.	8.79576		

Parameter Estimates

Variable	DF	Parameter Estimate	Standard Error	T for H0: Parameter=0	Prob > |T|
INTERCEP	1	5.872432	0.41120197	14.281	0.0001
LNSLOPE	1	0.148539	0.03465349	4.286	0.0001
LNSHEAR	1	-0.634782	0.14988376	-4.235	0.0001
LNCOMP	1	-0.190793	0.13123459	-1.454	0.1481
LNRAIN	1	0.570438	0.06268043	9.101	0.0001

The developed equation of this analysis is shown as follows.

$$U = 350 \cdot S^{0.15} \cdot \tau^{-0.64} \cdot \sigma^{-0.19} \cdot I^{0.57}, \qquad \text{Eq. [C-4]}$$

where

U = the 30 minute unit soil volume loss (cm^3/m^2),
S = slope of the soil bed (%),
τ = shear strength (N/cm^2),
σ = compressive strength (N/cm^2),
I = the rainfall intensity, (mm/hour).

Appendix E

Data and Unit Conversion

In Renard et al. (1997), ton/acre could be converted to kg/m^2 by multiplying the constant 0.2242. Therefore, we have

$$\frac{kg}{m^2} = 0.2242 \cdot \frac{ton}{acre}. \qquad \text{Eq. [E-1]}$$

We also have

$$\frac{g}{m^2} = \frac{1000 \cdot kg}{m^2} = 1000 \cdot 0.2242 \cdot \frac{ton}{acre} = 224.2 \cdot \frac{ton}{acre}, \qquad \text{Eq. [E-2]}$$

According to the defination of moisture content, we have

$$\omega = \frac{W_w}{W_s} \cdot 100, \qquad \text{Eq. [E-3]}$$

where

ω = Soil moisture content, (%);
W_s = Weight of soil, (g);
W_w = Weight of water, (g).

In our research, all the soils are 100% saturated. We have no air in the soil pore volume. Therefore, we have

$$V_s = \frac{W_s}{D_s} \text{ and } V_w = \frac{W_w}{D_w}$$

where

V_s = Volume of dry soil, (cm^3);
D_s = Density of dry soil, (g/cm^3);
V_w = Volume of water, (cm^3);
W_w = Weight of water, (g);
D_w = Density of water, (g/cm^3).

$$V_w = \frac{W_w}{1} = \frac{W_s \cdot \omega}{100 \cdot 1},$$

$$V_{total} = V_s + V_w = \frac{W_w}{D_s} + \frac{W_s \cdot \omega}{100} = W_s\left(\frac{1}{D_s} + \frac{\omega}{100}\right) \qquad \text{Eq. [E-4]}$$

Combine Eq. [E-1] and [E-4], we get

$$V_{total} = 224.2 \cdot A \cdot \left(\frac{1}{D_s} + \frac{\omega}{100}\right) \qquad \text{Eq. [E-5]}$$

where A is the result calculated from RUSLE with the unit of ton/acre. The Eq. [E-5] was used in the conversion of unit from RUSLE to the units used in this research.

Appendix F

Multiple Regression Analysis Results for

Erosion Power

EROPOWER = Erosion Power
LNPOWER = Ln(Erosion Power)

Multi-Variable Regression-Productive Model Analysis

Six Soils Regression Models for Dependent Variable: LNUNLOSS

Number in Model	R-square	Variables in Model
1	0.26514431	LNPOWER
1	0.13173210	LNCOMP
1	0.06649280	LNSHEAR
1	0.01577122	LNSLOPE
2	0.44015913	LNPOWER LNCOMP
2	0.33258108	LNPOWER LNSHEAR
2	0.27007140	LNSLOPE LNPOWER
2	0.19412060	LNSLOPE LNCOMP
2	0.17413692	LNSHEAR LNCOMP
2	0.08166428	LNSLOPE LNSHEAR
3	0.48240479	LNSLOPE LNPOWER LNCOMP
3	0.47984887	LNPOWER LNSHEAR LNCOMP
3	0.33715738	LNSLOPE LNPOWER LNSHEAR
3	0.23080026	LNSLOPE LNSHEAR LNCOMP
4	0.51758871	LNSLOPE LNPOWER LNSHEAR LNCOMP

--

Multi-Variable Regression-Productive Model Analysis

Six Soils Regression Models for Dependent Variable: LNUNLOSS

Number in Model	R-square	Variables in Model
1	0.26514431	LNPOWER
1	0.15160522	LNSHCOMP
1	0.01577122	LNSLOPE
2	0.44065923	LNSHCOMP LNPOWER
2	0.27007140	LNSLOPE LNPOWER
2	0.18659144	LNSLOPE LNSHCOMP
3	0.45843953	LNSLOPE LNSHCOMP LNPOWER

Multi-Variable Regression-Productive Model Analysis

Five Soils Regression Models for Dependent Variable: LNUNLOSS

Number in Model	R-square	Variables in Model
1	0.26934755	LNSHEAR
1	0.20319116	LNPOWER
1	0.19167658	LNCOMP
1	0.02317371	LNSLOPE
2	0.51996389	LNPOWER LNSHEAR
2	0.44595563	LNPOWER LNCOMP
2	0.34636094	LNSLOPE LNSHEAR
2	0.29841084	LNSLOPE LNCOMP
2	0.27079038	LNSHEAR LNCOMP
2	0.21294182	LNSLOPE LNPOWER
3	0.57168783	LNSLOPE LNPOWER LNSHEAR
3	0.52682818	LNSLOPE LNPOWER LNCOMP
3	0.51996970	LNPOWER LNSHEAR LNCOMP
3	0.34941439	LNSLOPE LNSHEAR LNCOMP
4	0.57721924	LNSLOPE LNPOWER LNSHEAR LNCOMP

Multi-Variable Regression-Productive Model Analysis

Five Soils Regression Models for Dependent Variable: LNUNLOSS

Number in Model	R-square	Variables in Model
1	0.23999107	LNSHCOMP
1	0.20319116	LNPOWER
1	0.02317371	LNSLOPE
2	0.49642429	LNSHCOMP LNPOWER
2	0.33985889	LNSLOPE LNSHCOMP
2	0.21294182	LNSLOPE LNPOWER
3	0.56952108	LNSLOPE LNSHCOMP LNPOWER